Master's Thesis

Revitalization of the *cabaña pasiega*:

A sustainable approach for the restoration of vernacular stone cattle buildings in rural Cantabria

Submitted by Ayelén Arceo
October 2024

Supervised by
David Briels, M.Sc.
Christian Hepf, M.Sc.

Master of Science (M.Sc.) in Energy Efficient and Sustainable Construction
Faculty of Civil, Geo, and Environmental Engineering & Faculty of Architecture

Technical University of Munich
Chair of Building Technology and Climate Responsive Design
Prof. Dipl.-Ing. Thomas Auer

Abstract

Today, vernacular heritage is at serious risk of disappearing. The absence of preservation policies and the resulting indiscriminate interventions are pressing issues that demand immediate attention. Meanwhile, the world is grappling with significant environmental challenges, such as rising levels of carbon dioxide (CO_2) in the atmosphere and resource scarcity.

This master's thesis explores how rural vernacular structures in northern Spain, which are becoming obsolete, can be sustainably and energy-efficiently rehabilitated. Adopting a holistic approach encompassing both ecological and cultural factors, the study identifies appropriate retrofitting strategies and incorporates them into an architectural design concept.

The thesis begins with a comprehensive study of local history and traditional building techniques, followed by a detailed climate analysis. It then focuses on a case study building, exploring the selection and evaluation of a suitable retrofit insulation system. The acquired insights are used to develop a preliminary design concept, which is assessed and refined for thermal comfort and heating energy consumption. This process culminates in the creation of a final architectural design proposal that aims to serve as a model for similar buildings.

Acknowledgements

My sincere appreciation goes to David Briels and Christian Hepf, whose guidance and expertise were instrumental in shaping the course of this master's thesis, especially in the early stages. I value your openness and positive attitude towards my topic proposal, as well as your mentoring and encouragement throughout the working process.

I would also like to extend my gratitude to Rosana Noce, whose coaching sessions helped me find focus and direction, enabling me to bring closure to an open chapter in my life. Thank you.

Special thanks to Donna Felten for taking the time to provide valuable advice and suggestions during the final phases of this work. Your keen eye and proficiency in linguistics are inspiring.

Lastly, I want to thank my family — my husband and daughters — for their patience during the long hours spent immersed in this pursuit. Without your unwavering support and independence, this would not have been possible. I am thankful and proud.

Table of contents

1. Introduction

1.1. On sustainability and the rehabilitation of vernacular heritage

As of 2024, a total of 1,223 properties have been inscribed on the UNESCO World Heritage List, reflecting global recognition of culturally and historically significant sites (UNESCO, 2024). However, despite some acknowledgment within the broader context of these exceptional sites, the “universal value” of vernacular heritage remains underappreciated (Dipasquale et al., 2020, p. 17).

In architecture, vernacular refers to regional building styles that have evolved organically within local communities. These structures are crafted by skilled, non-professional builders using techniques passed down through generations and locally sourced materials. They are harmoniously integrated into their natural surroundings, adapting to the whims of climate and challenges of topography (Rudofsky, 1964). Mostly involving settlements of a representative character rather than singular buildings, vernacular heritage provides a valuable glimpse into how people historically engaged with their environment. It stands as a vital expression of local identity and cultural diversity (Figure 1) (International Council on Monuments and Sites [ICOMOS], 1999). The immeasurable value of this form of heritage lies in the profound relationship between the tangible and the intangible, between nature and culture. It is this relationship that has allowed this type of architecture to endure through the ages, making it a testament to sustainability and an irreplaceable source of knowledge that cannot be neglected (Dipasquale et al., 2020, p. 15).

Today, vernacular structures worldwide are extremely vulnerable (ICOMOS, 1999). On one hand, global socio-economic changes, namely the shift from agricultural to industrial societies, have caused mass migration from rural areas to cities. This has led to a decline in rural populations and left many buildings in disrepair. On the other hand, damage to vernacular heritage is caused by the homogenization of architecture and culture. Rather than adhering to local traditions during restoration and new construction works, generic alternatives are often favored for their practicality (Council of Europe, 2008, p. 3).

Linked to both causes is perhaps the greatest threat: society’s general undervaluation of this form of heritage and the consequent lack of resources for safeguarding it (Council of Europe, 2008, p. 3). Overshadowed by the international attention and recognition given to monuments and sites listed under the concept of World Heritage, millions of anonymous structures, whose outstanding universal value is not evident, are hardly seen (Dipasquale et al., 2020, p. 21). Vernacular heritage is vulnerable because it is neither protected nor considered worthy of conservation. Despite several international UNESCO World Heritage conventions, constituting safeguards, and recommendations such as the ICOMOS charter on the built vernacular heritage ratified in 1999, it is still very difficult to act for the protection of these structures. As rural populations continue to leave their traditional habitats, the buildings are often sold to new owners who fail to recognize or value their cultural significance (Dipasquale et al., 2020, p. 15f.).

Figure 1: Examples of vernacular rural dwellings, clockwise from the top left: rural house in Cambodia, Mongolian ger, fortress-like tata somba houses in Togo and Benin, stone farmhouse in Portugal

In order to preserve vernacular habitats and to avoid the regrettable loss of historical constructions, it is essential to find adequate ways to recover and repurpose redundant buildings. A significant challenge is that the design and functionality of vernacular dwellings built decades or centuries ago do not meet the comfort requirements of modern society.

The present work attempts to develop strategies for the revitalization of rural vernacular structures currently facing obsolescence in northern Spain. An investigation of the cultural background, combined with a climatic examination and assessment of appropiate retrofitting measures, contributes to the design of an adapted re-use concept for a case study building, aiming to establish a prototype for the entire region.

1.2. Background and problem statement

In the Pasiego valleys of the Spanish province Cantabria, a specific technique for land use is reflected in a unique type of construction: the *cabaña pasiega*. These modest stone buildings, of which more than eleven thousand remain scattered over the rugged terrain, are the legacy of a way of life and an expression of the deep bond between the land and its inhabitants (Comisión Regional de Ordenación del Territorio y Urbanismo [CROTU], 2019, pp. 2, 10).

Figure 2: Impressions of the Pasiego cultural landscape

The physical setting straddling the provincial boundaries of Burgos and Cantabria is characterized by intricate valleys, pronounced altitudinal variation, and a harsh climate. The landscape we see today, however, was shaped by people who made the mountains their own and molded them according to their needs and preferences (Figure 2). Through the practice of transhumant herding, using the pastures as their primary resource, the Pasiegos were able to carve out a life in this inherently remote and challenging environment (CROTU, 2019, p. 13).

Their economic and productive system revolved around cattle meadows organized in clusters at varying altitudes. Each meadow was fully enclosed and featured a structure that, over time, evolved from a simple shepherd's shelter to a multi-use building combining both housing and stabling functions. Habitation in the Pasiego valleys was thus dispersed from meadow to meadow, with entire families moving with their cattle between cabins according to the weather and the feeding needs of the livestock. In this context, the *cabaña pasiega* is not merely a standalone construction but the micro-unit that forms the structural basis of the Pasiego landscape and thus, a vital element of cultural identity (CROTU, 2019, pp. 13ff., 53).

However, by the late twentieth century, the agricultural system that created this habitat became obsolete. The resulting decline in population and activity has led to widespread deterioration of the landscape, with numerous abandoned meadows and cabins that fall into disrepair with each passing day (CROTU, 2019, p. 2). Signs of this neglect can be found everywhere, although areas at high altitudes are particularly affected due to their difficult access.

Figure 3: Examples of renovations that profoundly alter the traditional character of the *cabaña pasiega*

This has led to the sale of land at low prices, often to those unfamiliar with its value. Consequently, many renovations have altered the heritage rather than preserving it. Issues include inappropriate urbanization, indiscriminate extensions, new openings, and the use of foreign materials and construction methods (CROTU, 2019, p. 46). Figure 3 illustrates some of these unfortunate modifications.

Like many other vernacular habitats, the Pasiego heritage is at risk due to insufficient protection. Although a regulation plan was initially approved in 2010, it was never fully enforced (Gobierno de Cantabria, 2024). Within the framework of this plan, a complementary study was carried out that included an inventory of cabins with over ten thousand structures listed. Moreover, a detailed guideline including intervention criteria and strategies for the preservation of this heritage was developed.

The idea of choosing the rehabilitation of the *cabaña pasiega* as a topic for a master's thesis came about through a personal connection to Cantabria due to family history. After having visited the place several times over the years, the possibility of engaging in a hands-on project arose. The present work encompasses the analysis and initial design phases that will ultimately lead to its realization.

1.3. Aim and methodological approach

The intent of this work is to develop a revitalization concept for the *cabaña pasiega*. As derived from previous discussions, this entails finding ways to adapt it for new uses without compromising its heritage value. Another key objective is addressing the urgent need to reduce energy consumption and greenhouse gas emissions in the European building industry (European Commission, 2020). The focus is thus on attaining an interior environment that meets modern standards of comfort while respecting the traditional character of the building and achieving a high degree of energy efficiency. In addition, mostly environmentally friendly materials are used. Through theoretical analyses, as well as the use of dynamic simulation software applied to a real-life context, the study identifies suitable retrofitting measures and intervention design strategies. The planning of building services is not included in this work.

The first part, Chapter 2, introduces the vernacular heritage under investigation, specifically the *cabaña pasiega*. This chapter provides an overview of the historical and socio-cultural background of the region's original inhabitants and examines the key formal characteristics of their vernacular structures. It also highlights the most relevant intervention criteria established by local authorities during the development of the preservation plan. Chapter 3 comprises a detailed climate analysis. After starting with a broad, macro-level examination of the region, the size of the area evaluated is narrowed down to the microclimate affecting the specific plot and building chosen for the case study.

Based on the findings of Chapters 2 and 3, the need to retrofit the building envelope with internal insulation is identified. Chapter 4 takes a closer look at the existing structure of the case study cabin, defines the desired level of insulation, and discusses the appropriateness of various insulation systems and materials. This is followed by the selection of a representative assembly for the exterior walls. Given the heightened risk of moisture damage associated with the installation of interior insulation, a standard cross-section of the chosen assembly is evaluated using the one-dimensional simulation tool WUFI Pro. Considerations include vapor diffusion, driving rain, and, in a separate part based on research, thermal bridges.

Chapter 5 draws on the theoretical analyses and hygrothermal simulations to develop a preliminary design concept. This concept is assessed in Chapter 6 using the software WUFI Plus to determine whether it provides a suitable indoor climate for modern use. Evaluation criteria are thermal comfort (measured in terms of the PMV index and operative temperature) and the energy requirements for heating. In the further course of the study, the influence of individual parameters on the building’s performance is surveyed and various scenarios of use are tested. This iterative process finally leads to a building variant that is optimized for energy efficiency during the winter and resilient enough to adapt to changing conditions in the future. Predicated on the results of this evaluation, a final architectural design proposal is elaborated and documented in Chapter 7. Figure 4 summarizes the methodological approach.

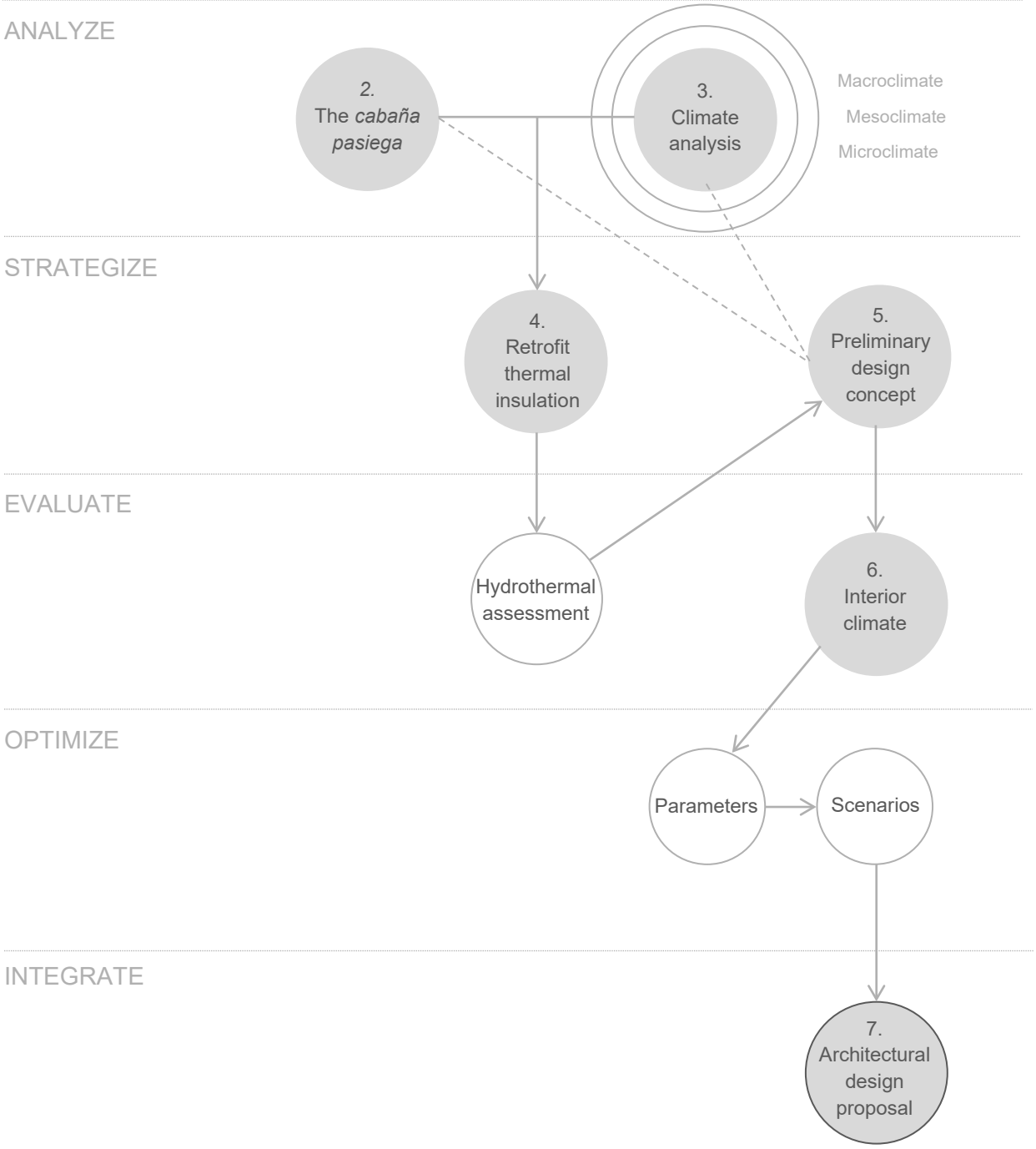

Figure 4: Methodological approach

2. The *cabaña pasiega*

The restoration of the *cabaña pasiega* primarily aims to extend the building's useful life by repurposing it. However, beyond ensuring long-term use, work on heritage buildings must maintain their historic and patrimonial value. Therefore, it is necessary to understand the cultural background and building traditions of the Pasiego people and incorporate this knowledge into the revitalization concept.

This chapter explores the historical processes and socioeconomic system that led to the construction of over eleven thousand cattle cabins scattered along the slopes of the Cantabrian valleys. It includes general reflections on the role of architecture in defining this territory, a brief description of the current situation, and general considerations about the *cabaña pasiega*, focusing on its essential typology and constructive, as well as structural, characteristics. Finally, it outlines the intervention criteria relevant to the case study.

2.1. Origin and evolution

Human activity in the region centered on the upper reaches of the Pas and Miera rivers (Figure 6) was not recorded in history until the year 1011. At this time, the Monastery of San Salvador de Oña was granted rights over an extensive Cantabrian area, allowing herders to pasture animals and expand the natural grasslands by clearing trees and building shelters from them. Despite this seasonal use of remote alpine pastures, the Pasiego territory remained uninhabited until the late Middle Ages (García Alonso, 2004, p. 21).

The study of extensive livestock grazing in the Montes de Pas, based on “brenas” (meadows) and “seles” (shelters), is of great interest in explaining the origins of the Pasiego pastoral system and its characteristic constructions. Brenas were natural grasslands, either alpine pastures or artificial ones created by deforestation in lower areas. In these brenas, seles to keep the livestock safe during the night and provide shelter for the herders were commonly found. Archaeological remains refer to one-story buildings assembled in dry stone, rectangular in shape and small in size, with a narrow access opening oriented to the southeast quadrant (Figure 5). The lack of evidence of covering materials suggests that during these early times, the use of plant-based roof coverings was common (García Alonso, 2004, p. 28ff.).

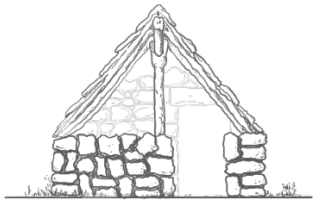

Figure 5: Shepherd’s shelter or “sel”

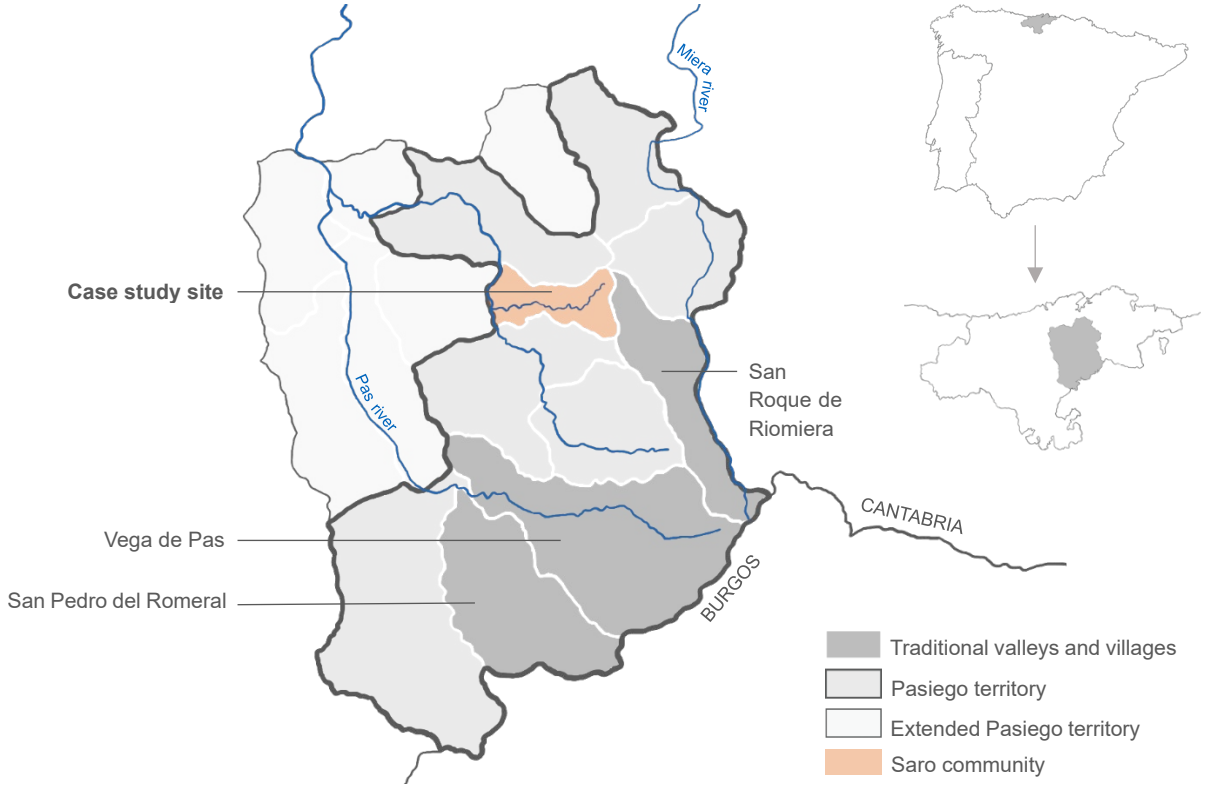

Figure 6: The Pasiego territory

In the sixteenth century, growing colonization efforts led to the gradual transformation of the landscape of forests, pastures, and seles into a mosaic of enclosed farms and cabins stretching over cleared slopes (Figure 7). After a series of disputes about land appropriation rights, the Pasiegos started building dry edge walls around the meadows and erecting cabins where the old seles once stood. These were buildings designed for permanence, as they were crafted with durable local materials such as stone, timber, and mud. The prevalence of slate roofs signals a change towards higher degrees of forest degradation, more stable and permanent settlements, and the improvement of the economic situation of the inhabitants (CROTU, 2019, p. 21).

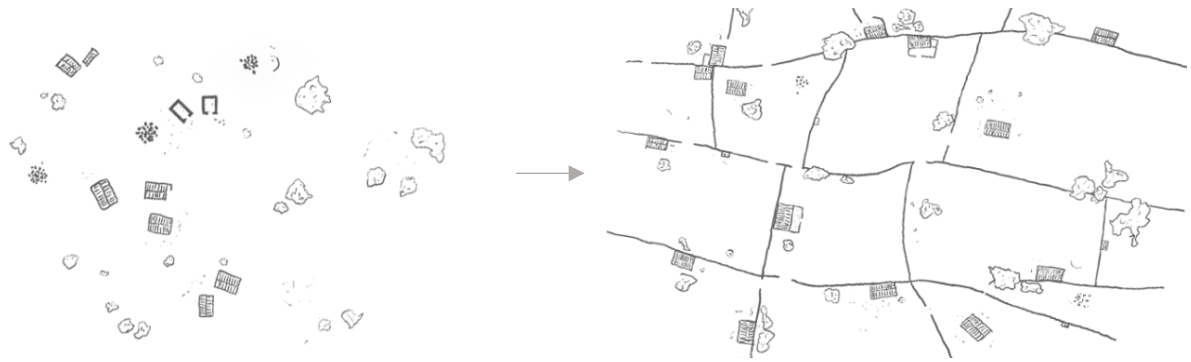

Figure 7: Transformation of landscape

By the late 1700s, seasonal transhumance for the intensive use of grasslands at various altitudes had become widespread. Throughout the year, the Pasiego people moved between several meadows, relocating their homes to meet the needs of their livestock. Central to this new economic model were the native cow, known for its “red” coat and small stature, and the commercialization of dairy products, particularly cheeses and butter, in local markets. Some impressions of the Pasiego lifestyle are shown in Figure 9. In this context, the cabin with its “ring fence” became the fundamental unit of land use and the symbol of a prosperous way of life that would endure for nearly three centuries (CROTU, 2019, p. 22f.).

In the final decades of the twentieth century, the Pasiego pastoral system fell into crisis. Numerous factors contributed to this decline, chief among them the new agricultural policies typical of the modern capitalist industrialized world (García Alonso, 2004, p. 130). The decrease in cattle activities led to the abandonment of the prairies and the decay of their cabins (Figure 8). In many cases, the ranches were sold due to their infrequent use. The lack of regulation resulted in inadequate interventions and modifications, leaving an architectural and historical heritage on the brink of ruin (CROTU, 2019, p. 46).

Figure 8: Abandoned cabins

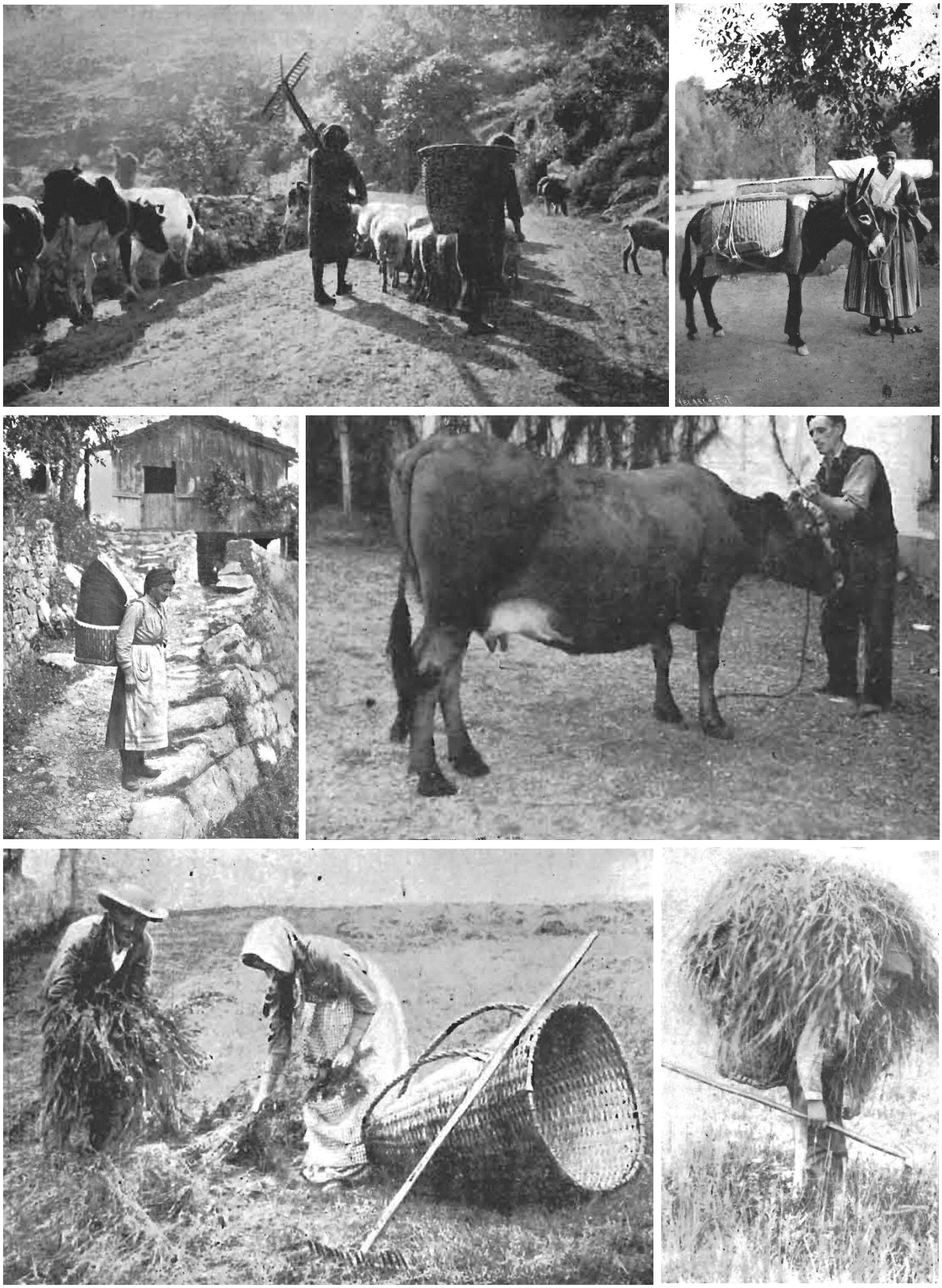

Figure 9: Impressions of the Pasiego lifestyle

2.2. Building characteristics

The strictly functional construction of the *cabaña pasiega*, executed with an economy of means, consists of two overlapping floors that are not connected from the inside. The ground floor serves as a stable, while the upper floor is used for storing hay and, in some cases, provides living spaces. The shape of the building is defined by its rectangular layout, compact volume, and gable roof. One of its most distinctive features is the short access façade, which has offset doors that are displaced to avoid the load of the main beams. These doors feature door leaves made of vertical wooden planks.

In many cases, the cabin is situated in the highest area of the land, along the stone boundary wall and close to the road. It is typically built with the long façade parallel to the slope and the short access front facing east or southeast (Figure 11). On steeply sloping terrain, the cabin's placement allows direct access to both floors with virtually no stairs. However, when the cabin is located on flat land, an exterior staircase is required to reach the upper level (Figure 10) (CROTU, 2019, p. 55).

Another characteristic feature is the gabled roof, with its ridge running parallel to the long façade and a pitch angle that ranges between 36% and 42%. In the more traditional areas, the roof is primarily covered with stone slabs, while the periphery of the Pasiego territory features several examples using Arabic clay tiles (CROTU, 2019, p. 61). Roof runoffs are consistently managed without rain gutters or downspouts. Constructive solutions to keep

Figure 10: Access situation on steep slope (left) and flat land (right)

Figure 11: Implantation

Figure 12: "Enrabadero"

water from dripping directly down the walls, one of which is the “enrabadero” shown in Figure 12, typically involve extending the roof slightly past the exterior walls.

Structurally, the building consists of load-bearing perimeter walls and two wooden posts with stone footings. These are made of oak or chestnut and symmetrically arranged in the center of the floor, parallel to the long façade. Loads from the intermediate floor and rafters of the roof are distributed across two longitudinal beams, which rest on the wooden supports and walls (CROTU, 2019, p. 68). The walls are about 70 to 80 cm thick, built with a double-faced technique using locally available stone and mud as a binder (García Alonso, 2004, p. 97ff.). In Figure 13, axonometric schemes portray the constructive systems described.

The components that make up the structure of the cabin define the geometry and proportions of the inner space (Figure 14). A characteristic feature is the lack of ceiling joists, allowing for the great height of the first floor, which contrasts with the low height of the space below. The only connection between both levels is through long gaps located directly above the mangers. These were conveniently used to feed the cattle and exemplify the productive and functional essence of these buildings. Only a small number of openings permit daylight to enter the interior, which is why it is rather dark. In some cabins, known as “cabañas vividoras,” a simple compartmentalization of the upper space has been carried out, defining differentiated rooms. These partitions are normally made with wooden planks and, in line with the austere character of the building, do not present interior finishes (CROTU, 2019, p. 69f.).

Throughout the Pasiego territory, several variants of the traditional *cabaña* enrich the landscape. The reasons for these differences stem from the unique characteristics of each site, such as topography, orientation, and availability of different stone types. Over time, many cabins have also been expanded to accommodate more livestock and improve their functional conditions (CROTU, 2019, p. 70ff.).

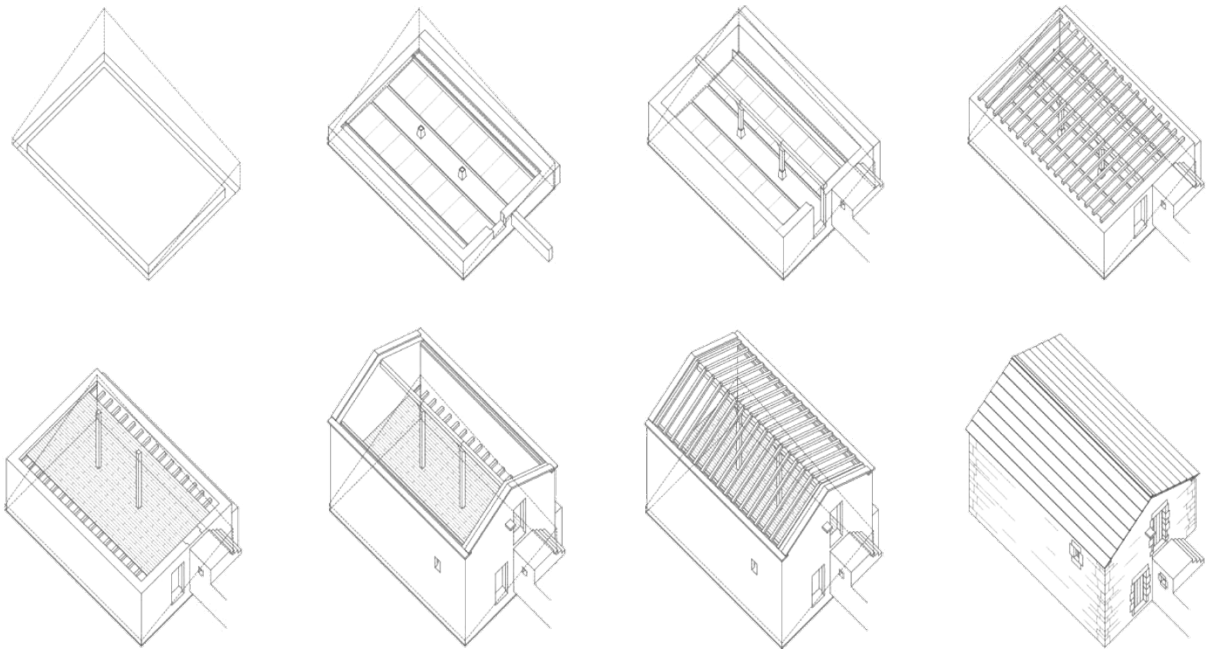

Figure 13: Structure and constructive system

Figure 14: Impressions of the interior space, clockwise from the top left: upper floor with partitions, upper floor, gap used to throw hay down to the feeders, ground floor

2.3. Intervention criteria

To increase economic activity and prevent rural depopulation, Cantabria's legislation has made changes to the law, specifically the content of the Law of Cantabria 3/2012, which amends the Law of Cantabria 2/2001. While allowing the construction of new buildings on rustic land and the renovation of existing ones with the possibility of adapting to new uses, the law does not define standards to ensure the preservation of the Pasiego cultural heritage (CROTU, 2019, pp. 2,3,79). Furthermore, municipal planning offices appear to ignore the territory's uniqueness, limiting themselves to establishing generic conditions for its protection (CROTU, 2019, p. 9).

In 2019, in response to the lack of specific regulation, the “Comisión Regional de Ordenación del Territorio y Urbanismo” [Regional Commission for Land Use and Urban Planning], from here on referred to as “CROTU”, approved the “Guía de Buenas Prácticas para la intervención en el patrimonio arquitectónico del territorio Pasiego” [Guide to good practices for intervention in the architectural heritage of the Pasiego territory]. This guide was originally created as part of the “Plan Especial de Protección y Ordenación del Territorio Pasiego” [Special Plan for the Protection and Planning of the Pasiego Territory] that was never fully enforced (Gobierno de

Cantabria, 2024). The purpose of the guide is to ensure that renovations and the incorporation of new uses to the *cabaña pasiega* are conducted in a way that preserves its traditional character and cultural value. Therefore, the criteria outlined in the guide serve as the foundation for all design decisions in this study.

Overall, the guide establishes that reforms must respect the essential and compact volume of the construction. Extensions and elevations are admissible only in justified cases and must be carried out in accordance with predefined criteria. The arrangement of the doors must be left unchanged, and their wooden panels have to be restored. In most cases, the layout and geometry of openings must be preserved; however, if the new program requires better lighting or ventilation conditions, new openings or expansions of existing ones are permitted. In every case, exterior blinds and shutters ought to be avoided and the new window frames must be made of wood, preferably oak or chestnut, with natural finishes (CROTU, 2019, pp. 82–85). When restoring the roof, the original cover material must be preserved and, if possible, reused (CROTU, 2019, p. 87). Rainwater collection systems based on gutters and downspouts are to be avoided and instead, traditional solutions like ledges and wooden eaves must be applied (CROTU, 2019, p. 89). The original structure of the building must be maintained. Restorations and reinforcements to improve safety and functionality need to be carried out using traditional construction techniques (CROTU, 2019, p. 92).

The guide hence states that interventions must protect or recover the original constructive characteristics of the *cabaña pasiega*. Its austerity, simplicity, stone- and carpentry work are values to be preserved. At the same time, to adapt to the new requirements for use and comfort, retrofit measures must guarantee safety, watertightness, and adequate thermal and acoustic conditions. In addition to maintaining heritage values, rehabilitation efforts should aim to reduce energy consumption by improving building envelope conditions and implementing efficient energy systems (CROTU, 2019, p. 109f.).

While this is only a general – and incomplete – overview of the do's and don'ts established in the guide, the forthcoming chapters will go into greater detail about the intervention criteria that are specifically relevant to the proposed revitalization concept.

In terms of possible new uses, a trend has been seen in the adaptation of cabins for residential and touristic purposes. To preserve the original constitution of the buildings, these transformations must avoid a literal translation of the habitability concepts of modern houses, flats, or hotels. It would be beneficial to experiment with less demanding residential solutions in terms of program, such as open and flexible designs that better adapt to the unique characteristics of the cabin's interior spaces (CROTU, 2019, pp. 82, 93).

When it comes to the cabins' suitability for permanent residential use, location is an important factor to consider. Remote sites are often difficult to reach, especially in the winter, making them more appealing for seasonal tourism. Given its good road connections and relative proximity to Santander, the case study cabin presented in the following chapters is well-suited to be inhabited year-round.

3. Climate analysis

The design of an adequate and energy-efficient revitalization concept for the *cabaña pasiega* requires close attention to the climate. In addition, through retrofit measures tailored to the local climate, both the quality of the indoor environment and the lifetime of the existing structure can be increased.

An overview of the macroclimate influencing the Iberian Peninsula opens this chapter and establishes the foundation for subsequent, more in-depth analyses of the Cantabrian regional climate and microclimate of the case study location (Hausladen et al., 2012, p. 12). Figure 15 illustrates a “zoom-in” sequence, beginning with a macro-level view of the region under investigation and progressively narrowing the focus to the smallest specific area.

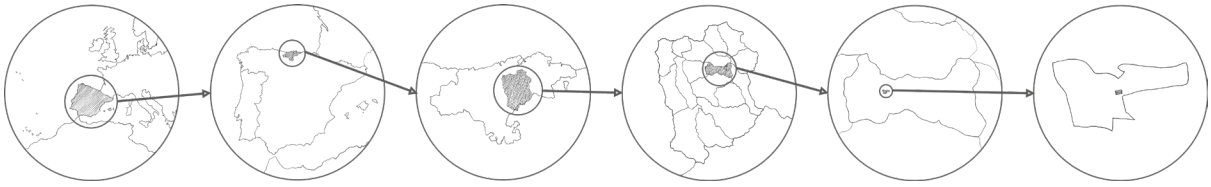

Figure 15: “Zoom-in”: Iberian Peninsula – Cantabria – Pasiego territory – Saro community – plot of land with cabin

3.1. Macroclimate

As a mighty trapezoid with a diagonal of 1,200 kilometers, the Iberian Peninsula adjoins the southwest corner of the European mainland and thus seals off the Mediterranean from the Atlantic Ocean. Its massive body is characterized by a central plateau, the Meseta, situated 600 meters above average sea level and large mountains that form chains surrounding it (Lautensach, 1969, p. 18).

Due to its prominent size, proximity to two very different bodies of water, and topographic relief, the Iberian Peninsula presents significant climatic variances within its territory (Figure 16). According to Köppen and Geiger, most of the Iberian Peninsula falls into a temperate climate, with no dry season in the north due to year-round influences of Atlantic fronts and a dry summer period elsewhere. The southern central plateau and Mediterranean coastal areas experience hot summers, while the northwest and most of the west coast have a temperate summer with an average temperature in the hottest month below or equal to 22°C. Cold climates are seen in mountainous regions at higher altitudes and the drier coastal areas of the south are classified as arid (Agencia Estatal de Meteorología [AEMET] et al., 2011, pp. 16–18).

Therefore, the climate of the northern province of Cantabria is expected to be temperate, with no major temperature variations, no dry season, and a mild summer.

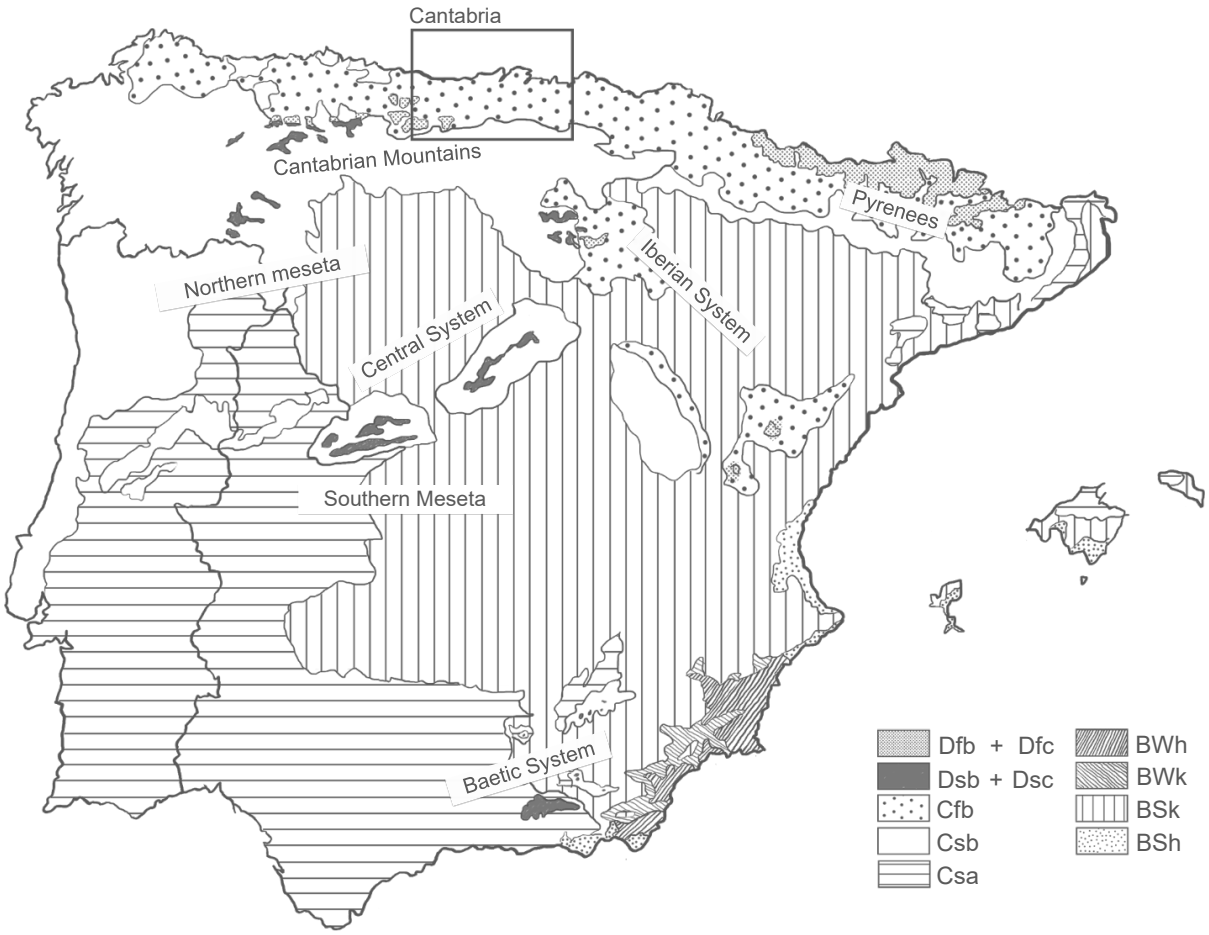

Figure 16: Köppen-Geiger climate classification for the Iberian Peninsula and Balearic Islands

3.2. Mesoclimate

Climate data for the town of Saro, located at 43.266° N and 3.824° W and 237 meters above sea level, in the Cantabrian municipality of the same name, is used to conduct the following regional climate analysis. For this evaluation, as well as for all simulations, Meteonorm is chosen as the data source. Data from the nearest stations is used to obtain interpolated values, which results in a small degree of inaccuracy. Nevertheless, interpolation errors are mostly within the variations of climate from one year to the next (Meteotest, 2017, p. 4).

Saro is located 19 kilometers south of Santander and 20 kilometers north of the border with the province of Burgos, in the transition area between the narrow fringe of lowland stretching parallel to the ocean and the abrupt reliefs of the Cantabrian range (Figures 17 and 18). The town and cattle cabin that are the object of this study are therefore situated in the northern periphery of the Pasiego territory at a relatively low altitude compared to other typical locations where such buildings can be found (see Figure 6, “The Pasiego territory,” p. 14) (García Alonso, 2004, p. 127). Differences in local climate, particularly greater annual and daily thermal amplitudes up in the mountains, but also variations in precipitation levels between different valleys, need to be taken into consideration in the individual renovation planning processes (CROTU, 2019, p. 15).

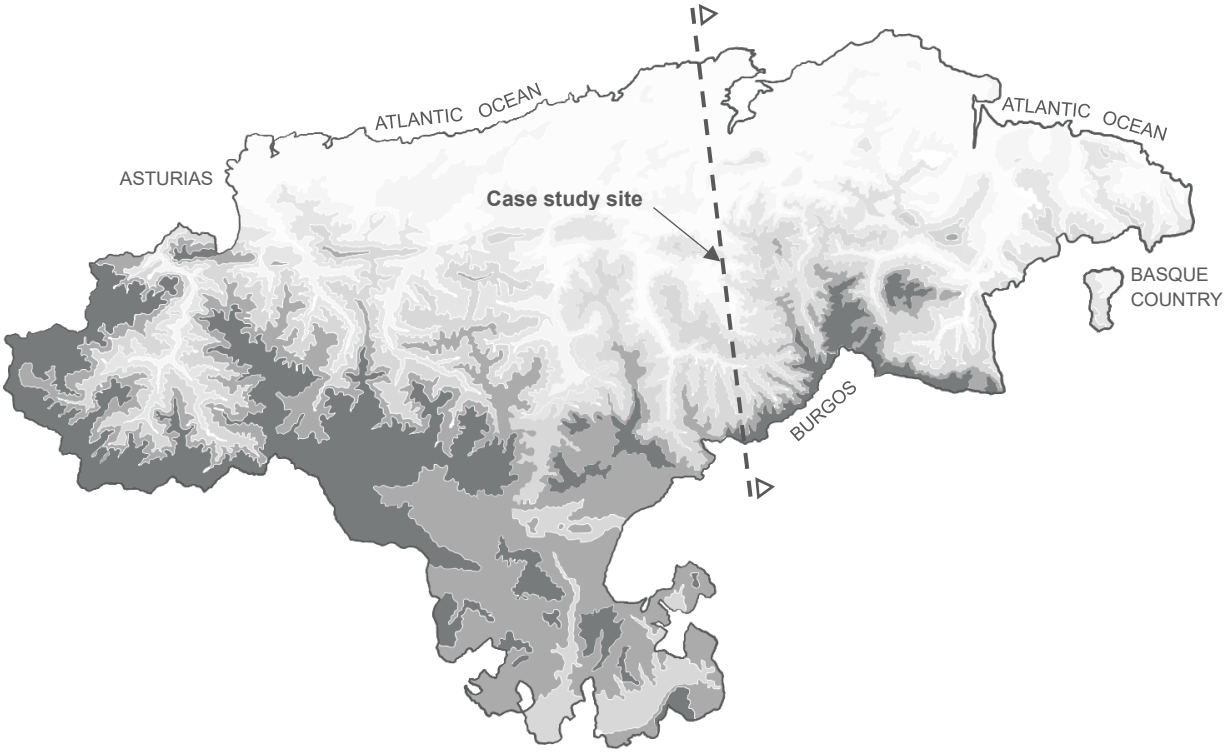

Figure 17: Relief of Cantabria

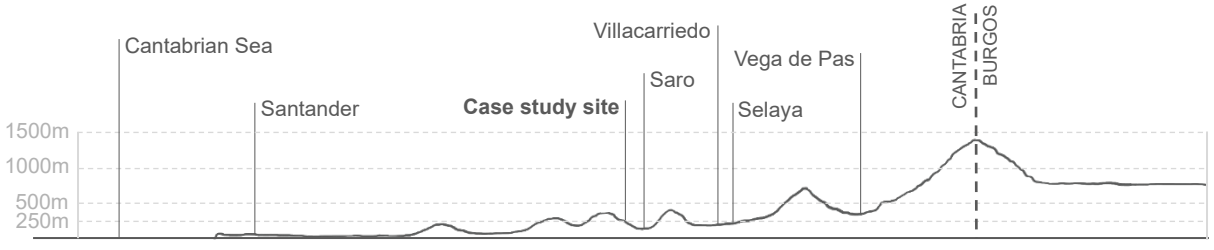

Figure 18: Topographic profile of the Pasiego territory

3.2.1. Solar radiation

Incident solar radiation is a key planning factor since it significantly influences the energy performance of buildings. The amount of solar energy received is primarily determined by the geographical latitude. Variations in day length, the angle of daylight incidence, and the intensity of solar radiation throughout the year become greater at higher latitudes (Hausladen et al., 2012, p. 25). Figure 19 depicts the sun's course across the sky in Saro for a given month.

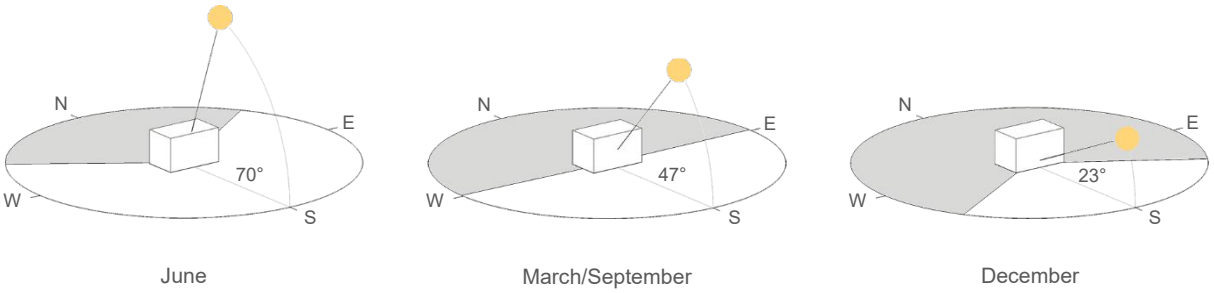

Figure 19: Course of the sun for the 21st of a given month

In summer, the elevation angle of the sun reaches a maximum of 70° on June 21, and days are about six hours longer than in winter (Hoffmann, 2024). Therefore, the highest radiation yields are to be expected during this time of the year, with horizontal surfaces and east and west façades receiving the biggest values of radiation energy. In winter, due to the lower position of the sun, usable solar gains occur primarily on the south façades.

The following graphic (Figure 20) shows the global radiation levels in kWh/m² for each month of the reference year:

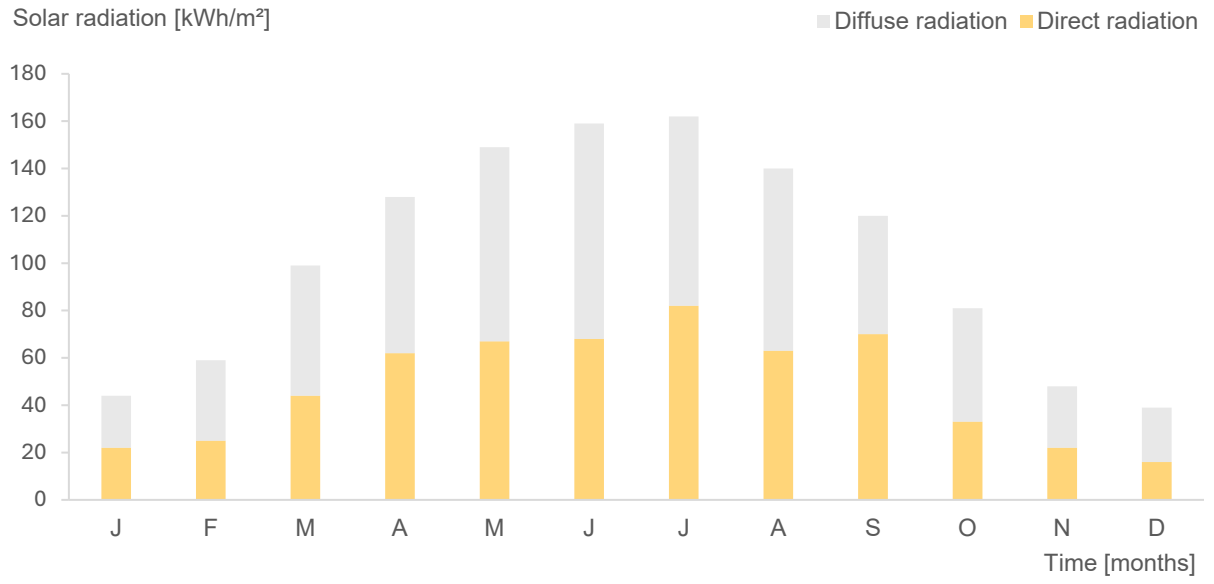

Figure 20: Monthly average solar radiation

Global radiation is the total radiation that falls on a horizontal surface. It is composed of direct solar radiation plus diffuse sky radiation. The global radiation received in Saro amounts to 1,226 kWh/m²a, with noticeably higher rates during the summer months. The fact that precipitation occurs all year round creates a high level of diffuse radiation, resulting in a reduced amount of radiation energy relative to other areas in the same latitude (Annex A1). Averaged throughout the year the proportion of direct (47%) to diffuse (53%) radiation is almost in equilibrium.

3.2.2. Temperature

In a typical year, the annual average temperature is 14.5°C. The coldest months are January and February, with an average of 9.5°C, and temperatures staying just above the freezing point during the coldest hours. This can be seen in Figure 21, where temperature fluctuations are depicted on an hourly basis for the described period. On the warmest day in August, the maximum value of 29.5°C is recorded. During summer, average temperatures oscillate between 18°C and 20°C.

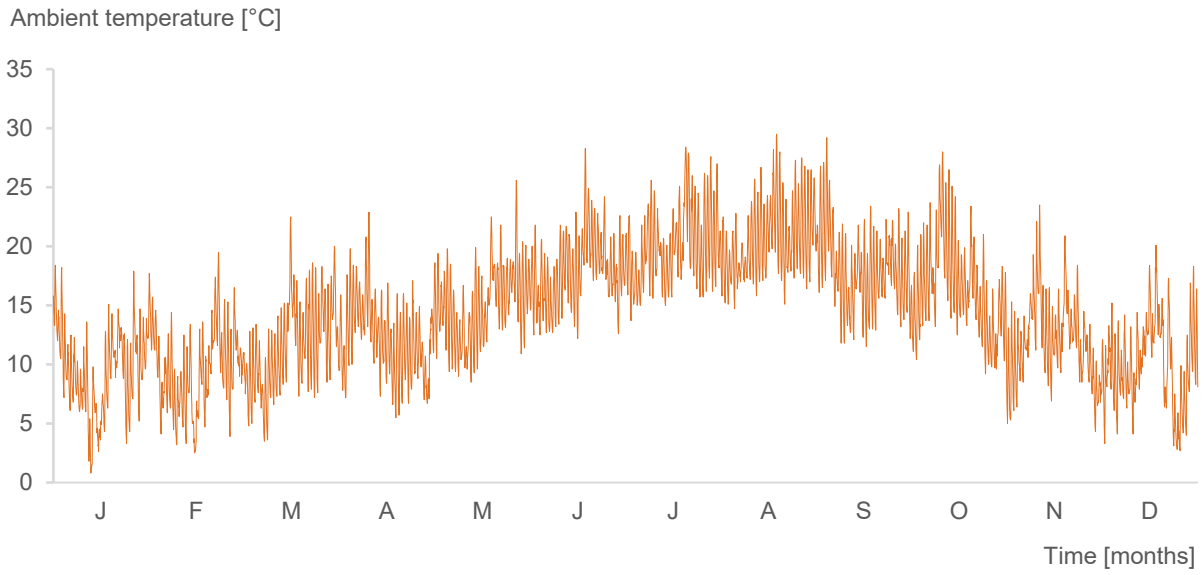

Figure 21: Hourly outside air temperature

The presence of the previously defined maritime climate can be confirmed, although a slightly greater variation in outdoor temperature is noticeable compared to areas closer to the coast (Lautensach, 1969, p. 328). Further analysis of the data indicates that, on the one hand, low requirements are to be expected for summer thermal protection. This is based on the fact that ambient temperatures rise above 26°C for only 114 hours of the year. On the other hand, a total of 4,760 hours with temperatures below 15°C are registered, indicating that heating demand during winter is a critical factor to be considered. The daily thermal amplitude oscillates between 2 and 12 degrees.

3.2.3. Air humidity

Due to the proximity to the ocean, high humidity levels are expected. This is supported by the data set, which reveals average monthly relative humidity levels between 75% and 81%. The determining factor in room climate and the outflow of moisture from indoor spaces is the absolute air humidity level, which, as can be deducted from the psychometric chart below, stays below the upper comfort limit of 12 g/kg most of the time (Figure 22) (Hausladen et al., 2012, p. 16). Only during the month of August do average humidity levels slightly exceed this value (Annex 2), increasing the risk of condensation on colder surfaces inside the building. The removal of moisture from the air through adequate ventilation must therefore be considered in the rehabilitation concept.

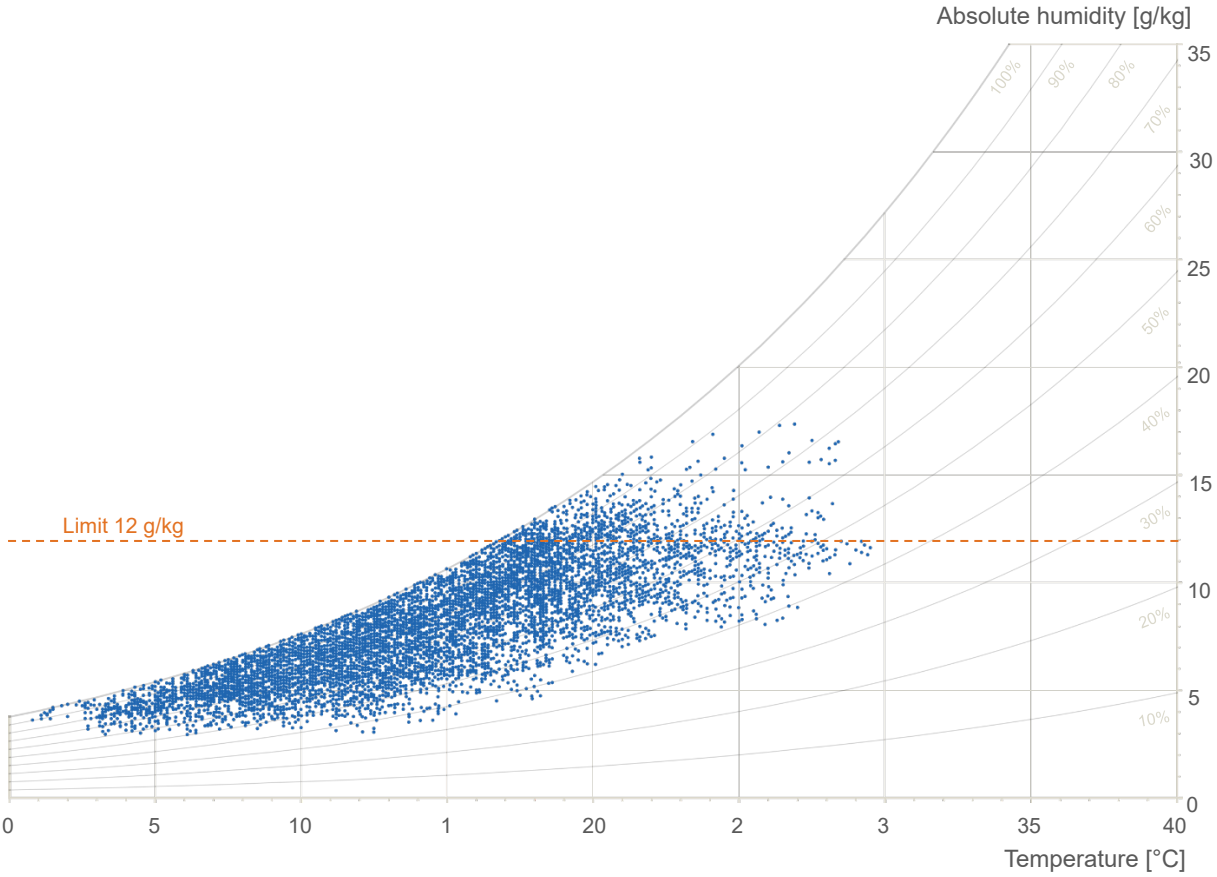

Figure 22: Psychometric chart Saro

3.2.4. Precipitation

Atlantic frontal systems affect the area of study all year round, with the moisture of the ocean getting trapped by the mountains. The amount of rain ranges between 1,100 and 1,300 mm on the coast of Cantabria, while it can exceed 2,200 mm in the inner mountains, where snowfall is also common during the winter (Lautensach, 1969, pp. 327–329).

Figure 23 confirms that abundant precipitation is expected year-round in Saro. At the same time a reduction in rainfall can be observed in summer, with July being the driest month.

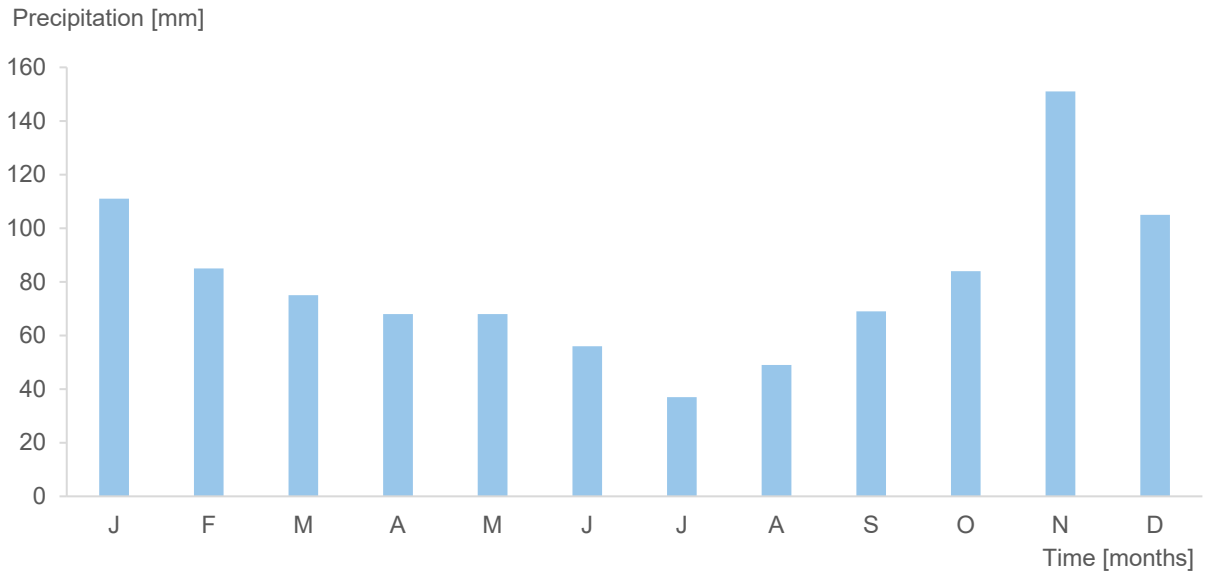

Figure 23: Monthly average rainfall

When characterizing rainfall patterns, it is important to consider both the annual average rainfall and its seasonal distribution throughout the year. It is therefore necessary to examine the average number of days per year in which precipitation exceeds several thresholds (AEMET et al., 2011, p. 55). Figure 24 shows the number of days with precipitation equal to or greater than 1 mm, 10 mm, and 30 mm for a given month.

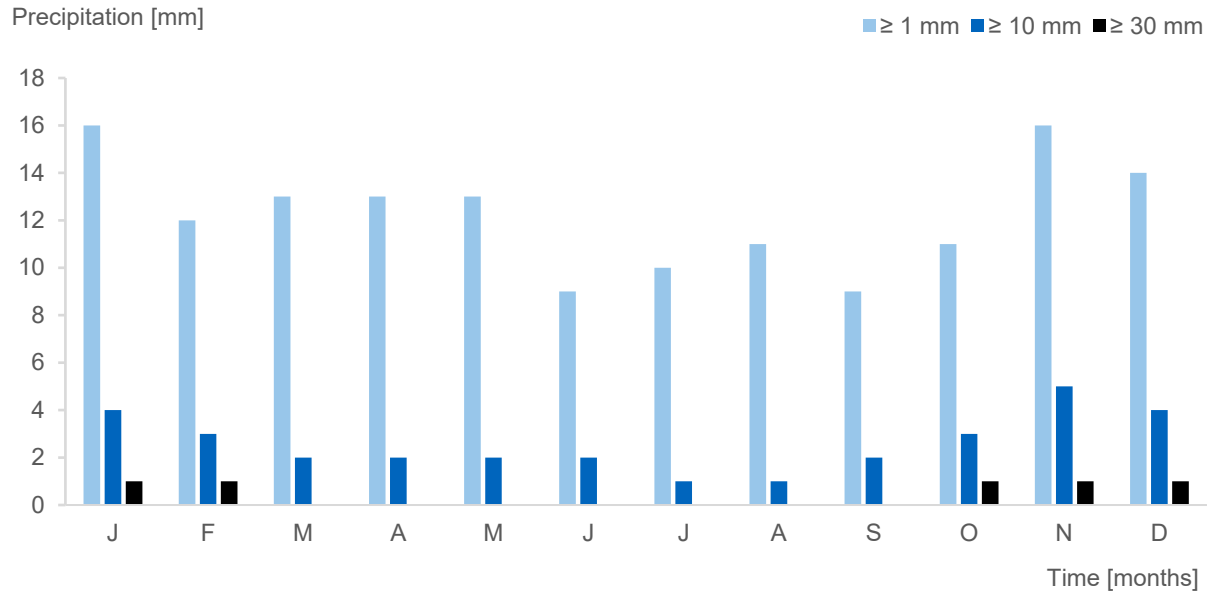

Figure 24: Monthly number of days with precipitation above 1 mm, 10 mm, and 30 mm

The monthly average number of days with precipitation equal to or greater than 1 mm is 12, with values fluctuating between 16 days in January and November and 9 days in June and September.

A greater frequency of daily heavy or intense precipitation can be observed during the winter months. In November, a single day registered 46 mm of rainfall in just a few hours, which also explains the notable spike in the previous graph. Cloudburst events like this are most common in fall and make it essential to plan protective measures for flood prevention and wind-driven rain (Lautensach, 1969, p. 328).

3.2.5. Wind

Atmospheric motion related to two centers of action (the Icelandic Low cyclone and the Azores High anticyclone) is the driving force of the Cantabrian wind regime. The complex situation is further shaped by geographical factors such as relief and the proximity to the sea (Giménez & Álvarez, 2016, p. 11).

An analysis of the dominant wind directions for the location Saro reveals a clear seasonality for winds blowing from the south and southwest, reaching notably higher frequencies in winter (Figure 25, left). This wind is named Surrada by the locals and speeds down the mountains, bringing sudden increases in temperature thanks to the Föhn effect (Giménez & Álvarez, 2016, p. 14). It is also usually the prelude to an abrupt change in weather causing most of the monthly precipitation, which in winter is associated with frequent Atlantic storms and frontal systems over the north of the peninsula. With the arrival of spring, modifications in atmospheric circulation cause these winds to practically disappear, and, due to the thermal contrast between land and sea, maritime breezes from the northeast become predominant (Figure 15, right) (Fernández García & Rasilla, 1992, pp. 277–280) (Murioz, 2005, pp. 214–217).

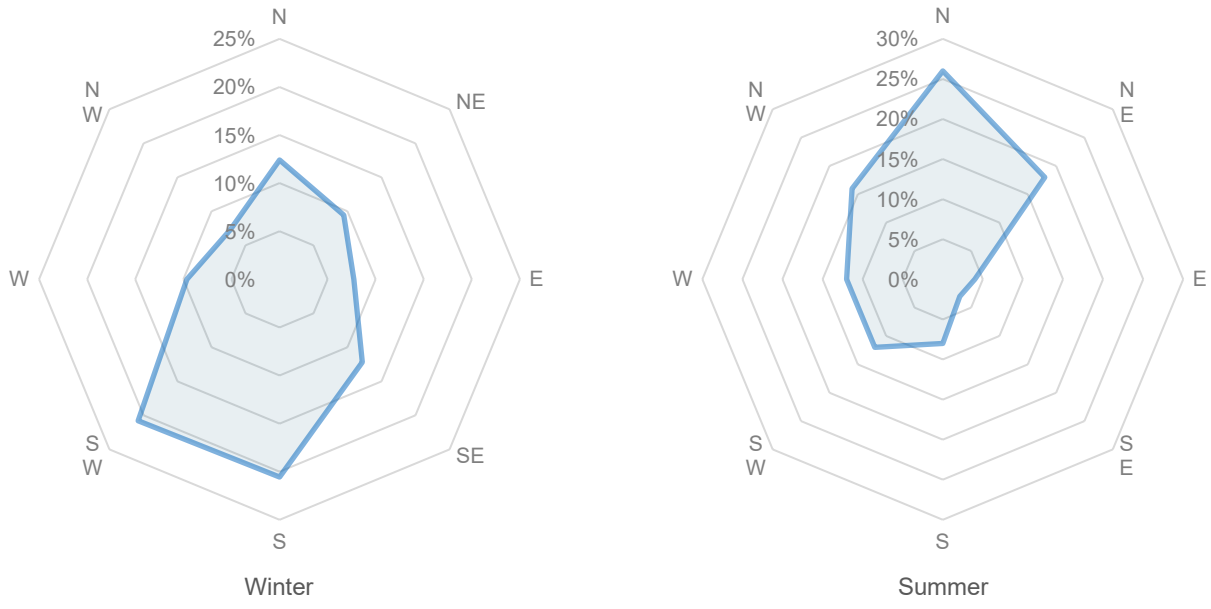

Figure 25*:* Directional distribution of the wind depending on the time of the year

Figure 26 shows the general wind direction and speed for the sampling period. Light to gentle breezes with wind speeds up to 5.5 m/s are the most common. Stronger winds, with speeds up to 11 m/s (and in some cases over 15m/s), are recorded for 664 hours of the year. The wind is almost never calm in Saro.

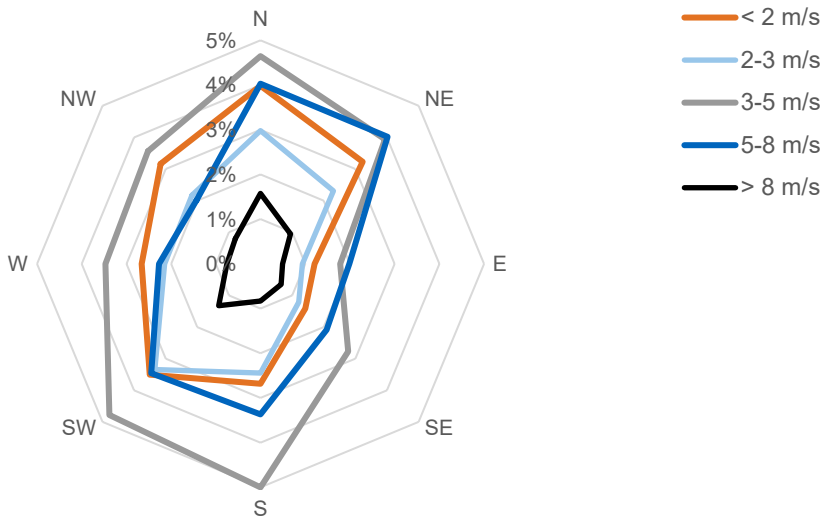

Figure 26: Wind speeds and overall directional distribution

The results of the wind analysis make it essential to plan protective measures against wind-driven rain. Moreover, the building concept should provide a sufficiently windtight construction to minimize infiltration energy losses via the external walls and roof and avoid uncomfortable drafts in indoor spaces. On a positive note, the moderate wind speeds can be useful for natural ventilation (Hausladen et al., 2012, p. 142).

The above information and conclusions are based on meteorological data and can therefore paint only a generalized picture of the onsite wind situation (Hausladen et al., 2012, p. 16). For this reason, a more detailed evaluation of the influence of topography, surrounding buildings, and vegetation is presented in the next chapter.

To summarize, the climate of the Pasiego valleys can be characterized as wet and temperate, with mild winters and cool summers closer to the coast and greater temperature variations in the inner valleys and mountains.

3.3. Microclimate

Having described the large-scale climatic conditions in the previous section, the focus now shifts to a smaller unit of space. This “zooming in” enables an exploration of the site’s immediate surroundings, which can significantly impact the local climate (Hausladen et al., 2012, pp. 12, 16).

The property chosen for the case study is located on a south-facing slope, nestled between green meadows and remnants of native forests, in the hilly territory of the Llerana river basin. Figure 27 shows the cabin in the center of a uniquely shaped plot of land and a few neighboring buildings. The drawing also illustrates topographic contour lines and existing trees. To the north and extending to the northwest and northeast boundaries of the plot, a steep hillside covered in dense forest blocks the wind. This sheltering effect leads to higher perceived temperatures on the site's central plane, especially during summer (Fredo, personal communication, January 2024). The south-facing orientation of the slope amplifies this condition as there is virtually no shading by surrounding obstacles, except for one tree. Consequently, the construction is exposed to intense winds from the southwest (3rd quadrant) during the winter months and transitional periods.

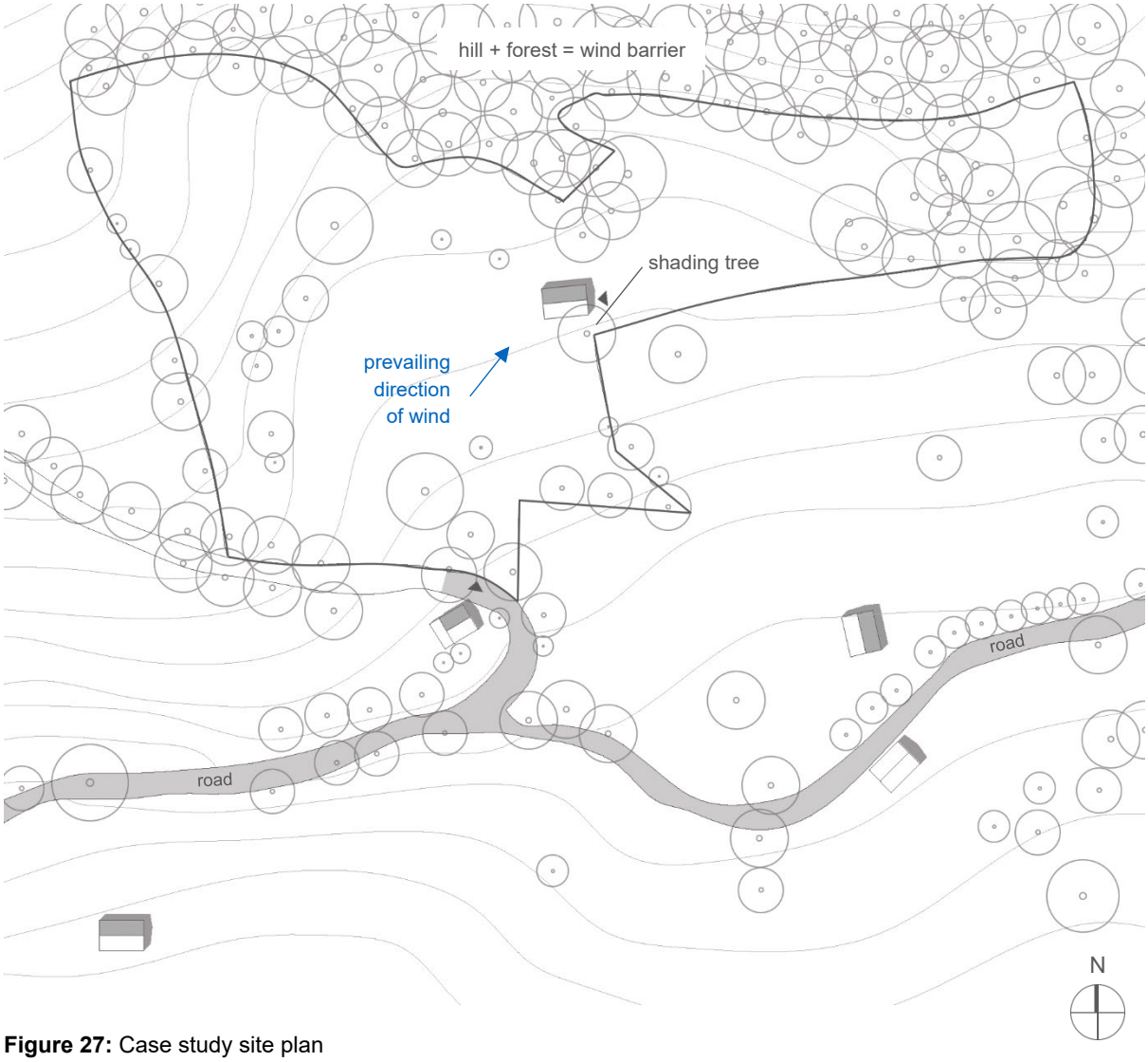

Figure 27: Case study site plan

4. Retrofit thermal insulation

Based on the foregoing analyses of both vernacular architecture and the unique climatic conditions of the Pasiego valleys, it becomes clear that the rehabilitation concept for the cabin located in Saro must fulfill a variety of tasks. While its heritage value must be protected in accordance with the guidelines discussed, the building must also be modified to allow for long-term use. At the same time, environmental sustainability should be ensured by using mostly biodegradable or recyclable construction materials for the renovation. The examination of the outdoor climate revealed that emphasis needs to be placed on the provision of heating during the winter months. To reduce heat losses and achieve high degrees of energy efficiency, good thermal protection is required. Changes to the external surface of the *cabaña pasiega* are not permitted due to conservation requirements. For this reason, the attachment of an internal insulation layer is the only alternative.

With the aim of designing an effective and long-lasting internal insulation system, this chapter begins with a brief assessment of the case study's building structure. Once the current condition of the cabin has been recorded, the target level of insulation is defined (Scheffler, 2016, p. 53). Then, following a discussion about the suitability of various insulation systems and materials, a final wall assembly is selected and evaluated in terms of its hygrothermal performance.

4.1. Assessment of existing structure

As described in the microclimate analysis, the case study building is located on a south-facing hillside. To the north, topography and vegetation provide a sheltering effect against the high levels of rainfall expected in the region. Rain will also rarely reach the short access façade. This is mainly because winds blowing from the east are uncommon, but also because the original structure has a roof overhang that protects the entrance. The north and south façades are somewhat protected from water dripping down the walls by short wooden eaves with exposed rafter tails. Almost no constructive protection measures against wind-driven rain can be found on the façade facing west.

The exterior walls of the cabin are assembled in uncoursed rubble masonry. The stones employed are very irregular in shape and size and the type is, based on visual on-site evaluation, estimated to be mostly sandstone. Larger and roughly square stone blocks are employed at quoins and jambs to increase the strength of the wall. On the exterior surface, especially on the north and east façades, traces of a white-colored plastering can be found. The west façade appears completely washed out, underlying the premise of a greater exposure to wind-driven rain. Indices of recent pointing and cleaning of the stones can be seen on the south-facing surface, particularly towards its western edge.

Inside, the surface of the masonry has been left uncovered, showing wooden elements, such as lintels and beams, laying longitudinally inside the stonework. In addition, the wooden beam ends from the main structure and joists from the intermediate floor are embedded in the load-bearing wall.

Figure 28 depicts the cabin and surrounding landscape. The first two shots were taken in 2023 at the end of September, and the third one at the beginning of January. The images show the damage caused by a fallen tree branch to the northern part of the roof overhang, as well as the poor condition of the exterior staircase. A large chestnut tree standing on the southeast corner of the building (on the left side of the first image) provides shade during the summer. The short west-facing façade is well exposed to the elements, as evidenced by the last two photographs.

Figure 28: Case study building

4.2. Determination of insulation standard

As previously stated, this *cabaña pasiega* is suited to be converted for permanent residential purposes. The installation of thermal insulation aims to improve thermal comfort while reducing heating energy demand. For the subsequent parts of this study, the level of insulation to be achieved is set to meet the Documento Básico HE Ahorro de energía [Basic Document on Energy Conservation] [DB-HE] of the Spanish Código Técnico de la Edificación [Technical Building Code], which regulates the energy use and demand of buildings. The document proposes a zoning of energy demand according to defined climatic zones. For buildings located in Cantabria at altitudes between 200 and 600 meters, a minimum U-value of 0.41 W/m²K is required for walls in contact with outside air (DB-HE, 2022, pp. 16, 46).

To determine the necessary level of insulation, first, the U-value of the existing construction must be known. The wall's thickness was measured on site and is roughly 70 to 75 cm. Because insufficient information about its physical properties is available at the time of this evaluation, a thermal conductivity of 2.3 W/mK is estimated using the standard DIN EN ISO 10456 (value for sandstone). Assuming a wall thickness of 70 cm, this results in a thermal transmittance or U-value of 2.11 W/m²K for the existing wall.

4.3. Selection of internal insulation system

The primary function of an insulating layer is to limit heat transmission through the building envelope. If there is a temperature difference between inside and outside, heat flows from warm to cold and a temperature profile is created across the wall. When internal insulation is

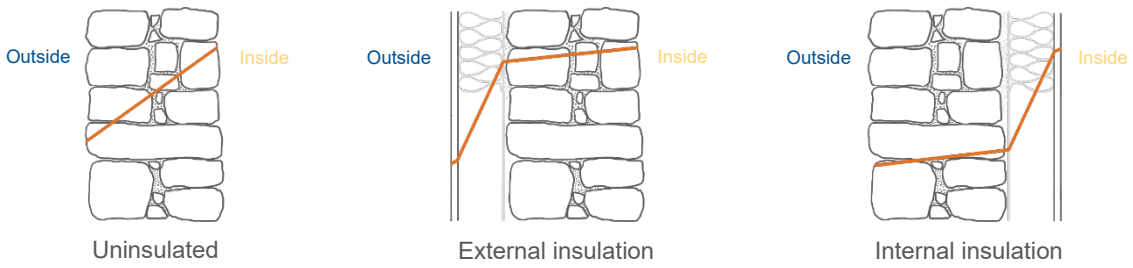

Figure 29: Comparison of possible wall assemblies in terms of thermal insulation with schematic temperature profile in winter

added retroactively, the layer that primarily restricts the heat flow is on the inside of the wall. As shown in Figure 29, this leads to a cooling down of the wall in winter (Scheffler, 2016, p. 11). Due to the relationship between temperature and relative humidity, temperature differences also act as a driving force for water vapor transport. This occurs in the same direction that heat flows. To avoid moisture damage caused by condensation on the colder inner face of the masonry wall, water vapor diffusion must either be effectively reduced by attaching a vapor barrier to the inside of the insulation or absorbed by the insulation system (Scheffler, 2016, p. 13).

Water does not only enter the wall from the inside as water vapor, but it can also enter from the outer surface and be transported inside via capillary forces. In this context, the main

consideration is that the resulting moisture can dry off and does not accumulate over time (Fachverband Innendämmung, 2016, p. 53). Figure 30 shows that while vapor-inhibiting and vapor-retarding insulation systems limit the vapor diffusion flow from the indoor climate into the wall, they also lower the drying-out potential of moisture towards the interior.

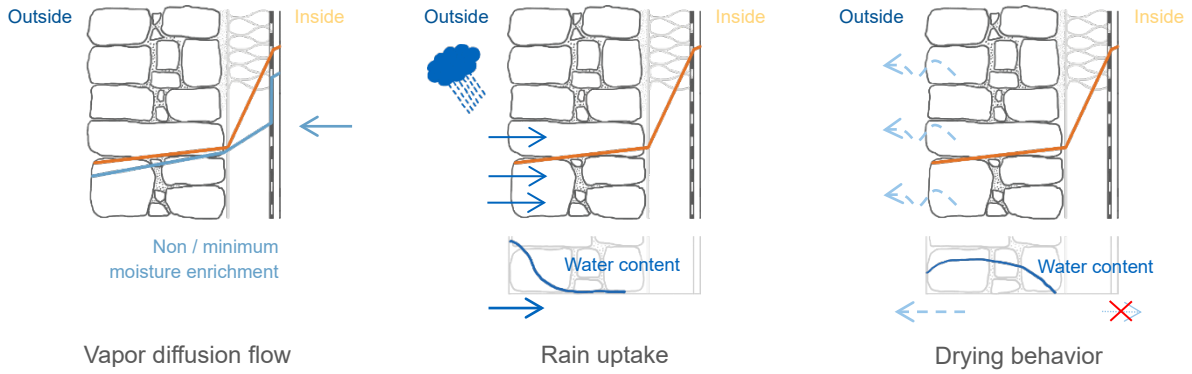

Figure 30: How vapor-retarding interior insulation works

As an alternative, it is possible to use insulating materials that can absorb large quantities of water vapor and, above a certain moisture level, release it in liquid form to the interior (Figure 31). These vapor-permeable, capillary-active insulation systems have a greater fault tolerance for vapor diffusion and thus can often be installed more easily (Scheffler, 2016, p. 19). With such a solution, it is critical that moisture be dissipated through normal air exchange in the interior (Hegger et al., 2008, p. 88).

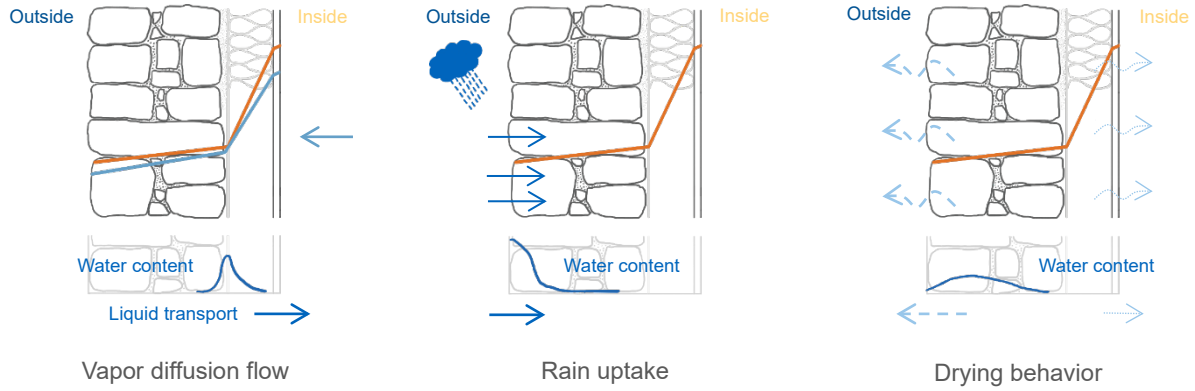

Figure 31: How vapor-permeable, capillary-active interior insulation works

Based on the climate analysis, a large amount of wind-driven rain must be considered in the rehabilitation concept. Due to the exposed state of the masonry and the inability to install rain gutters, water entry from the outside cannot be safely ruled out. Thus, insulation systems that maintain a certain level of drying potential to the inside, i.e., vapor-permeable and capillary-active materials, should be used.

4.4. Choice of insulation materials

Condensate-tolerant interior insulation systems can be further classified according to their mechanical properties. Rigid insulation boards that are fitted to the wall and covered with vapor-open plastering are available in a wide range of materials. Alternatively, insulating plasters or renders can be used (Arbeiter, 2014, p. 73). When selecting an interior insulation system, the nature and condition of the substrate are often decisive criteria (Fachverband Innendämmung, 2016, p. 140). To mitigate the risk of condensation inside the wall, convective moisture entry must be prevented by ensuring an airtight connection between layers (Scheffler, 2016, p. 19). While rigid boards require an even basis to guarantee a full-surface bonding, plastic materials create a seamless and homogeneous layer that allows for the leveling out of bumps and irregularities (Arbeiter, 2014, p. 73). Given that the inner face of the evaluated wall is rough and uneven, the use of a malleable material is convenient.

In agreement with ecological construction practices, the proposed renovation concept seeks to avoid environmentally harmful materials such as plasters containing synthetic additives or products that have energy-intensive manufacturing processes. Ideally, the insulation of the case study building should be addressed with locally available materials that have a low carbon footprint and are either biodegradable or recyclable. Loam-based insulating materials are especially well-suited to all the above requirements and have several advantages in comparison to common industrial alternatives. Loam can absorb and desorb humidity to a great extent, enabling it to balance the indoor climate. Thanks to its high capillarity, it helps conserve the timber elements that remain in contact with it by keeping them dry. From an ecological point of view, loam has the benefit of requiring little energy during its production process, especially if clayey soil is found on the construction site, in which case loam produces virtually no environmental pollution. Lastly, if it is unbaked, this material can be recycled an indefinite number of times or returned to nature (Minke, 2009, pp. 13–17).

To enhance the thermal insulation of loam, porous plant-based substances or mineral particles are added. Loam with aggregates is termed lightweight loam if its dry-state density is less than 1200 kg/m³ (Minke, 2009, p. 48). Mineral aggregates include pumice, expanded clay, glass, and perlite. Organic additives include straw, expanded cork, sawdust, or wood shavings, among others (Minke, 2009, p. 49f.). Except for cork, these latter additives have certain disadvantages when implemented wet, due to their sensitivity to moisture. Especially in moderate or humid climates, fungal growth can occur after just a few days (Pilz et al., 2012, p. 46).

To be on the safe side in terms of mold growth, a mixture containing expanded clay aggregate is chosen. The thermal insulation properties of the mixture depend mainly on its density, which is affected by the grain size distribution of the expanded clay (Minke, 2009, p. 50). According to DIN 4108-4, which lists hygrothermal design values for building materials, mixtures with a density of 600 kg/m3 have a thermal conductivity of 0.17 W/mK. This means that a 33 cm thick insulating layer is needed to achieve the required U-value of 0.41 W/m²K. A lightweight loam layer with a density of 700 kg/m3 would need to be 41 cm thick to meet this requirement (DIN 4108-4, n.d., p. 22). This solution is therefore considered problematic due to the loss of space and the prolonged drying times associated with the initial moisture content.

A viable alternative is to level the surface of the wall with lightweight loam and then add permeable insulation boards. Figure 32 depicts an assembly in which the specified level of

insulation is achieved by applying a 6 cm thick lightweight loam layer and a 6 cm layer of wood fiber insulation. Other renewable and biodegradable options include boards made of expanded cork, hemp, or reed. The latter is the best choice from an environmental standpoint, but its thermal conductivity of 0.055 W/mK is slightly higher than that of other insulation materials (Fachverband Innendämmung, 2016, p. 156). Due to the problems related to space loss, the wood fiber variant is selected and set as the basis for upcoming evaluations.

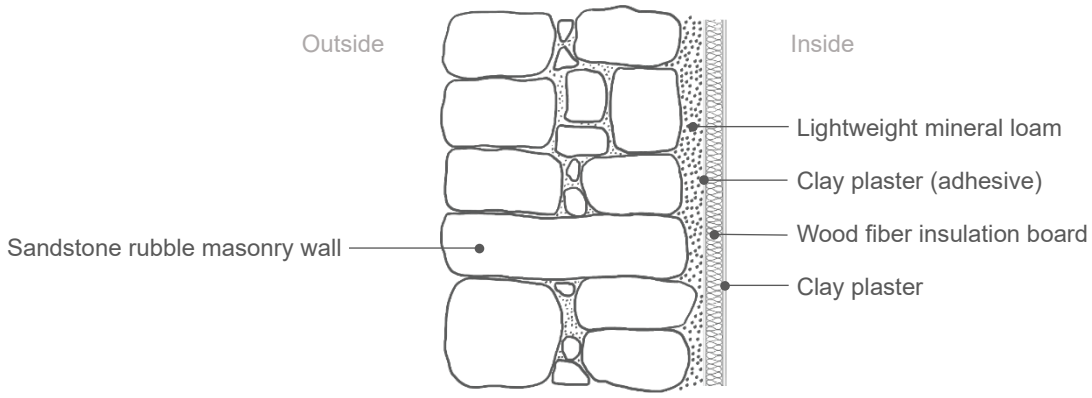

Figure 32: Wall assembly

4.5. Hydrothermal assessment

When selecting an interior insulation system, it is critical to evaluate the impact of heat and moisture processes to avoid damage to the building envelope. According to the German standard DIN 4108-3 and WTA 6-4, the hygrothermal performance must be – except for minor thermal improvements – assessed using either the simplified Glaser method or computer simulations. The Glaser method assesses the risk of interstitial condensation in steady-state conditions. Moisture storage and liquid transport through capillary suction are not considered. This method is thus unsuitable for evaluating insulations with capillary-active properties or for situations in which additional moisture sources from wind-driven rain cannot be ruled out (Scheffler, 2016, p. 87). Based on foregoing considerations, the risk of moisture damage in the present case study must therefore be assessed by numerical simulation.

4.5.1. Simulation setup

Wufi Pro, a software developed by the Fraunhofer Institute for Building Physics, is used to develop a model of the wall under investigation. Since precise knowledge of material characteristics is necessary to obtain realistic results in hygrothermal component simulation, all materials modeled are sourced from the MASEA- and Fraunhofer-IBP databases. These databases are readily available in the WUFI program and contain typical data for common materials. While they are thus primarily suitable for use in standard cases, it is also possible to carry out sensitivity analyses in cases where specific material properties are unknown (Schmidt, 2002, p. 130).

Because the material parameters of the existing wall are unavailable at the point of this study, simulations are run with three different sandstones representing the range of those available in the database. Table 1 summarizes their properties. Further information regarding their hygrothermal functions can be found at the end of this document (Annexes A4, A5, and A6).

Sandstone type	Density **ρ** [kg/m³]	Porosity [m³/m³]	Diffusion resistance factor **μ** [-]	Sorption **u80** [kg/m³]	Free water saturation **uf** [kg/m³]	Water absorption coefficient **w** [kg/m² √h]
Bad Bentheim	1933	0.27	10.5	1.5	147	40.1
Baumberger	1980	0.23	20.0	35.6	210	2.64
Zeitzer	2300	0.05	70.0	8.5	40	0.15

Table 1: Material properties of the sandstones used in the WUFI Pro model

The Bad Bentheim sandstone has the lowest moisture storage capacity but the highest water absorption- and liquid transport coefficients of the three types modeled. The Baumberger pore system accumulates the most water molecules until the equilibrium moisture corresponding to the humidity of the ambient air is reached (WUFI-wiki, 2013). Both have a lower diffusion resistance factor than the denser Zeitzer sandstone.

As it is impossible to represent the rubble masonry in WUFI Pro, a simplified model of homogenous stonework is assumed. All simulations are carried out using the Meteonorm climate file for Saro and the wall is set to be facing north since this façade receives less solar radiation and corresponds with the prevailing direction of wind-driven rain. The adhering fraction of rain is set to 70%, based on the inclination and type of wall. Microclimatic influences like topographic wind-sheltering effects and roof overhangs are therefore disregarded. Further information concerning the simulation settings can be found in Annex A3.

Running simulations of the masonry wall in its pre-renovation condition until equilibrium moisture is reached provides an estimate of the three sandstones' initial water content. Since the building is currently uninhabited and has no windows, the indoor climate is considered equivalent to the outdoor boundary conditions. When this type of climatic arrangement is chosen, WUFI automatically turns off driving rain and solar radiation for the right (indoor) side of the construction. Table 2 shows the resulting average moisture content values for the three sandstones at steady state.

Sandstone type	Bad Bentheim	Baumberger	Zeitzer
Initial water content [kg/m³]	12.5	43	7.8

Table 2: Initial water content of the three sandstones

The initial condition of the materials comprising the insulation system is assumed to be constant across all layers at 80% relative humidity and a starting temperature of 20°C. As their hygric material properties are unknown at the point of this analysis, similar materials are chosen from the WUFI database. Their relevant parameters and sources are listed in Table 3 and Annexes A7, A8, and A9.

Material	Density **ρ** [kg/m³]	Porosity [m³/m³]	Thermal conductivity **λ** [W/mK]	Diffusion resistance factor **μ** [-]	Sorption **u80** [kg/m³]	Free water saturation **uf** [kg/m³]
Lightweight loam (Exp. Clay - MASEA)	719	0.67	0.119	7	17	97
Loam plaster (Clay Rend. - MASEA)	1514	0.42	0.65	11.3	18.8	294
Wood fiber board (Fraunhofer-IBP)	140	0.91	0.039	3	21	350

Table 3: Relevant parameters of the insulation materials used in the simulation

As there is no lightweight loam material available in WUFI, a comparative test simulation is run by adjusting the values of “Expanded Clay” to match the material “Blähtonlehm 1” from the MASEA database available online (MASEA, n.d.). However, results were found to deviate only slightly between the two variants. Because not all values of “Blähtonlehm 1” are known, simulations are therefore run with “Expanded Clay.”

To accurately evaluate the construction, both the initial behavior and the hygrothermal conditions during dynamic equilibrium are analyzed. For this reason, simulations are run until there aren’t any changes in moisture content from one year to the next. Because the Baumberger sandstone’s high sorption capacity results in significant hygric inertia, simulations to determine the sandstones’ initial moisture content are run for a 15-year period. Once the water content of the existing wall is known, a five-year period is defined for all calculations. For the indoor climate, the option in accordance with the standard EN 15026 is selected.

Figure 33 depicts the WUFI Pro model of the insulated wall. The thickness of the layers corresponding to the insulation system is set according to the assembly defined under “Choice of insulation materials” (p. 35f.). Aside from the monitor positions that are automatically assigned to the inner and outer surfaces, three additional positions are inserted at critical points inside the construction: one at the leftmost grid element of the wood fiber, one at the leftmost grid element of the mineral lightweight loam layer, and a third one at a depth of approximately 60 cm within the existing wall. For each monitor position, the courses of relative humidity and temperature are output after simulation, which allows for a quick evaluation of their hygrothermal conditions.

For a better assessment of the post-renovation scenario, the wall component is simulated both with and without insulation for the three sandstone variants. Once all calculations are completed, the results are analyzed using WUFIGraph and Microsoft Excel.

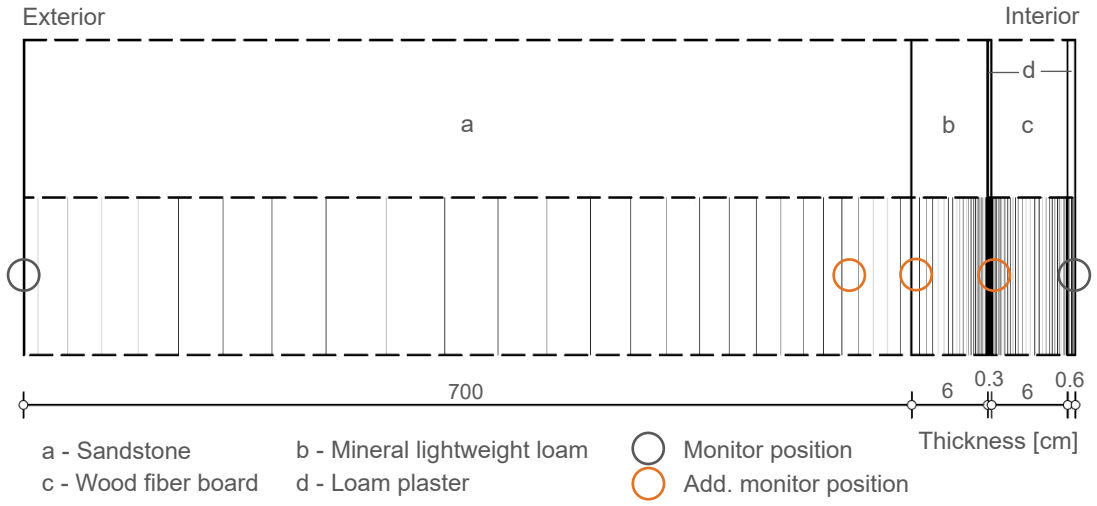

Figure 33: Component assembly of the insulated wall as modeled in WUFI Pro

4.5.2. Evaluation of results

Figure 34 shows the water content at equilibrium state for each of the three sandstones considered in the evaluation. The Baumberger sandstone contains more water than its counterparts. Notable is also the difference in moisture load fluctuations: while the water content inside the Zeitzer stone remains constant throughout the year, it varies to a much greater degree in the Bad Bentheim type.

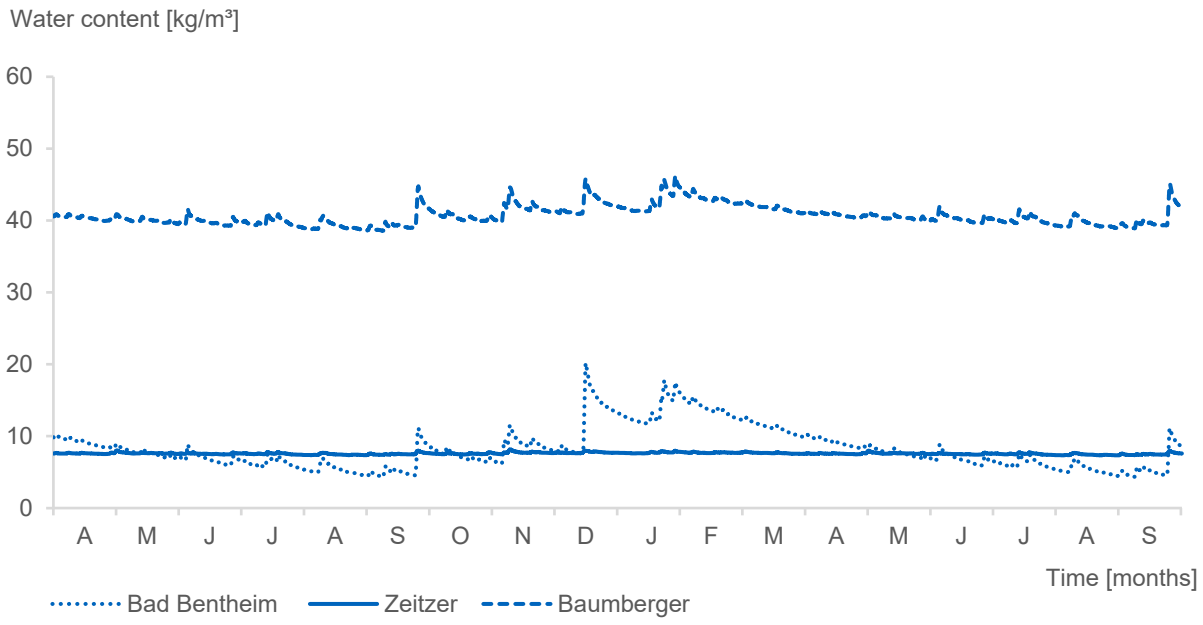

Figure 34: Overall sandstone water content in uninhabited condition (daily average)

Once the initial moisture content of the three sandstones has been determined, a qualitative evaluation of the moisture balance within the insulated wall is undertaken. Figure 35 shows the total water content of the wall over a five-year period. The blue lines represent the initial uninhabited state of the construction. The orange lines represent the insulated variant, while the grey lines depict how the moisture content would change if the building were adapted for residential use without insulation.

The diagram shows that, for all three stone types, the uninsulated wall would dry out if the building were inhabited. Retrofit thermal insulation, however, affects the water content of the walls differently for each type of sandstone masonry. While the Baumberger (B) wall continues to dry out compared to its initial state, the Zeitzer (Z) variant exhibits a higher overall moisture content and slightly greater seasonal fluctuations. The addition of internal insulation to the Bad Bentheim (BB) wall allows moisture accumulated during the winter season to dry out more slowly and to a lesser extent during the summer. In either case, no continuous moistening of the structure can be observed.

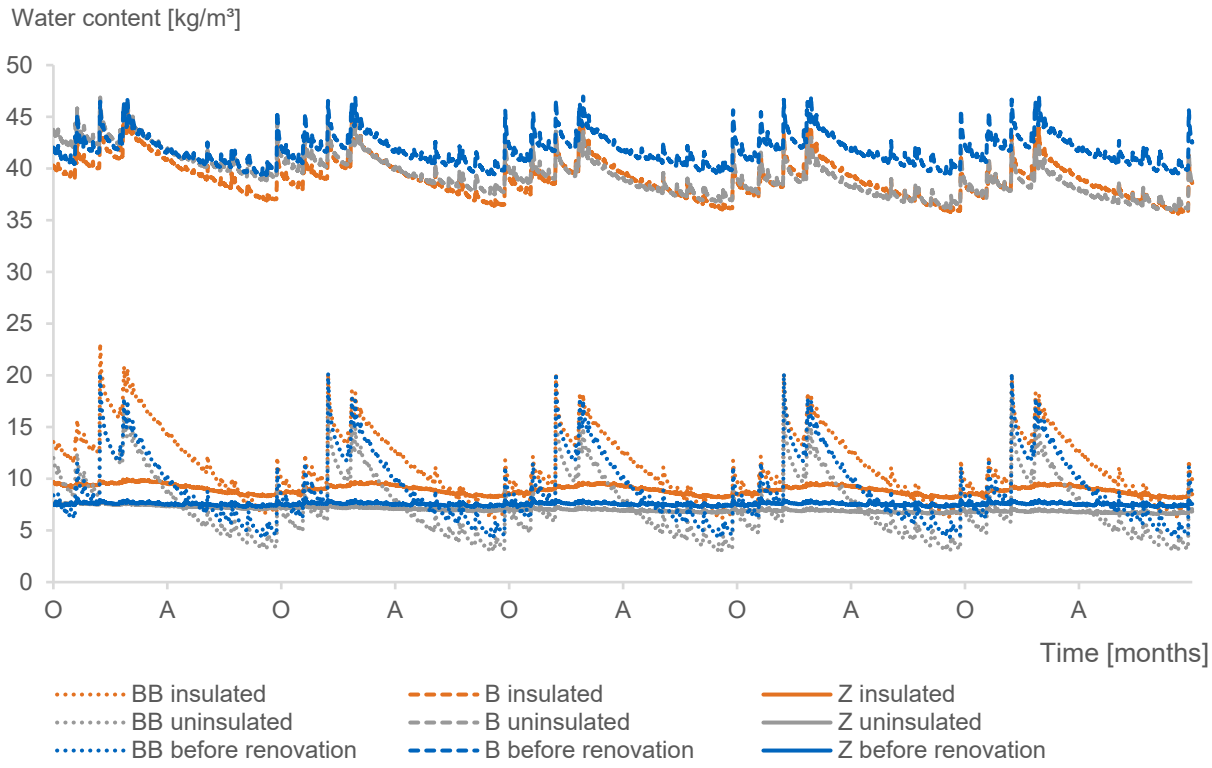

Figure 35: Total water content of the wall, with and without insulation (daily average)

In accordance with the planning guide WTA 6-5, achieving a steady state is the first requirement that needs to be met when verifying the functionality of an interior insulation system. In a further step, the maximum water content of the individual component layers must be assessed so that long-term moisture damage can be ruled out.

First, the interior surface of the component must be analyzed in terms of the risk of mold growth. For the construction to be regarded as safe, mold growth on its interior surface must

be excluded (WTA Guideline 6-5, 2014, p. 7). This is assessed by studying WUFI's quick graphics for the relevant monitor position. The diagram "Mon. Pos. Isopleths" plots the relative humidity against the simultaneous temperature and contains limit isopleths that represent the minimum growth requirements for the usual nutrient supply on building materials (limit curves LIM B I and LIM B II) (Fraunhofer IBP, 2024, p. 8). In the investigated case, conditions continuously stay below the limiting isopleths for all three sandstone variants (Annex A10). Hence, at normal indoor moisture loads, the interior surface is considered risk-free in terms of mold growth. A comparative analysis of the uninsulated wall results in slightly higher values but can also be regarded as being on the safe side and no further investigations are required.

Second, critical conditions inside moisture-sensitive materials must be identified. Wood-based materials such as the modeled wood fiber insulation are subject to the risk of rot if critical water contents are surpassed. The norm states that the mass-related water content of such materials must not exceed 18.-% (WTA Guideline 6-8, 2014, p. 10). Figure 36 shows the daily average moisture content of the modeled wood fiber board, measured across the entire layer.

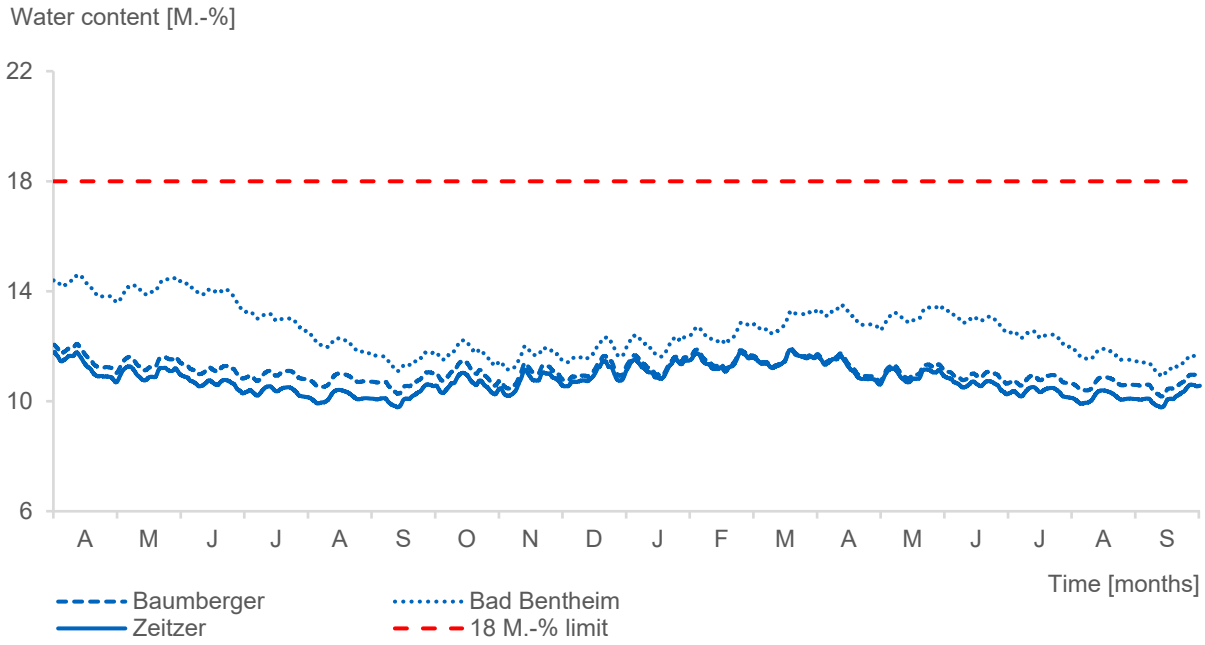

Figure 36: Overall moisture content of the wood fiber insulation (daily average)

All three evaluated variants stay below the limiting value, even during the first year. It is worth noting, however, that the Bad Bentheim stone allows for more water hitting the outer face of the wall to pass into the wood fiber.

In a further step, the hygrothermal conditions at critical points inside the insulation system are investigated. Because of the higher relative humidity values, the cold side of internal thermal insulation is defined as being most at risk of interstitial condensation (Scheffler, 2016, p. 18) (Fachverband Innendämmung, 2016, p. 50). Running the WUFI film for the three variants reveals that the humidity level at the interface between the masonry and insulation never hits 100%. However, hygroscopic materials can have a significant moisture content even without the occurrence of "condensation" in the Glaser sense (Scheffler, 2016, p. 18) (Krus & Rösler,

2011, p. 142). To determine the resulting water content, which can vary greatly within a layer, a 1 mm thick sub-layer in which the highest moisture content occurs is evaluated. This is done both for the wood fiber board (Figure 37) and the mineral lightweight loam layer (Figure 38).

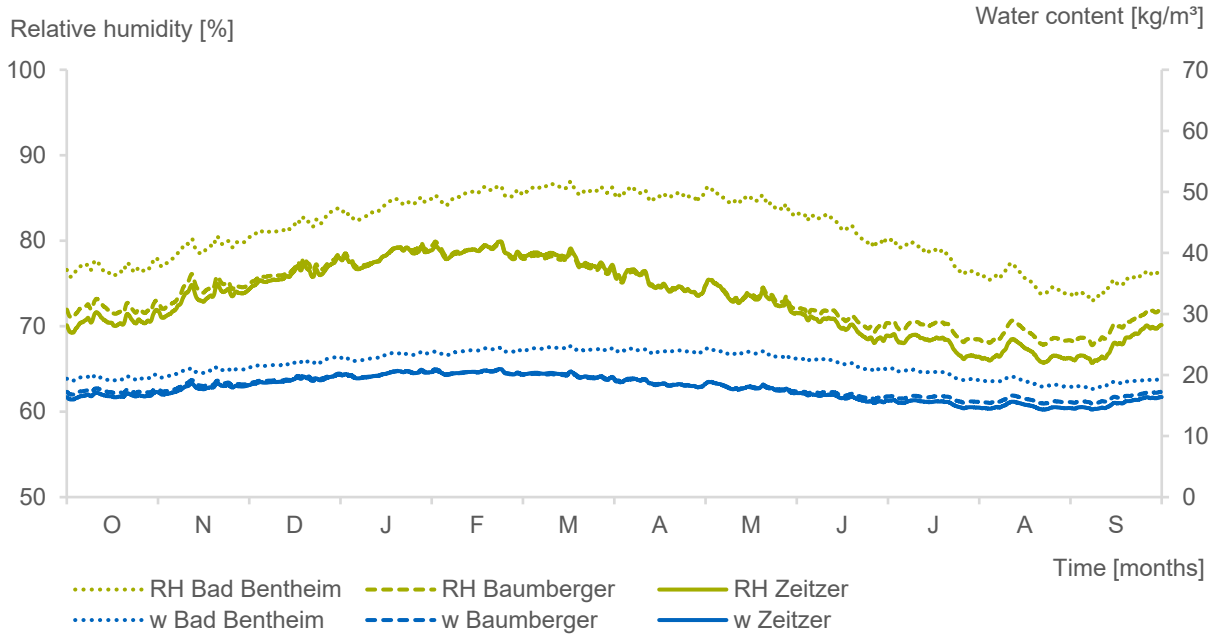

Figure 37: Relative humidity and water content of the wood fiber insulation in the critical outer 1 mm thick sub-layer

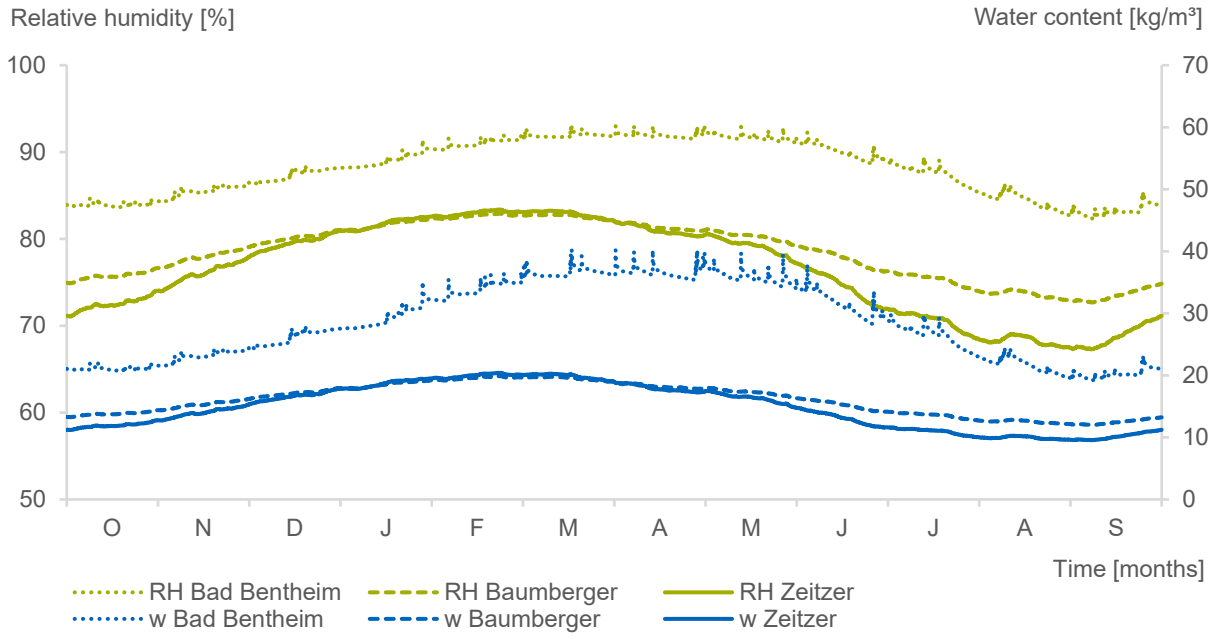

Figure 38: Relative humidity and water content of the lightweight loam insulation in the critical outer 1 mm thick sub-layer

The graphs show that the highest values are reached for the Bad Bentheim wall and correspond to a water content of 25 kg/m³ in the wood fiber insulation and 40 kg/m³ in the mineral lightweight loam. Since the modeled wood fiber retains up to 350 kg/m³ (Annex A5) and the free water saturation level of the expanded clay layer is 97 kg/m³ (Annex A6), no liquid water is expected to run off inside the construction (Fraunhofer IBP, 2017, p. 10). However, it is worth mentioning that the moisture content simulated using the Bad Bentheim stone rises as the monitor position moves outwards.

Another important evaluation criterion is the possibility of mold growth caused by high humidity levels inside the insulation system. Figure 38 shows a maximum of 93% for the Bad Bentheim sandstone. The German standard DIN 4108-3 defines a relative humidity limit of 80% for exposed surfaces, but this is explicitly not required for the interior of the construction. If airtightness between layers is ensured, mold growth is improbable (DIN 4108-3, n.d., p. 81). The Baumberger and Zeitzer variants are unlikely to develop mold because their relative humidity levels remain close to 80%. Further information on the assembly's airtightness is required to evaluate the Bad Bentheim case.

A third and last critical position to be evaluated in terms of its relative humidity level and water content is defined at a depth of about 60 cm inside the existing wall, which is where moist-sensitive structural wooden elements are embedded. Adding internal insulation poses the risk of increased moisture content inside the wooden beam heads. Figure 39 depicts the water content and relative humidity profiles at a specific point in time at the end of the winter period for all investigated sandstone masonries. For each type, the variant with adjacent insulation is shown in color, whereas the dark and light grey profiles represent the uninsulated wall before and after renovation respectively.

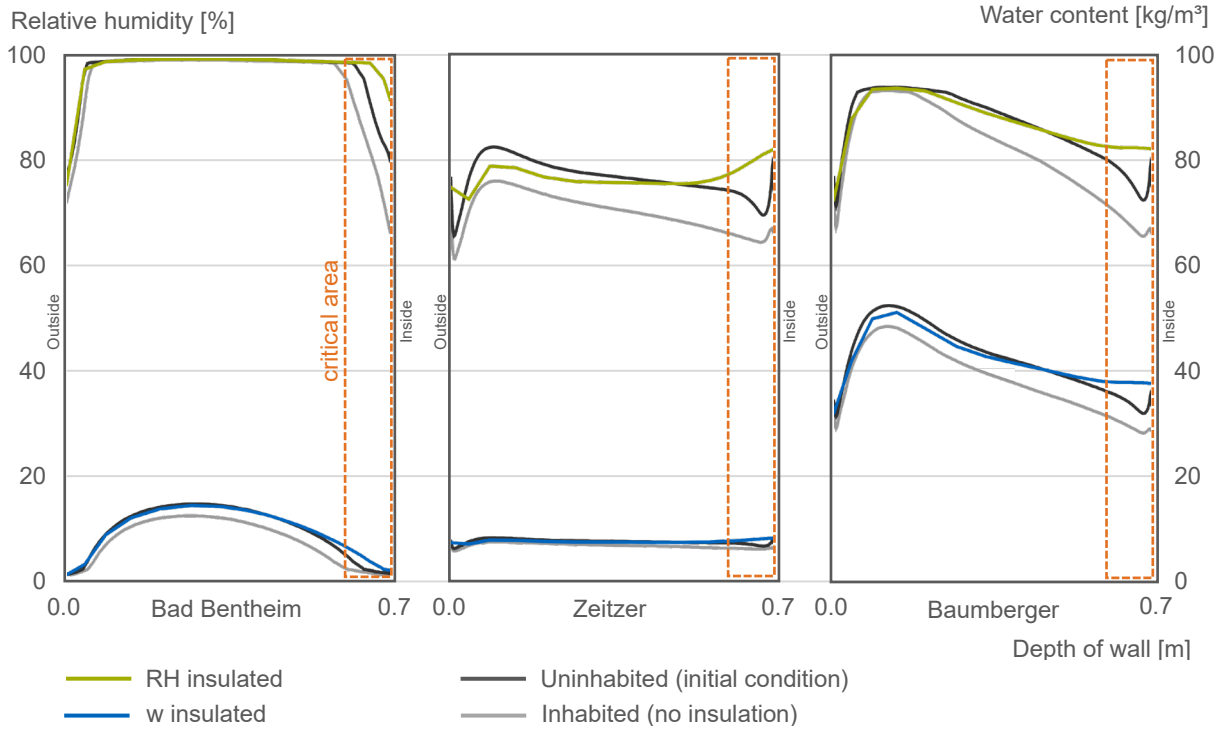

Figure 39: Moisture and relative humidity profiles across the sandstone masonry on April 1, 2029 at 12 AM, with and without adjacent insulation

A divergence between the profiles can be recognized towards the rightmost side of the wall, indicating that internal insulation reduces the drying-out potential of the absorbed rainwater towards the inside. Increased moisture levels in the analyzed area are the result. However, critical values are primarily recorded in simulations using the Bad Bentheim sandstone. In this case, lowering relative humidity levels requires protecting the façade from wind-driven rain. In WUFI Pro, this is simulated by gradually lowering the adhering fraction of rain (AFR) (Figure 40).

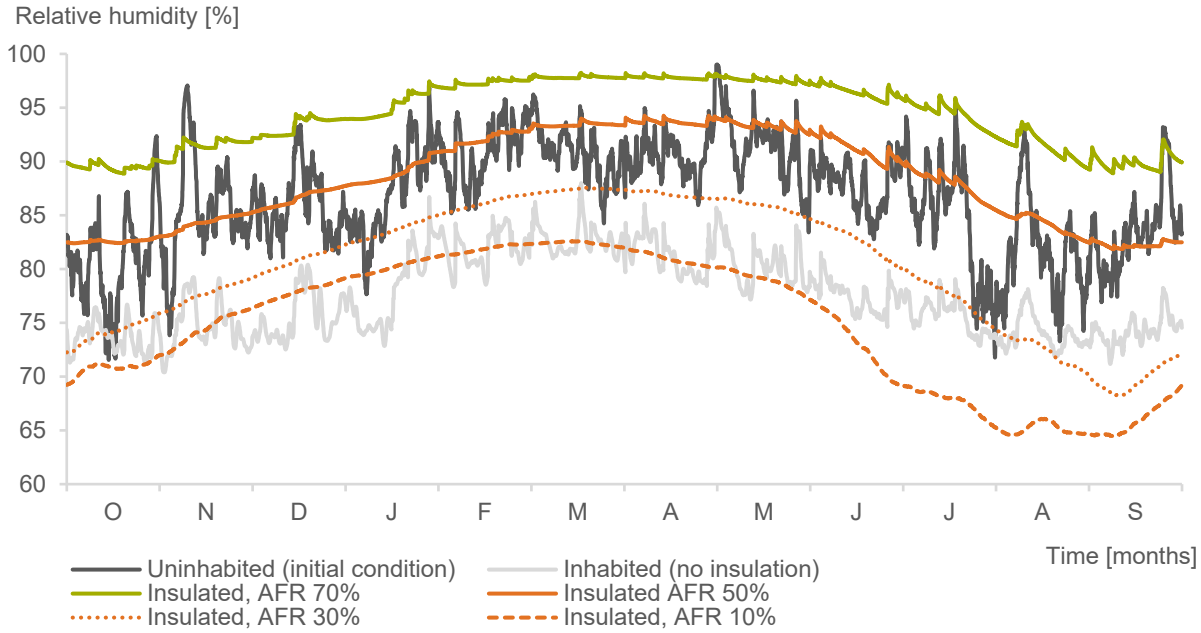

Figure 40: Relative humidity levels inside the critical area, Bad Bentheim sandstone

Throughout the year, the uninsulated wall experiences more fluctuations in relative humidity levels at the critical position. Reducing the amount of rain hitting the outer surface of the insulated wall by 40% (curve for AFR 30%) results in humidity levels lower than those before renovation.

4.5.3. Discussion

The hydrothermal analysis demonstrates that results heavily depend on the capillary rainwater absorption of the external surface. To draw accurate conclusions, more detailed information about the material properties of the sandstone used must be gathered. The simulations also reveal that internal insulation increases humidity levels in the rightmost (inner) layer of the masonry. However, for the same reasons just mentioned, the risk of damage to the beam heads cannot yet be reliably assessed. As for the insulation system, the study finds that using permeable and capillary-active materials is suitable. If water uptake from the outside is controlled and airtightness between layers is ensured, moisture issues are unlikely to arise within the construction.

Consideration must be given to the model's simplification compared to the actual complexity of the stone and mortar matrix in rubble masonry. Stone and mortar have different capillary structures, creating resistance to moisture transport. In this case, the small size of the stones and the tight joint network, along with the significant thickness of the walls, may offer enhanced protection against driving rain (Künzel, 2015, p. 61). However, rain protection depends largely on the quality of the exterior joints. Because of the irregularities of the stonework, grouting is a challenging task and mortar detachment may become an issue. If the joints get damaged, rain can seep into the wall and – not being able to drain out again because of improper capillary contact – may lead to unpredictable water buildup. Thus, regular maintenance of the exterior joints is crucial to ensure adequate rain protection (Künzel, 2015, p. 69ff.).

In addition, the simulation does not account for rising dampness, which affects both the external walls and the ground floor of the cabin. Key concerns include managing roof rainwater runoff without gutters and potential damp issues related to the cabin being built into the sloping ground. Installing a French drain to direct water downhill and away from the building is a practical solution. In addition, horizontal moisture barriers must be carefully planned and executed in order to prevent structural damage. Membranes are suitable for damp-proofing the floor, sometimes combined with the creation of a ventilated sub-floor (Gamazo, 2020, p. 135). In many renovations, methods such as wall cutting with impermeable sheet insertion, chemical injections, or electro-osmosis are additionally required to prevent moisture from traveling up the walls through capillary suction (Balak & Pech, 2008, p. 145). Because of the complexities involved and their low impact on the indoor climate, this paper does not explore these barrier layers in detail.

4.6. Thermal bridges

Thermal bridges are local disruptions in the insulating enclosure that allow more heat to flow from inside to outside than the surrounding surfaces. Typical effects include heat losses and decreased temperatures at inner surfaces, which can lead to high humidity levels and moisture problems inside the construction. Therefore, a primary design goal for the building enclosure assembly is to have a continuous and aligned layer of insulation (Hegger et al., 2008, p. 90) (Arbeiter, 2014, p. 92).

In the case study, thermal bridging occurs where beams and joists are integrated into the exterior wall. The amount of energy lost is determined by the temperature difference between inside and outside and the thermal conductivity of the disrupting component (Arbeiter, 2014, p. 91). Winters in Saro are mild and the thermal conductivity of timber is relatively low. Thus, from a thermal point of view, ceiling supports embedded in the loadbearing wall can be regarded as unproblematic. (Oswald, 2011, p. 64). However, as shown by the hygrothermal assessment, an internal insulation layer worsens the drying behavior of the external wall. As a result, the area around the beam head is likely to experience increased air humidity. This affects the wood's pore air humidity, causing its moisture content to slightly increase. According to the standard DIN 68800, long-term damage can occur if wooden components are permanently exposed to moisture levels greater than 20 M.-%.

As the ceiling joists are in poor condition and will need to be replaced during the renovation, it is recommended to evaluate whether decoupling them from the existing wall is feasible. Otherwise, insulation must be placed as close to the wooden beams as possible to avoid

moisture ingress through convective air flow and protection against driving rain must be ensured (Oswald, 2011, p. 68). Since the water absorption of wood across the grain is very low, insulating the interior is not a problem for wooden beams that run parallel to the outer wall (Künzel, 2015, p. 107) (Oswald, 2011, p. 65).

Thermal bridges also develop in the window reveals. To lower their impact, the thickest insulation layer technically possible should be installed in this area. (Oswald, 2011, p. 43). It should be noted that heat losses in the area of window connections are higher for windows that are positioned further outwards (Oswald, 2011, p. 50). The insulation must be installed on all four sides of the opening, with special care taken to ensure a tight connection to the new window construction (Arbeiter, 2014, p. 137).

5. Preliminary design concept

Optimizing the building envelope of the *cabaña pasiega* is crucial for ensuring an interior environment that meets the new comfort demands while keeping heating energy requirements low. However, previous analyses have revealed that retrofit interior insulation carries risks associated with increased moisture content inside the existing wall. Therefore, in addition to protecting the exterior surface against driving rain, the building must provide adequate ventilation to remove moisture and facilitate drying to the inside. Interior spaces must be designed in such a way that high levels of daylight utilization are possible despite constraints imposed by conservation requirements. Furthermore, they must remain comfortable during the summer months without the need for active cooling. Lastly, as one of the most important preconditions for sustainable building planning is a long usage period, the architectural layout must not only consider the current change of use but also leave room for flexible adaptations in the future. The following chapter addresses the design perspective of the building's intervention in response to these challenges.

5.1. Volume

One of the main characteristics of the *cabaña pasiega* is its basic form, which is defined by a pitched roof with two end gables and a rectangular floor plan. The cultural landscape of the Pasiego valleys is nonetheless enriched by several variants of this basic shape. The reason for this diversity lies in history: as the productive system of the Pasiegos evolved over time, such as with the introduction of the taller Dutch cattle breed, so did their buildings. Hence, in many cases, the basic volume of the building has been altered by way of volumetric additions or elevations. With the decline of the Pasiego economic model, the original use of the *cabaña pasiega* finishes its life cycle. In alignment with its history, the principle of volume modification can be applied to enable the accommodation of living spaces and therefore extend its lifespan. Figure 41 shows possibilities defined by the guideline for the intervention of architectural heritage in the Pasiego valleys to expand the volume of the building. As the cabin used for this case study is not cataloged, additions are permitted to increase the built surface by up to 15% (instead of the 20% allowed for listed cabins). The current building's footprint of 78 m^2 can therefore be enlarged by 11.7 m^2. Based on the implantation of the building, the fourth of the options depicted in Figure 41 is the most suitable. For the purpose of flexibility, the primary design proposal will be planned without this addition but will consider its construction in the future.

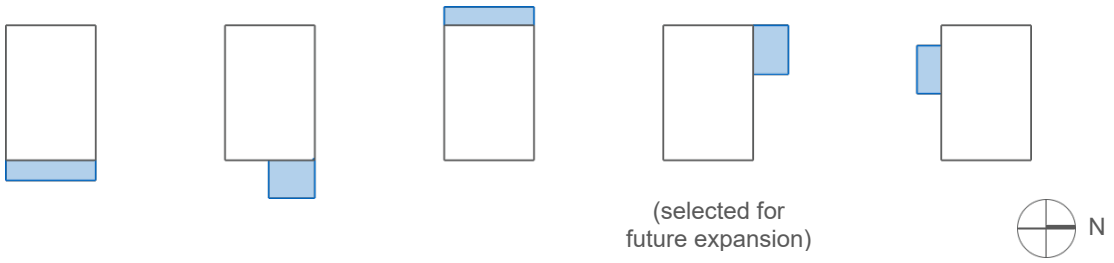

Figure 41: Expansion possibilities

Currently, the height measured from the ground level floor to the lower edge of the beams is 1.8 meters. Since most of the structural elements must be replaced due to their poor condition, an elevation of the intermediate floor, combined with an increase in eave and ridge height to the maximum admissible, is recommended (Figure 42). Specifically, the joist ceiling and cornice are elevated by 20 cm and the ridge is raised by a maximum of 60 cm, depending on the roof's slope, which must be less than 42% (CROTU, 2019, p. 105).

One of the main challenges that the design concept faces is wind-driven rain. In the hygrothermal simulation, the north-facing façade is defined as the most critical. In reality, this side of the building is sheltered from the wind by topography and a dense forest (see Figure 27, "Case study site plan," p. 30). On-site evaluation has furthermore confirmed that rain primarily hits the west- and south-oriented surfaces of the cabin. The southern façade is protected, although to a minimum extent, by a small roof overhang and, towards its eastern edge, by the large chestnut tree (see "Assessment of existing structure", p. 31).

In response to the described conditions, the west side of the building enclosure is pushed back about 1.8 meters, and a small functional patio is created. The existing west wall hinders rain from reaching the thermally active layer while also shading it from the critical afternoon sun in summer. According to page 87 of CROTU (2019), 15% of the roof can be left uncovered in this area. In addition, because the new façade is imperceptible from the outside, a more open layout is possible. In accordance with these intervention criteria, a significant proportion of glazing is allocated towards the courtyard, allowing daylight to enter the building. The loss of space is justified by the benefits achieved through this measure.

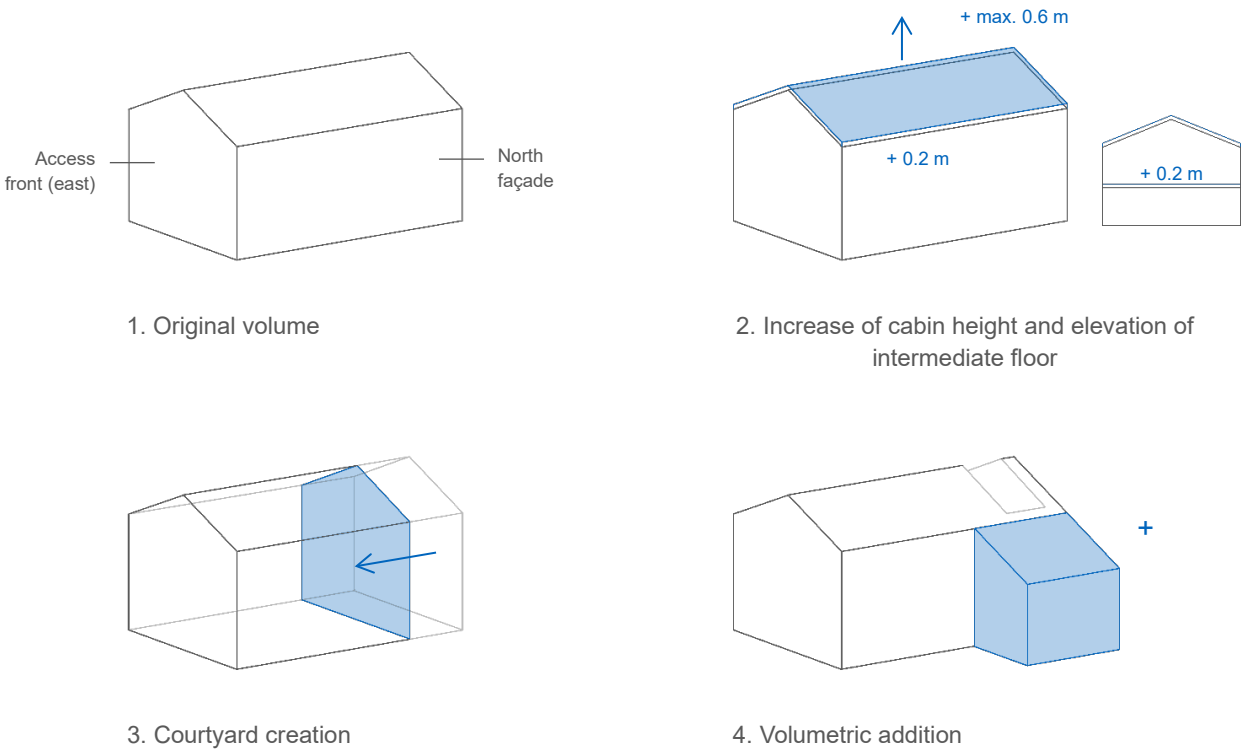

Figure 42: Scheme of volumetric modifications

5.2. Openings

Several requirements influence the planning of transparent components. Besides protecting the interior through thermal separation and permitting natural ventilation, windows allow for the use of daylight and visual contact with the outdoors. Furthermore, due to its physical properties, glass enables the passive use of solar radiation to heat the interior of the building. However, it is critical that the benefits of solar gains during the cold months do not lead to negative consequences during the hotter part of the year (Hegger et al., 2008, pp. 91–92).

In contrast to new building projects, where the size and arrangement of openings can be tailored to the architectural program, the rehabilitation of the *cabaña pasiega* is subject to several constraints. The façades, with their massive constitution and small random openings, are essential in defining the character of the building type. Therefore, according to the guideline for the intervention on the architectural heritage in the Pasiego valleys, the following conditions apply for the creation of new openings or expansions of existing ones:

- The disposition and geometry of all existing openings, including the front doors, must be conserved.
- Exceptionally, one single opening may be expanded, and the height of the doors may be increased to adapt for new uses.
- No additional openings are allowed on the access front.
- A maximum of three new openings can be created on the south façade, yet a total number of six must not be exceeded. The proportion of glazing is limited to 20%.
- Two new openings are permitted respectively on the north- and west-facing walls, although the total number on each side must be less than four. The maximum proportion of glazing permitted here is 12%.
- The size of new openings must be equal to or smaller than the largest existing one, and a distance of at least 1.5 meters must be maintained. A larger window may exceptionally be allowed on the south-facing front. In this case, no additional openings are to be created.
- Shading elements on the exterior are prohibited.

Shown in Figure 43 are the new openings planned for the case study building. In accordance with conservation requirements, no changes are made to the design of the eastern access façade. Natural light is allowed inside the building through the installation of glass doors behind the existing wooden panels, which are restored and used for solar protection during hot days. A total of three new openings are planned on the south wall. Through the creation of the courtyard, the existing west wall and a portion of the north and south walls are thermally inactivated. New openings in this area (green line) serve the purpose of increasing the daylight yield and generating visual connections to the outdoors. Because it is not advisable from a thermal point of view, no new windows are accommodated facing north.

In total, six new square openings with an individual area of 0.49 m^2 are thus created. Only two of them, oriented towards the south, enclose the conditioned area of the cabin. The four remaining ones are situated at different heights surrounding the courtyard. Despite the addition of these openings, the cabin’s appearance, defined by the unique relationship between solids and voids, with the stone walls dominating the small openings, is conserved.

Only on the short access façade does the proportion reach close to 10%. On the south wall, it amounts to roughly 6%, and on the west and north walls to 3.3% and 1.2% respectively.

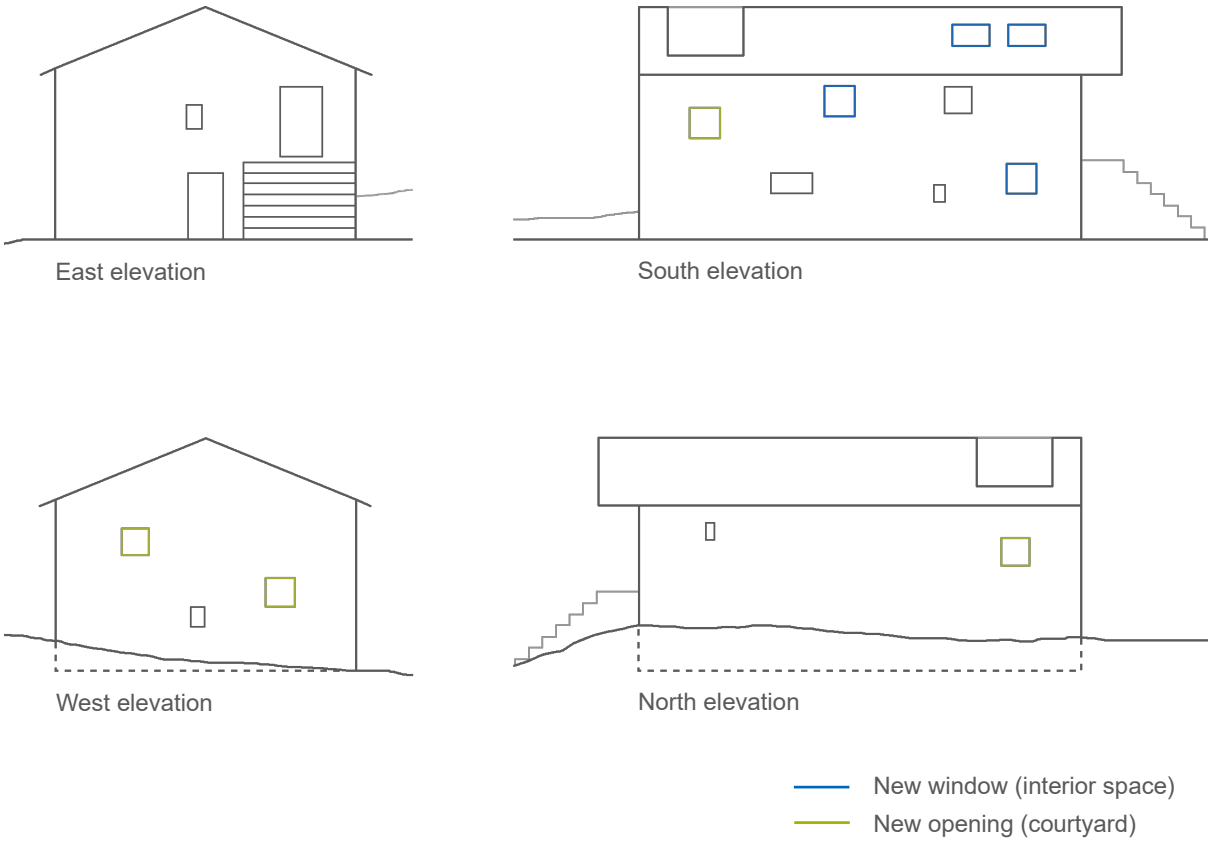

Figure 43: Scheme of existing and planned new openings

Windows set within the existing wall are installed using traditional construction methods, partially concealing the frame behind the ashlar surround, as shown in Figure 44. By beveling the reveals towards the interior of the building, the utilization of daylight is maximized. Frames are made of oak or chestnut wood and treated with natural sealants.

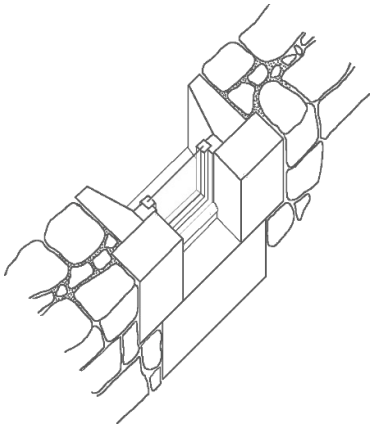

Figure 44: Mounting of window behind ashlar surround

While the outer shell of the cabin retains its original closed character, the rear of the interior is predominantly glazed to open out to the new courtyard. Aside from increased daylight acquisition, the use of glass allows for the patio to be visually integrated into the interior and thus creates a larger sense of space. A critical aspect to be considered here is the increased risk of overheating. As can be seen in Figure 19 “Course of the sun for the 21st of a given month” (p. 24), the east and west façades receive high solar yields during summer. Without adequate sun protection, a large percentage of glazing could therefore lead to unpleasantly high temperatures inside the building. However, because the sunlight coming in at a shallow angle is largely blocked by the surrounding walls, in this case, it is acceptable. Any additional shading devices required should be installed in such a way as to avoid hindering the use of the courtyard. The final layout of this façade will be designed in the last chapter of this thesis.

Depending on use and orientation, a window area of 30-60% of the façade area is generally ideal for optimizing daylight (Richarz & Schulz, 2011, p. 23). Despite having increased the number of windows in the exterior wall and using transparent components towards the courtyard, natural light inside the cabin might still be scarce. For this reason, two additional windows – each measuring about 1 m^2 – are allocated on the southern plane of the roof. In terms of visual comfort, a smaller area would probably suffice, because the illuminance for the inclined surface of the roof is higher than that for the vertical wall. However, larger windows lead to higher passive solar gains in winter. To avoid an excessive increase in heat input during summertime, the glazing is positioned towards the eastern side of the roof, where it will be mostly shaded by the tree.

5.3. Interior layout

To ensure the drying out of external walls towards the interior of the cabin, sufficient ventilation must be provided. Cross-ventilation, which relies on air movement between opposite windows, is particularly effective at removing moisture. To guarantee proper airflow across the building and along the surface of the insulation, spaces are arranged around a central core housing the sanitary and mechanical functions (Figures 45 and 46). The continuity of space is maintained by setting this core away from the building’s edges and deliberately avoiding rigid divisions intersecting with the exterior walls. Rather than compartmentalizing space, different configurations are made possible through the use of versatile furniture modules and sliding doors. Air circulation is further improved by the integration of double-height spaces into the design.

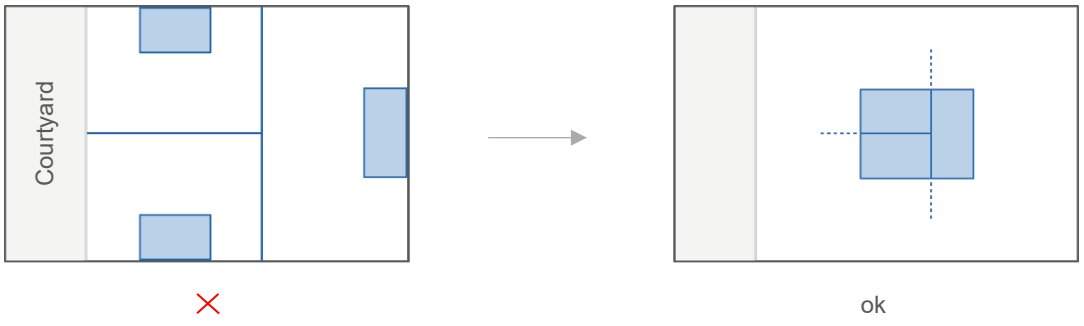

Figure 45: Interior layout with: a) conventional partitions and furniture against exterior walls and b) central core

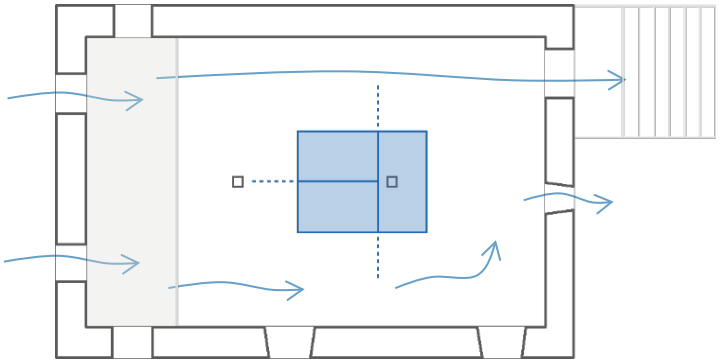

Figure 46: Cross-ventilation and air movement along exterior walls

6. Evaluation and optimization of the interior climate

The preliminary design concept was developed to provide comfortable living conditions for the occupants of the cabin while minimizing the energy demand for heating. In the following, these conditions are examined and optimized where applicable. To do so, the building is modeled with the tool WUFI Plus, which can calculate the interior climate and energy consumption. In order to analyze and evaluate the simulations, first, a basis upon which the results are assessed must be determined.

6.1. Assessment criteria

Thermal comfort is defined as the principal criterion for evaluating the proposed rehabilitation concept. A thermally comfortable environment is primarily influenced by physical factors such as the temperature, humidity, and speed of the internal air as well as the average external temperature. However, the perception of users is subject to individual and varying factors such as their age, type of clothing, and activity level (Hegger et al., 2008, p. 57). Taking these subjective parameters into account, the assessment is carried out using the PMV (Predicted Mean Vote) model according to DIN EN ISO 7730. PMV is an index that aims to predict the mean value of votes of a group of occupants on a seven-point thermal sensation scale. Within the PMV index, +3 translates as too hot, while -3 translates as too cold, as shown in Table 4.

PMV [-]	**-3**	**-2**	**-1**	**0**	**1**	**2**	**3**
Perception	Cold	Cool	Slightly cool	Neutral (comfortable)	Slightly warm	Warm	Hot

Table 4: Assessment scale for the predicted mean vote (PMV)

Once the PMV value is known it is then possible to determine the PPD (Percentage of People Dissatisfied) value according to the following formula (DIN EN ISO 7730, p.4):

$$PPD=100-95\cdot\exp(-0{,}03353\cdot PMV^4-0{,}2179\cdot PMV^2)$$

The PPD is an index that provides information about the number of people who can be expected to be unhappy with the prevailing interior climate. Given the individual perception, even with a PMV value of 0, the number of dissatisfied persons will still be 5% (Table 5).

PMV [-]	**-2**	**-1**	**-0.7**	**-0.5**	**0**	**0.5**	**0.7**	**1**	**2**
PPD [%]	75	25	15	10	5	10	15	25	75

Table 5: PPD value in relation to PMV value

In its current edition, the DIN EN ISO 7730 standard defines four categories for the interior climate (Table 6).

Category	PPD [%]	PMV [-]
I	< 6	-0.2 < PMV < +0.2
II	< 10	-0.5 < PMV < +0.5
III	< 15	-0.7 < PMV < +0.7
IV	< 25	-1.0 < PMV < +1.0

Table 6: Categories of thermal environment, thermal state of the body as a whole

Ambient conditions corresponding to the first two categories are difficult to achieve in the case of natural ventilation (Hegger et al., 2008, p. 57). Hence, category III is chosen as the desired thermal environment for this evaluation. The PMV and PPD values are calculated using WUFI Plus for every hour that a person is inside the building. Afterward, the hours in which the PMV value deviates from the defined comfort range are summed up in Microsoft Excel. The interior climate of the building is regarded as too cold for values below -0.7 and too hot for values greater than +0.7.

In addition to PMV, the operative temperature is analyzed for each of the 8,760 hours of the simulation period. This metric, which combines both air temperature and radiant temperatures of surfaces, reflects the temperature that occupants perceive. As a first criterion, the yearly maximum and minimum temperatures are documented for each simulation. Moreover, the sum of hours with temperatures below 19°C and above 26°C is examined. These limits are set for a better understanding of thermal comfort during the different seasons of the year and are not based on official requirements. Table A.5 of DIN EN ISO 7730 provides example design criteria for the operative temperature in different types of space. According to it, temperatures between 22°C and 27°C are recommended for category III thermal environments during summer (0.5 clo; 1.2 met), and between 19°C and 25°C during winter (1.0 clo; 1.2 met).

Besides influencing the human heat balance, thermal comfort has a direct influence on the energy consumption of a building (Hegger et al., 2008, p. 55). For this reason, the third and last criterion defined for evaluating the proposed revitalization concept is the simulated heating energy. This value provides information on how much energy is needed to keep the interior temperature at a certain level during the heating period.

6.2. Boundary conditions

To efficiently estimate the building's energy performance, geometrical and non-geometrical data, such as construction materials and assemblies and the boundary conditions of occupancy, must be specified. The following briefly describes the model setup and input parameters.

6.2.1. Building geometry and climate

For the simulation, the cabin is represented in a single-zone model with a net floor area of 40.8 m^2 and a net volume of 188.7 m^3. Adjacent shading elements such as roof overhangs and the exterior walls of the courtyard are included to improve the accuracy of results (Figure 47). In addition to the exterior climate, an optional climate is created and assigned to components in contact with the ground. This climate is specified as a sine curve with a mean value of 14°C and an amplitude of 3K. The day of the maximum is September 15, and the relative humidity is set to a constant value of 99%.

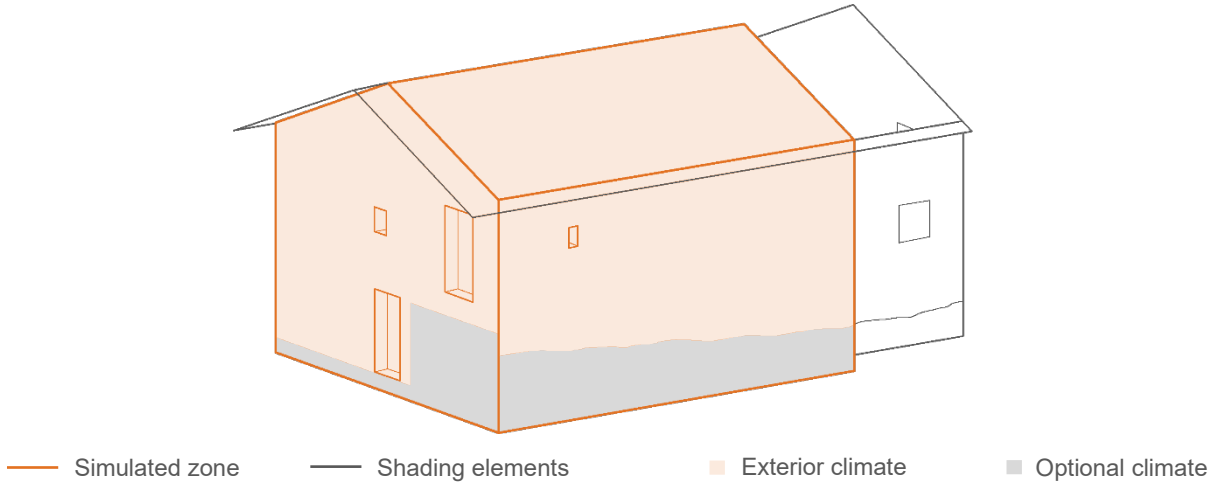

Figure 47: Simulated zone with adjacent shading elements and assignment of external and optional climates

6.2.2. Components

Once the building geometry is created and the climatic boundary conditions are set, individual parameters are specified for each component connected to the zone. This includes visualized components enclosing the interior space and non-visualized components affecting the interior environment such as the intermediate floor and partition walls. The window parameters assigned are shown in Table 7 and are based on DB-HE (2022, p.16) and the recommendations of the guideline for the intervention of the architectural heritage of the Pasiego valleys. Annex A11 provides detailed information on the assemblies and material parameters used for opaque components, which include a rammed-earth floor on the ground level and a vented roof with over-rafter insulation. The resulting U-values are summarized in Table 9.

Uw [W/m²K]	Frame factor [-]	Solar energy transmittance [-]	Depth of window reveal [m]
1.8	0.7	0.6	0.3

Table 7: Window parameters

WUFI Plus can simulate both the hygrothermal conditions in a building component and the interior climate. For the evaluation at hand, the calculation mode of the software is switched to “thermal only” and – as they are redundant from a thermal point of view – all assemblies are entered without membranes. The pitched roof is simulated without explicit consideration of the roof cladding and the ventilated air layer. Instead, it is calculated using effective transfer parameters according to Kölsch (2015). This involves applying the solar emission coefficient ε (= 0.84 for matt clay tiles) directly to the surface of the sub-roof and switching on the explicit radiation balance in the simulation settings (Kölsch, 2015, p. 9). In addition, the coefficient of absorption of the cladding (a=0.77 for matt red clay tiles) is multiplied with a reduction factor in dependency of the ventilation of the air layer and the position between the eave and ridge, as shown in Table 8. Under the assumption of normal ventilation and the use of the parameters for the coldest position, the input for the effective short-wave coefficient of absorption results in ae = 0.77 · 0.69 = 0.53.

	Eaves position (coldest)	Middle position		Ridge position (warmest)
Strong ventilation		$\alpha_{k,e}$= 30 W/m²K		
	$a_e = a \cdot 0.71$	$a_e = a \cdot 0.90$		$a_e = \alpha$
Normal ventilation		$\alpha_{k,e}$= 19 W/m²K		
	$a_e = a \cdot 0.69$	$a_e = a \cdot 0.92$		$a_e = \alpha$
Low ventilation		$\alpha_{k,e}$= 13.5 W/m²K		
	$a_e = a \cdot 0.75$	$a_e = a \cdot 0.89$		$a_e = \alpha$

Table 8: Effective transfer parameters of the roof in dependency of the ventilation type and the position between eave and ridge

For the simulation model to be represented realistically, it is necessary to account for the junctions and connections of the enclosing components. Heat losses due to uncontrolled ventilation are determined by the airtightness of the building and are estimated according to the following formula (DIN 18599-2, p.58):

$n_{inf} = n_{50} \cdot e \cdot f_{ATD}$

$n_{inf} = 6\ 1/h \cdot 0.07 \cdot 1$

$n_{inf} = 0.42\ 1/h$

with
n_{inf} = air change through infiltration
n_{50} = air change at 50 Pa pressure difference
e = shielding coefficient
f_{ATD} = factor for air transfer device

The air change at 50 Pa pressure difference (n_{50} = 6 1/h) for a category III building is taken from Table 7 of the DIN 18599-2 and table B.6 of EN 12831-1. The shielding coefficient e

corresponds to more than one façade being exposed to the wind and a building height below 10 meters. As there are no air transfer devices planned, the f_{ATD} value has no effect on the calculation. In the simulation, the infiltration air change that takes place in an hour (ACH) is set to 0.5 1/h, as this is the minimum air change rate defined for living spaces in EN 12831. This value is also typical for unconditioned rooms with sealed joints between components and no ventilation openings (ISO 13789, p.27).

Thermal bridges are accounted for by means of general surcharges. If a solid ceiling is attached to an external wall, the adjustment for internal insulation is + 0.15 W/m²K (DIN 18599-2, p. 56). Since this is not relevant to the case study, a surcharge of + 0.10 W/m²K is applied to all resulting U-values (Table 9). This is achieved in the simulation model by reducing the thickness of the insulation accordingly.

Component	**U [W/m²K]** recommended for climate zone by DB-HE (CTE)	**U [W/m²K]** resulting from assembly	**U [W/m²K]** + 0.10 surcharge
Roof	0.35	0.298	0.398
Wall uninsulated*	-	2.108	2.208
Wall insulated	0.41	0.415	0.515
Floor	0.65	0.633	0.733

**Surcharge accounted for by reducing the thickness of the wall in the simulation*

Table 9: U-values

6.2.3. Occupancy and schedules

People, lighting, and appliances cause internal thermal loads that influence the room temperature. Although the cabin is intended to accommodate up to four people, the number of occupants for the simulation is assumed to be one. This results in lower internal heat gains and therefore represents the most unfavorable situation during the heating period (Hegger et al., 2008, p. 113). To encompass the effects of occupancy on the energy performance of the building, a predefined profile for a single household is selected from the WUFI database. The resulting internal thermal loads are standard based and consider the use of a washing machine every four days and one bathroom. During the week, the person is assumed to sleep from 11:00 pm to 6:00 am. He then leaves the building around 8:00 am and spends the day elsewhere until 5:00 pm. To simulate a wider spectrum of usage times, a different profile is used for the weekends. Here, the user sleeps a little longer (8:00 am) and then stays inside until going to bed at 11:00 pm. Over the course of a year, the building is thus occupied for a total number of 6,348 hours.

The amount of heat produced by the person is influenced primarily by the level of activity. Figure 48 depicts the metabolic rate at different activity levels throughout both simulated day-profiles. While not sleeping, the occupant alternates between relaxing (1.0 met) and a sedentary activity (1.2 met) (DIN EN ISO 7730, Annex B).

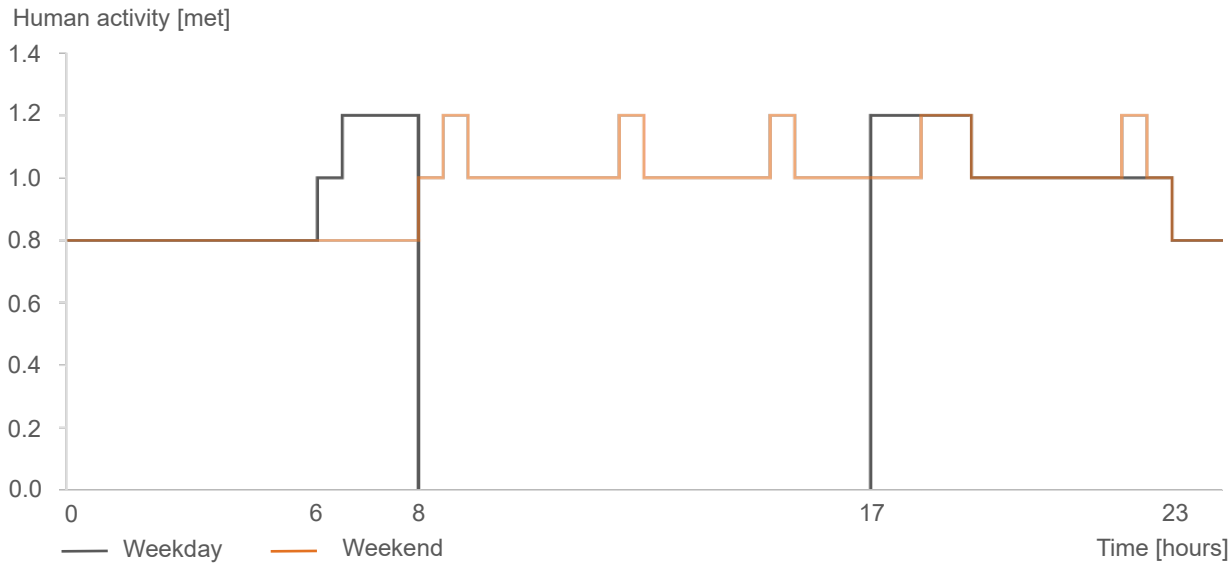

Figure 48: Periodic day profiles for human activity level (single household)

The user's clothing represents a thermal insulation layer and therefore affects his perception of the interior temperature. This value is adjusted in the daily profiles and assigned to customized periods, as shown in Table 10.

	1.2 met and 1.0 met	0.8 met
July/August	0.6	1.8
June/September	0.8	1.8
May/October	0.9	2.5
November - April	1.1	2.5

Table 10: Clothing insulation

A clothing insulation of 0.6 clo (shirt with short sleeves and light trousers plus – as the user is assumed to be sitting most of the time – insulation of a chair) is considered during the warmest period of the year and 1.1 clo (shirt, trousers, jacket plus insulation of a chair) during the heating period. In addition, intermediate values are estimated for transitional periods. As temperatures during summer nights and especially in between seasons tend to drop, higher insulation values are entered for the sleeping hours (0.8 met) and represent the insulation of the bedding system. The effect of changing the thermal insulation of the bedding on the optimum operative temperature is approximately 5.3°C per clo (Lin & Deng, 2008, p. 80). Two types of bedding insulation are assumed: one for summer (1.8 clo) and one for winter (2.5 clo).

Air velocity and relative humidity are two additional variables that influence the user's perception of the interior environment. However, because the effect of relative humidity on thermal comfort is relatively small, it is ignored during the assessment (Lin & Deng, 2008, p. 78) (DIN 7730, Annex F). The air velocity is set to 0.1 m/s for all simulations.

By opening the windows, the user can control the exchange of air as required. Natural ventilation is assumed to occur in the morning and before the occupant goes to bed, as well as a third time when he enters the cabin at 5:00 pm. During weekends, because the building is constantly occupied, windows are scheduled to be opened four times per day. The duration of window openings is varied throughout the year according to Table 10.

Time of year	Duration [h]	Air change rate [1/h]
Heating period	0.1	10
June, July, August	0.5	10
May, September, October	0.25	10

Table 11: Variation of window opening duration

For solar protection, the wooden doors are kept shut during the mornings in July and August. This is modeled by scheduling a shading device with a reduction factor of 0.1 from 8:00 am to 12:30 pm. From April to October, a factor of 0.5 is additionally set for windows affected by the shading of the chestnut tree (eastern side of southern façade and roof) (Musso, 2012, p. 6). Lastly, the exposed roof construction above the new courtyard is assumed to have a constant shading effect equivalent to a factor of 0.9 on west-facing windows.

6.3. Assessment of preliminary revitalization concept

One of the most important factors influencing the design concept is the interior insulation of existing walls. Its effect on improving the climate-related energy performance of the building is evaluated by running simulations both for the insulated and the uninsulated case. Figure 49 summarizes the results. It should be noted that the PMV values shown refer to 6,348 total usage hours, while the values for the operative temperature (OT) are based on the 8,760 hours that make up the simulation period. The assessment reveals that by installing internal insulation, the number of hours that are perceived as too cold (PMV < -0.7) can be reduced by 15%. In contrast to the positive impact on thermal comfort during cold periods, an increase in the count of hours with PMV values greater than +0.7 and operative temperatures above 26°C is registered.

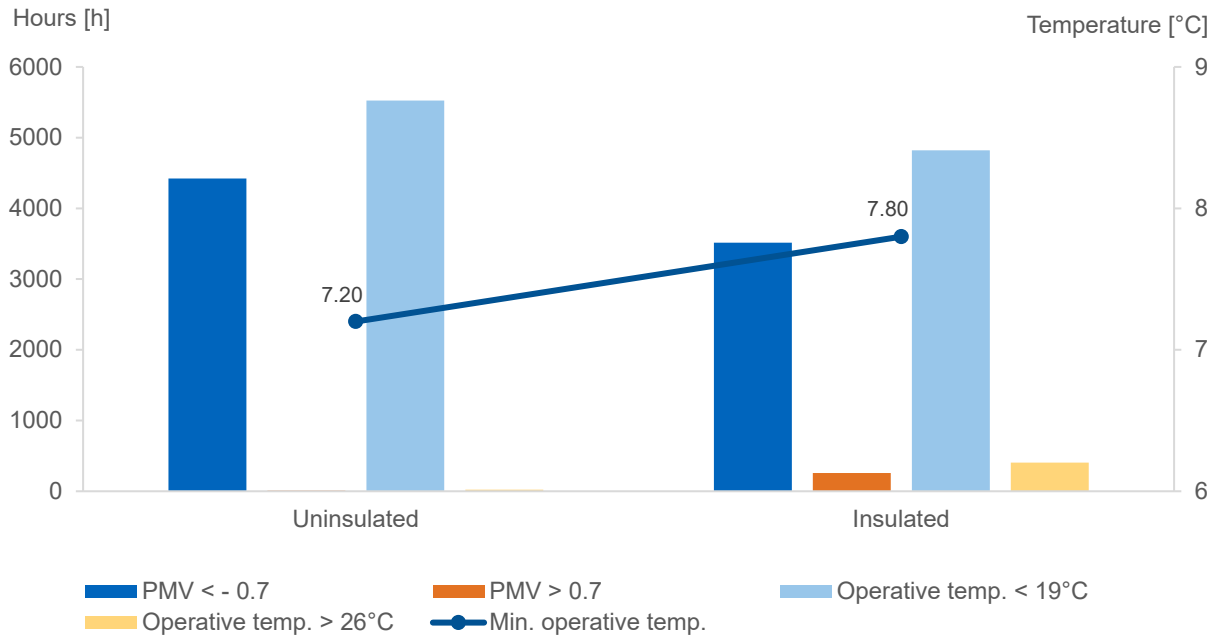

Figure 49: Thermal comfort dependent on level of insulation (unheated)

Figure 50 clearly shows that the decoupling of the thermal mass from the interior caused by the insulation layer leads to higher operating temperatures during hot summer afternoons. The maximum reached is 30°C and occurs on August 20 at 5:00 pm.

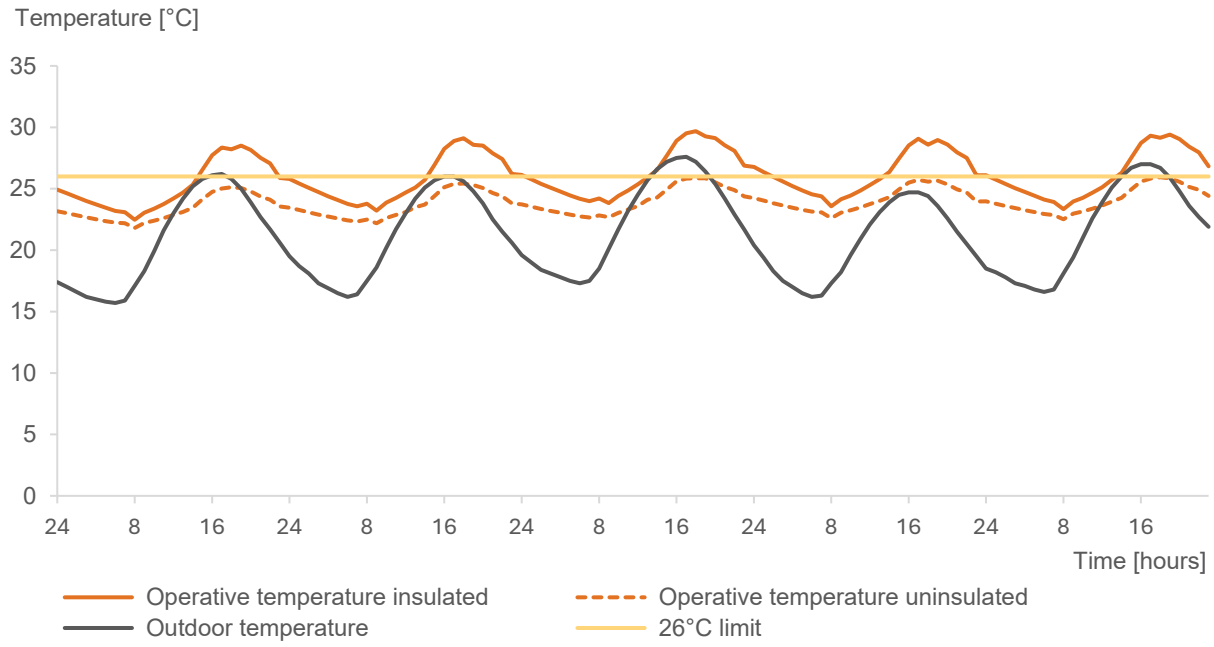

Figure 50: Operative temperature with and without interior insulation from July 27 to July 31

During the winter, both building variants require additional heating to keep occupants comfortable. To assess the impact of internal insulation on heating demand, an ideal heating system is set to maintain the interior temperature at 21°C from November 1 to April 30. The evaluation shows that insulation reduces heating-related energy consumption by more than 50% (Figure 51). Both models record hours in which the interior environment is still perceived as too cold, though this is the case less than half of the time in the insulated variant. These uncomfortably cold hours occur in October and May, when the heating system is turned off.

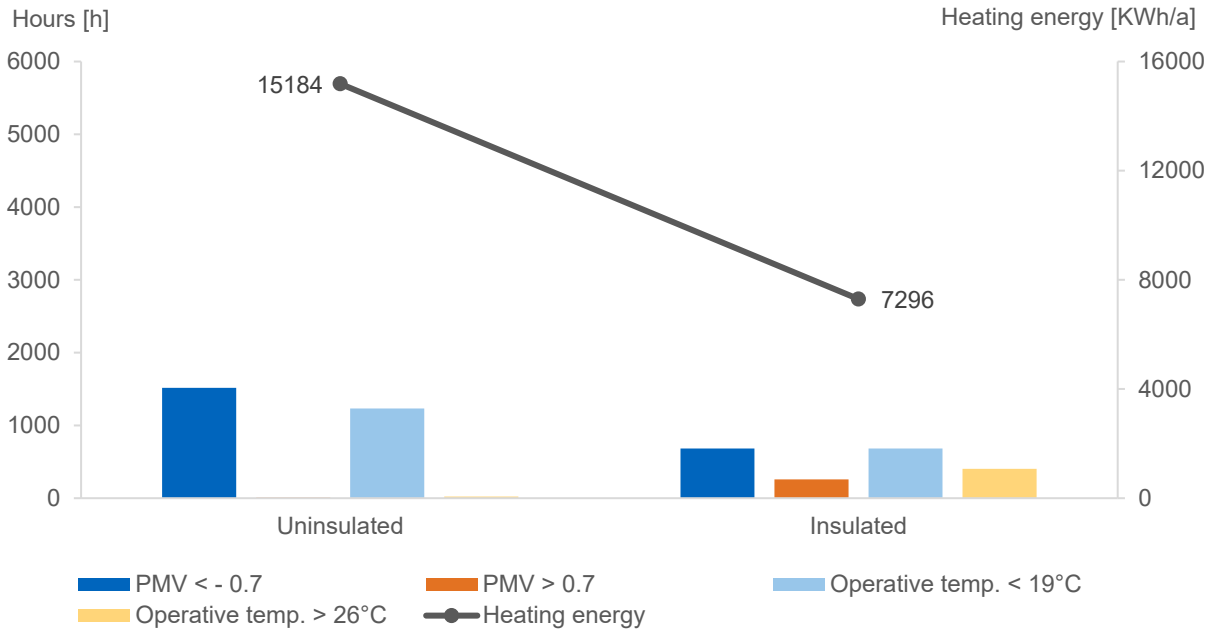

Figure 51: Thermal comfort dependent on level of insulation (heated)

6.4. Optimization of interior climate

The preceding analysis confirms that installing interior insulation positively impacts thermal comfort and the energy efficiency of the cabin. Building on these findings, further improvements to the interior environment are explored. The focus is on reducing the number of uncomfortably cold hours while at the same time avoiding excessive heat. To accomplish this, individual parameters are modified in the simulation settings and their effect on thermal comfort is determined. The resulting model is then further evaluated for suitability under various use and climate scenarios. Figure 52 illustrates the optimization strategy employed. The goal of the parameter study is to identify ways to refine the preliminary design in terms of indoor climate, ultimately leading to a finalized architectural design proposal.

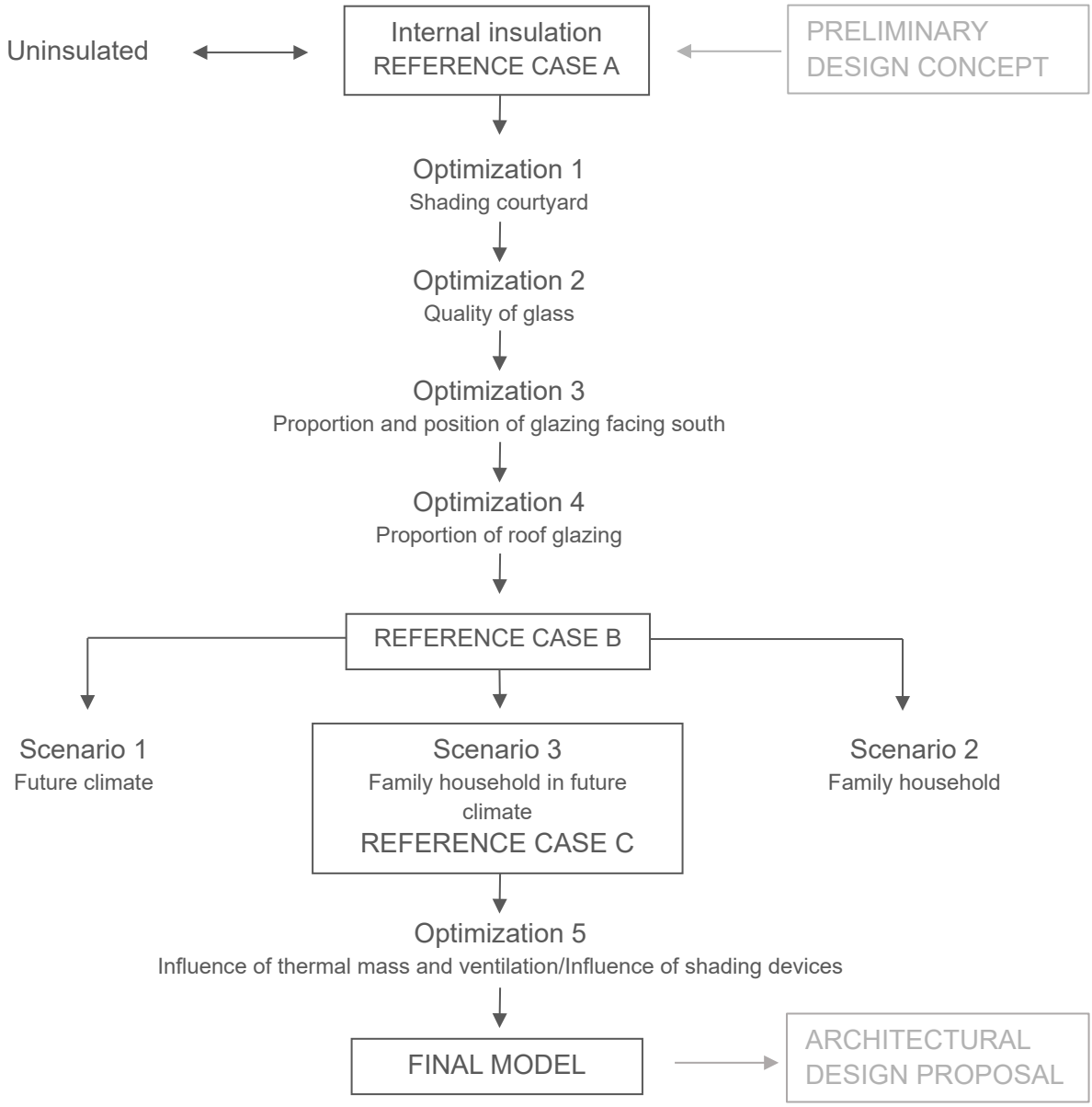

Figure 52: Optimization strategy

6.4.1. Optimization 1: Shading courtyard

Installing internal insulation increases the risk of overheating (see Figure 50, “Operative temperature with and without interior insulation from July 27 to July 31,” p.60). One way to counteract this problem is by blocking out the low afternoon sun from west-facing windows. Shade is, in part, already provided by the surrounding walls of the courtyard. In the following, additional protection is given by an external shading device as soon as the interior temperature rises above 25°C. A reduction factor of 0.3 is set. This corresponds to partially closed shutters (75%) to avoid an increased energy requirement for artificial light (DIN 4108-2, p. 25). The examination aims to determine whether the amount of uncomfortably warm hours can be minimized by this measure.

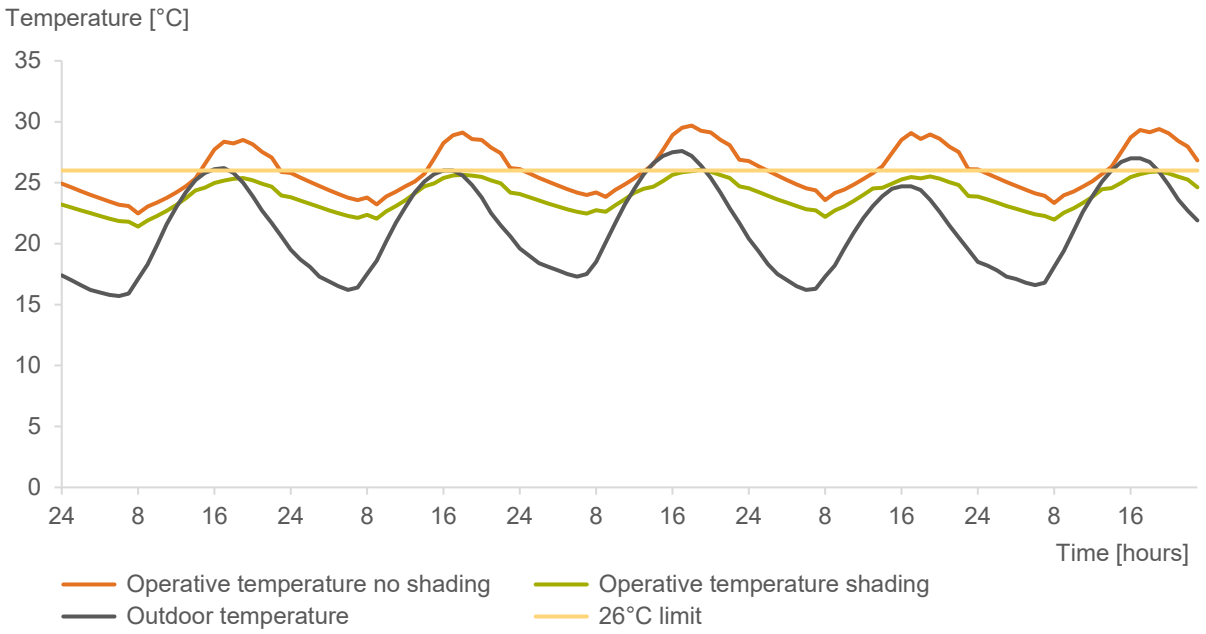

Figure 53: Operative temperature dependent on sun protection from July 27 to July 31

Overheating is avoided through sun protection of the west façade (Figure 53). The shading system allows the maximum operative temperature to be reduced to 26.7°C, which is lower than the maximum reached in the uninsulated building (26.9°C). The number of hours with values greater than 26°C is only 21. Occupants feel warm (PMV > 0.7) during 11 hours of the reference year.

6.4.2. Optimization 2: Quality of glass

Without heating, users perceive the interior environment as too cold 55% of the time. Changing the quality of glazing improves the Uw-value of windows and therefore helps minimize transmission heat losses. The Uw-value is the overall heat transfer coefficient of a window. It is composed of the U-value of the glazing (Ug) and the U-value of the frame (Uf). To analyze the impact of windows with differing thermal performances on the interior environment, simulations are run with Uw-values ranging from 2.0 to 1.4 W/m²K. For simplification, all other parameters are kept constant. It should be noted, that modifying the type of glazing often entails a change in the solar energy transmittance (g-value), which in turn may lead to lower or higher passive solar gains.

Figure 54 shows that as the quality of the glass increases, the number of uncomfortably cold hours in the building (PMV < -0.7) decreases and the minimum operative temperature rises. At the same time, the number of excessively warm hours (PMV > +0.7) remains negligibly low. For the following parts of this study, windows are therefore upgraded to the best value, i.e., a heat transfer coefficient of 1.4 W/m2K. Through this measure, 11% less energy is required to heat the building compared to the reference case (see Figure 58, “Optimization of heating energy requirement,” p. 67).

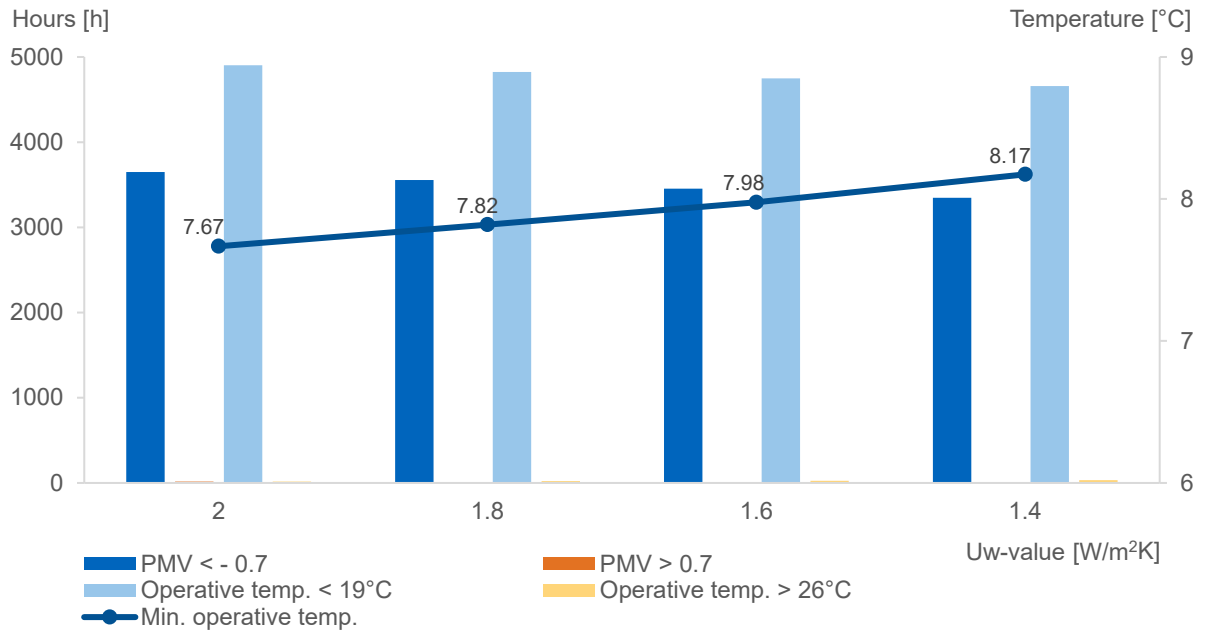

Figure 54: Thermal comfort dependent on Uw-value

6.4.3. Optimization 3: Proportion and position of glazing facing south

Upcoming simulations analyze whether the interior climate can be improved further by maximizing the solar heat gains through south-facing glazing. The position of the window inside the wall is closely related to the amount of shade cast by the reveal and thus the amount of solar radiation entering the interior space. As of now, the distance between the outer reveal edge and the glazing is set to 0.3 meters. Aside from this solution, the conservation guideline also allows for windows to be placed further outside, even flush with the exterior wall surface (CROTU, 201 p. 84). This positioning favors solar heat gains but also increases transmission losses due to thermal bridging. For the study, it is assumed that the heat losses caused by enhanced thermal bridging are compensated for with increased reveal insulation. Therefore, only the position of the glazing is adjusted.

First, the depth of the reveal is set to zero for all five windows facing south (option a, Figures 55 and 56). Next, a model is generated in which, rather than creating new openings, one existing opening is enlarged in accordance with CROTU (2019, p. 84). This allows for a greater overall glazing area of the façade (options b and c). In the model, only the large window is placed on the outer edge of the wall. To determine which existing window to expand, two simulations are run: one considering the tree's shading (option b), and one assuming an internal shading device with a reduction factor of 0.7 (option c). Figure 55 shows the three resulting design possibilities for the southern façade. Figure 56 compares the effect of each variant on thermal comfort.

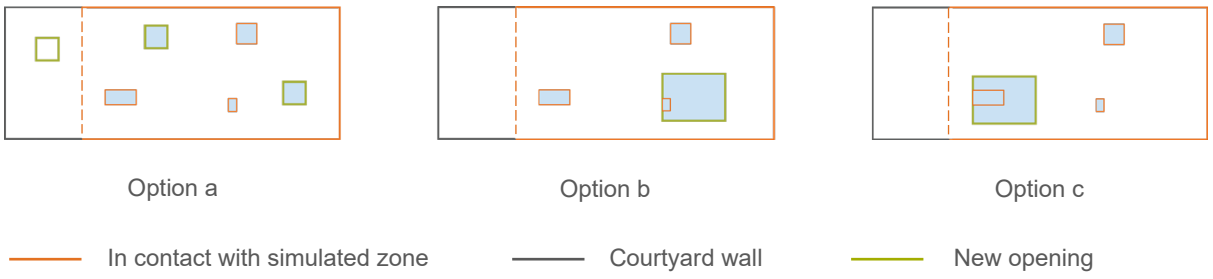

Figure 55: South façade design options

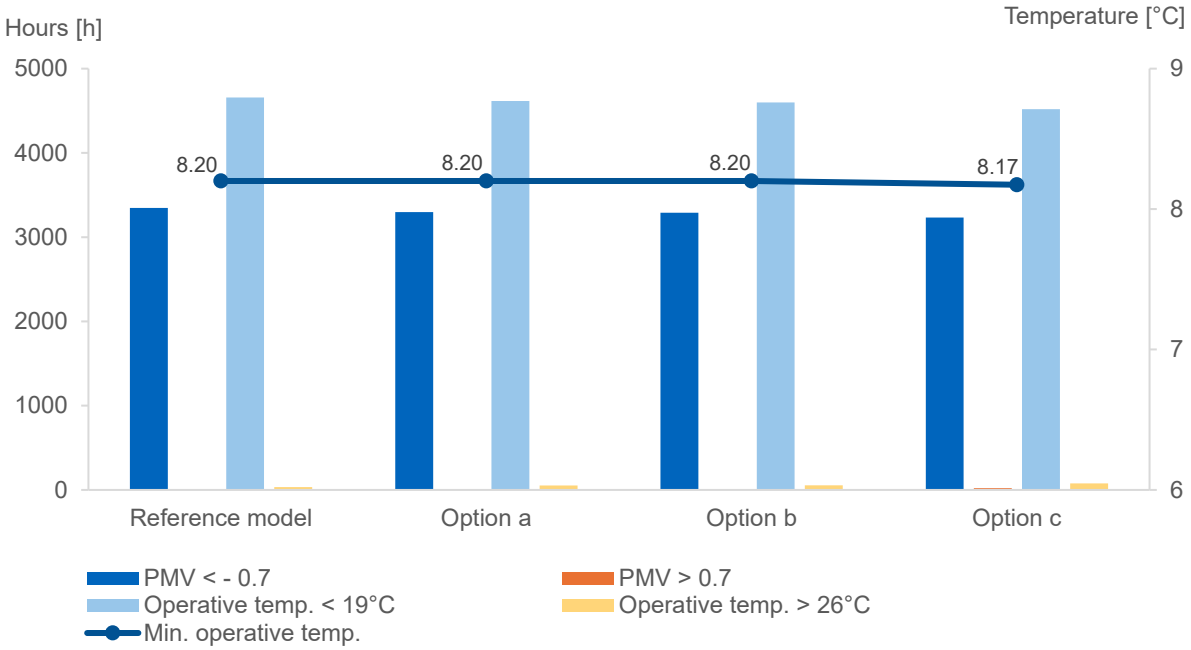

Figure 56: Thermal comfort dependent on the proportion and position of glazing facing south

Moving all south-facing windows to the outer edge of the wall decreases the number of hours with a PMV < -0.7 by 49 (option a). However, expanding one existing window instead of creating new small ones delivers better results. The best choice from a thermal point of view, with a reduction of the uncomfortably cold hours by 115, is the variant that does not receive shade from the tree (option c). An enlargement of any of the two eastern windows (option b) would furthermore not comply with the required minimum distance of 1.5 meters to existing openings (see “Openings,” p. 49). Consequently, the preliminary design of the façade is modified in accordance with option c.

6.4.4. Optimization 4: Proportion of roof glazing

The following assesses the influence of the size of the roof’s glazing. In the simulation model, this is realized by increasing the glazed area in steps of 1m^2. All windows are placed on the

south-facing plane of the roof and are assumed to be shaded by the foliage of the tree from April through October. The resulting impact on thermal comfort is depicted in Figure 57.

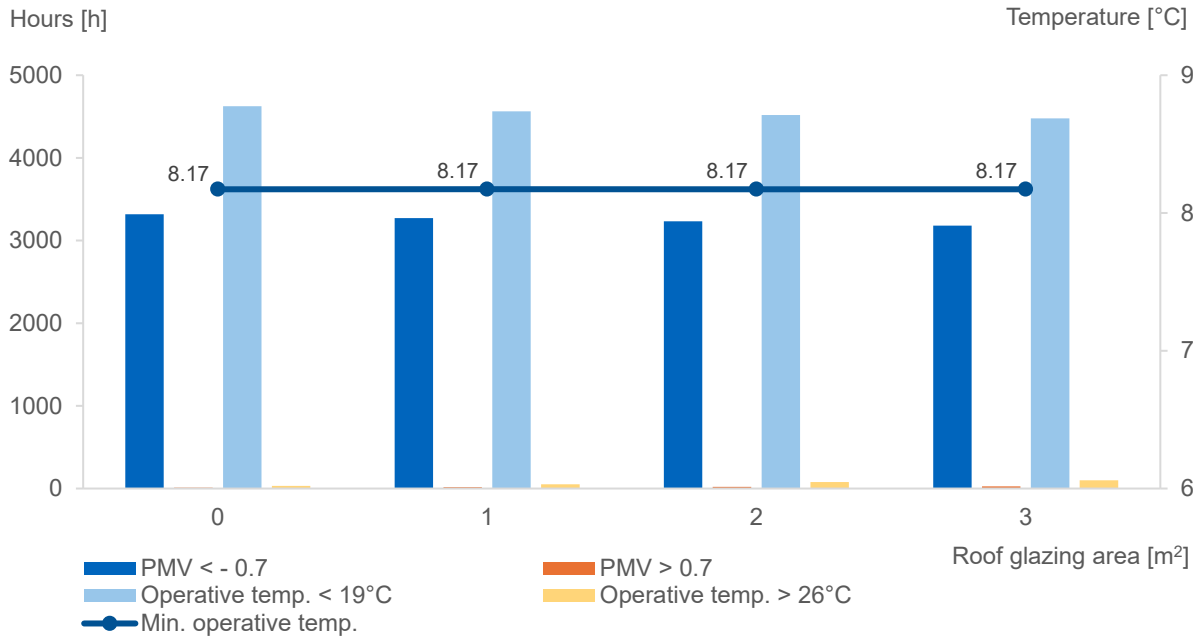

Figure 57: Thermal comfort dependent on the area of the roof glazing

For each square meter of glazing added, the number of uncomfortably cold hours is reduced by roughly 100. An evaluation of the heating energy requirements for each case reveals that approximately 73KWh/a can be saved with every meter the glass area is increased (Annex A12). For the purpose of maximizing passive solar heat gains, a larger proportion of glazing therefore seems to make sense. However, the simulations also show that with larger glazing areas the number of hours with temperatures above 26°C starts to increase. As the boundary conditions of use under “Occupancy and schedules” (p. 57), have been defined to represent the most unfavorable case during the heating period, further assessments must be carried out to rule out the risk of overheating.

Figure 58 summarizes the improvements achieved by each optimization in terms of heating energy requirement.

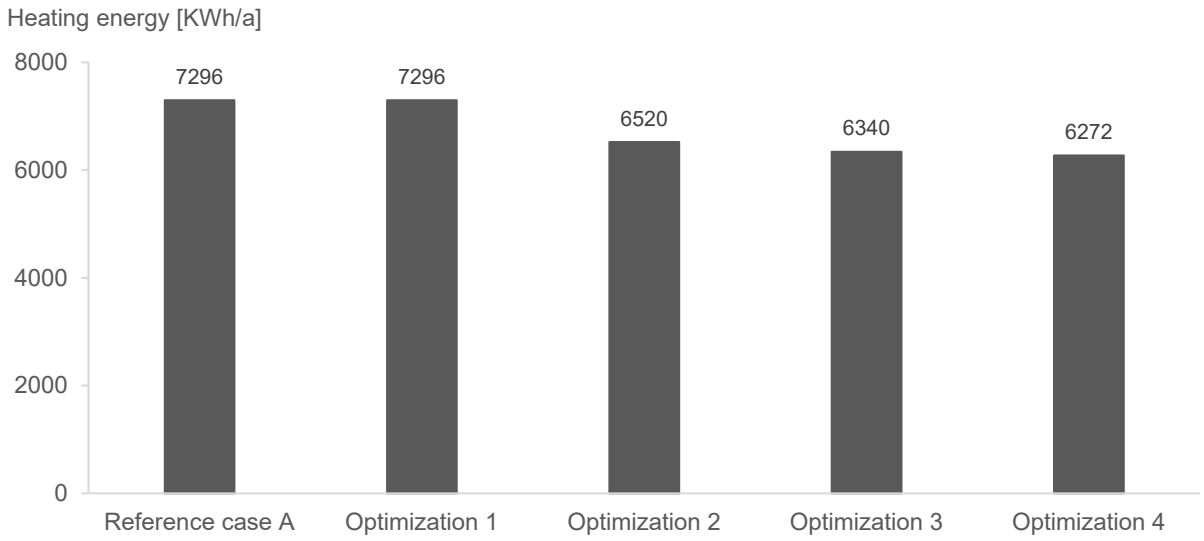

Figure 58: Optimization of heating energy requirement

6.4.5. Evaluation of different scenarios

To maintain long-term value, the cabin must be adaptable to various uses and capable of regulating changing exterior climatic conditions. The following chapter aims to determine whether the proposed retrofit measures and design concept are robust enough to ensure a habitable indoor environment under alternative circumstances. To achieve this, first, a climate file containing future data for the year 2050 is imported and assigned to the model (scenario 1). The data is obtained from Meteonorm and is based on the A1B scenario of the IPCC's Special Report on Emissions Scenarios (SRES). A1B describes a future world with very rapid economic growth, a global population that peaks in mid-century and declines thereafter, and a balance across all energy sources (IPCC, 2000, p. 4). Next, the impact of increased internal heat gains is examined (scenario 2) by selecting daily profiles (weekday and weekend) for a family household of four from the WUFI Plus database (Annex A13). Lastly, a variant where both occupancy and the exterior climate are changed is evaluated (scenario 3). Please refer to Figure 52, "Optimization strategy" on page 62, for an overview of the proceeding.

In Figure 59, the PMV values for scenarios 2 and 3, refer to a total of 7,388 usage hours. Based on this data, it is evident that users in scenario 2 feel cold 10% less of the time they spend inside the building compared to the single user in the reference case. A similar trend can be observed when comparing scenario 1 to the reference case: while the single occupant perceives the interior climate as being too cold 50% of the time in 2005, this is the case only 40% of the time in 2050. It can therefore be concluded that changes in the exterior climate and/or occupancy have a considerable impact on the interior environment. Figure 60 further supports this, showing that under the same climatic conditions, the family household requires roughly 1,200KWh/a less heating energy than the single person. The theoretical heating energy savings for the future cases (scenarios 1 and 3) are estimated to be approximately 766KWh/a.

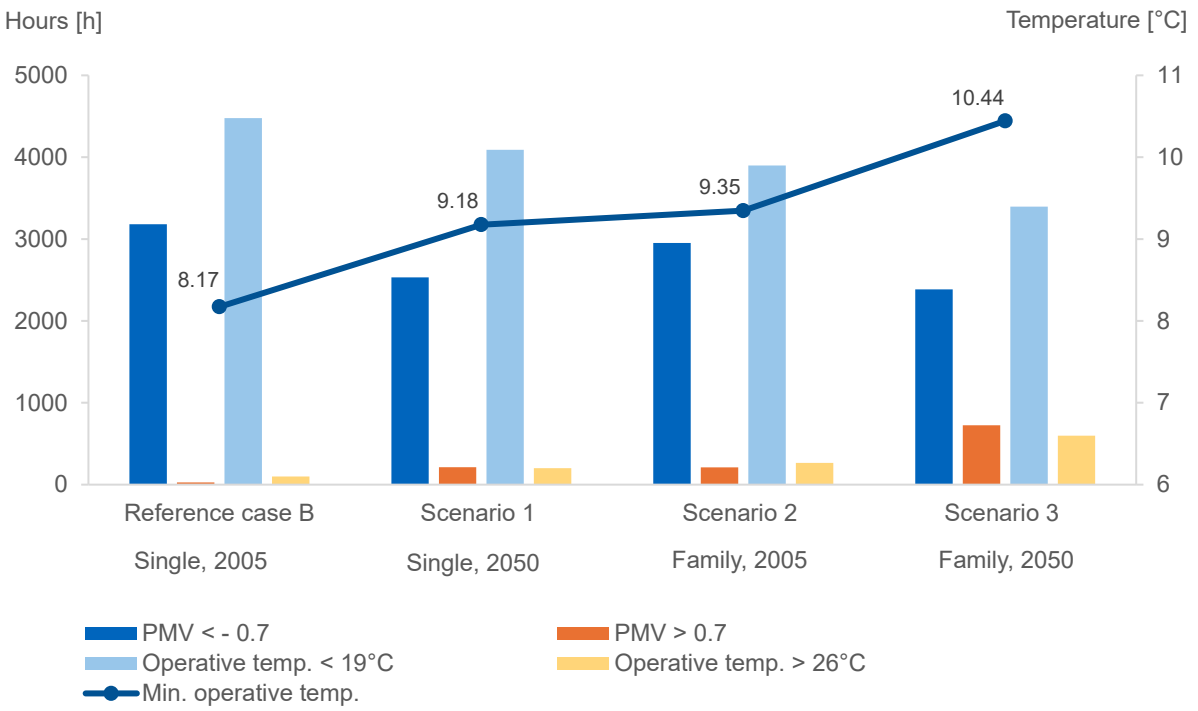

Figure 59: Thermal comfort dependent on varying scenarios

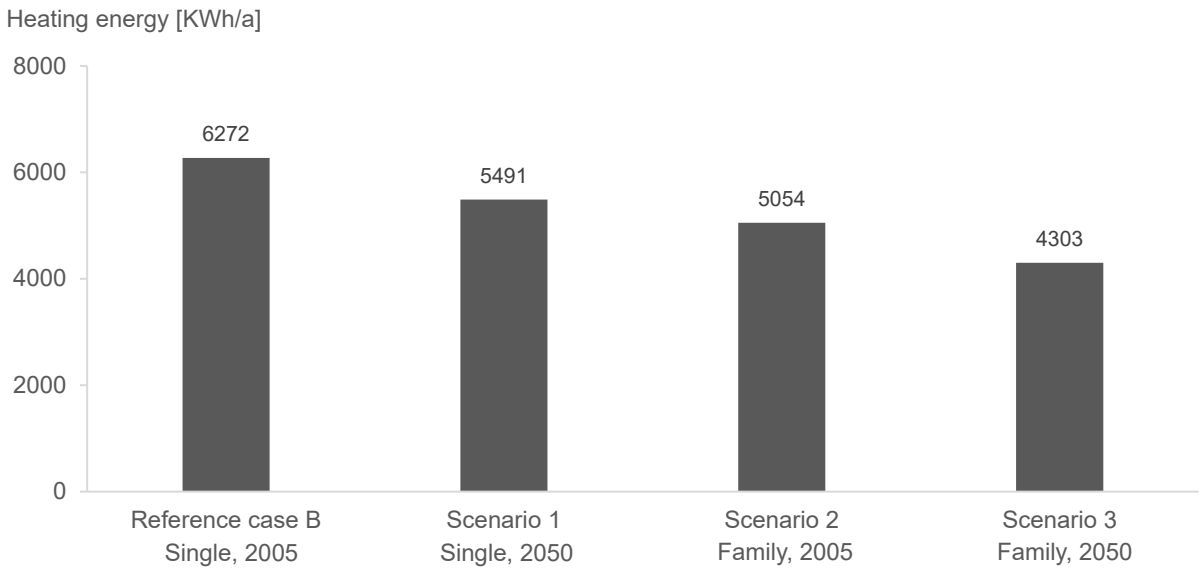

Figure 60: Heating energy requirements dependent on varying scenarios

However, with a greater number of persons inhabiting the building in the future (scenario 3) the number of uncomfortably warm hours (PMV > +0.7) increases to over 700 (9.8%), and the operative temperature stays above 26°C for almost 600 hours (6.8%) of the year. It should be noted that 224 of the uncomfortably warm hours occur in September and October, when the clothing insulation is higher. Conversely, high operative temperatures (>26°C) are mostly recorded from July to the beginning of September. According to Table NA.3 of the standard DIN EN 16798-1, the limit for cooling in category III buildings is 27°C. An evaluation of the

simulated data reveals that this limit is surpassed for 204 hours (2.3%) of the reference year. In the following section, further assessments are carried out to find out which strategies are the most effective in preventing excessive heat inside the building. Scenario 3 is used as the base model.

6.4.6. Influence of thermal mass and night ventilation

In addition to external shading systems, night ventilation and thermal mass are commonly used passive cooling methods. Currently, occupants open the windows for short periods of time during the day (see Table 11, “Variation of window opening duration,” p.59). Opening them during the night allows cool air to flow inside and the heat stored in the building materials to dissipate. The choice of using rammed earth for the floor of the cabin has been made, among other reasons, to compensate for the mass lost by the installment of internal insulation. For the next investigation, the thermal mass of the floor is varied by increasing the thickness of the loam layer in steps of 5 cm. To ensure a constant U-value, the thickness of the insulation is reduced accordingly. For each floor variant, the effect of night ventilation from July to September at different rates is evaluated.

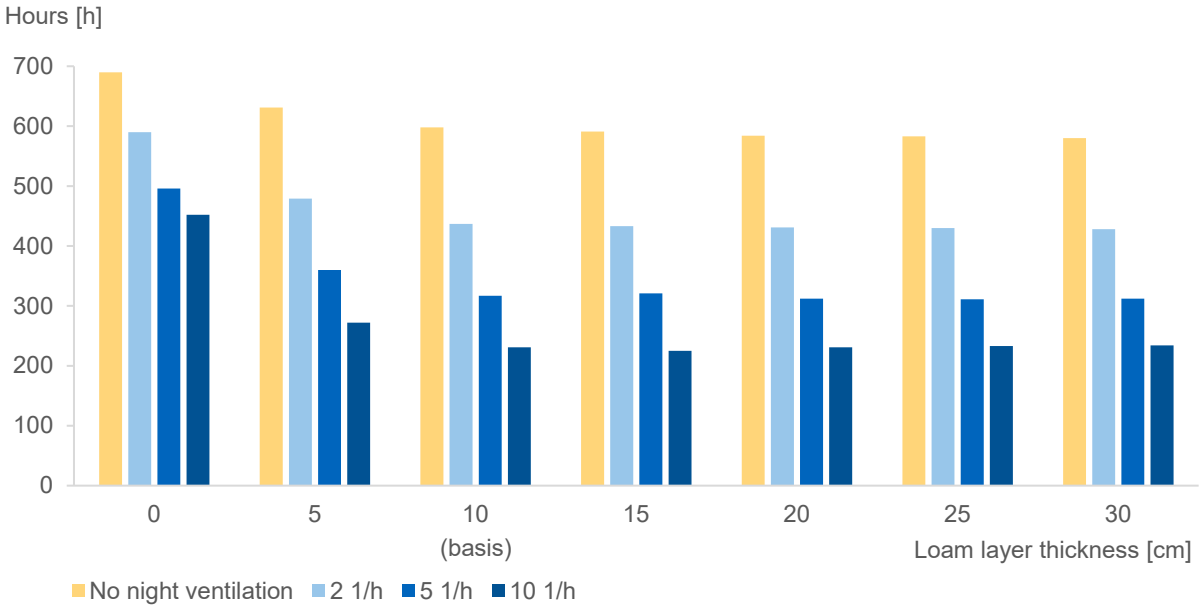

Figure 61: Hours above 26°C dependent on night ventilation and the thickness of the loam flooring (scenario 3)

Figure 61 shows that increasing the floor thickness beyond 10 cm does not enhance thermal comfort. Conversely, a greater number of hours with operative temperatures above 26°C is seen for thinner loam layers. Therefore, neither an increase of the flooring thickness above 10 cm nor a reduction below this value is recommended. Meanwhile, night ventilation is found to significantly reduce overheating, with its impact highly dependent on the number of air exchanges occurring per hour. An air change rate of 5 1/h reduces the number of hours with temperatures above 26°C from 598 to 317 (taking a 10 cm thick loam layer as the basis). A rate of ten air exchanges per hour reduces these hours to 231.

A further evaluation is performed to analyze the effect of increasing the mass of the intermediate floor. For this purpose, a loam infill between the wooden beams is modeled. The area of the upper level of the cabin is set to 30 m^2 and the thickness of the loam layer is increased in steps of 2.5 cm. As before, the impact of night ventilation at varying rates is also assessed.

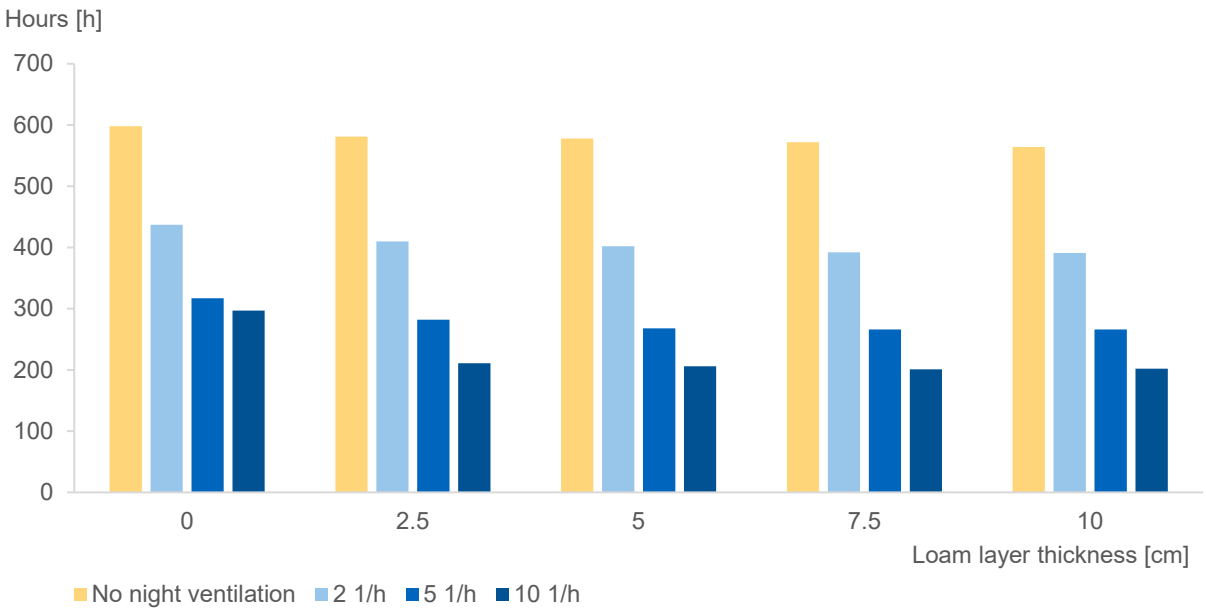

Figure 62: Hours above 26°C dependent on night ventilation and the thickness of the intermediate floor's loam infill (scenario 3)

Without night ventilation, a 2.5 cm thick loam infill leads to 17 fewer hours above the threshold of 26°C (Figure 62). Further thickness increments show almost no impact on overheating. However, at an air change rate of 5 1/h, a 5 cm thick layer results in an improvement of 15% related to the variant without the infill. Adding mass to the design of the intermediate floor furthermore provides insulation against airborne and structural noise. To eliminate the drying time, adobes without mortar can be used. The position between the beams has the advantage of a lower structural height (Minke, 2009, p. 111). A layer thickness of more than 5 cm is not recommended due to the additional weight the joists must carry.

6.4.7. Influence of shading devices

In addition to the strategic use of overnight natural ventilation, overheating is prevented by shading transparent components from sun radiation. As of now, the external shutters in the courtyard are set to close automatically to 75% (reduction factor 0.3) when the temperature inside the building reaches 25°C. In the following, these parameters are optimized and their effect on reducing the count of warm hours is analyzed. In the first step, the temperature threshold at which shutters are closed is gradually lowered. Then, two further simulations are run to estimate the impact of adjusting the reduction factor. In all cases, a 5 cm thick loam infill

is modeled between the joists of the intermediate floor and an air exchange of 5 1/h is set during the night.

Like in the previous graphs, Figure 63 depicts the number of hours with operative temperatures above 26°C for each variant simulated. To provide more detailed information about the thermal performance of the building during summer, the yearly maximum temperature and the number of hours with operative temperatures greater than 27°C are also shown. It should be noted that lowering the design temperature in the simulation affects both the sun protection of the glazing facing the courtyard and the large south-facing window.

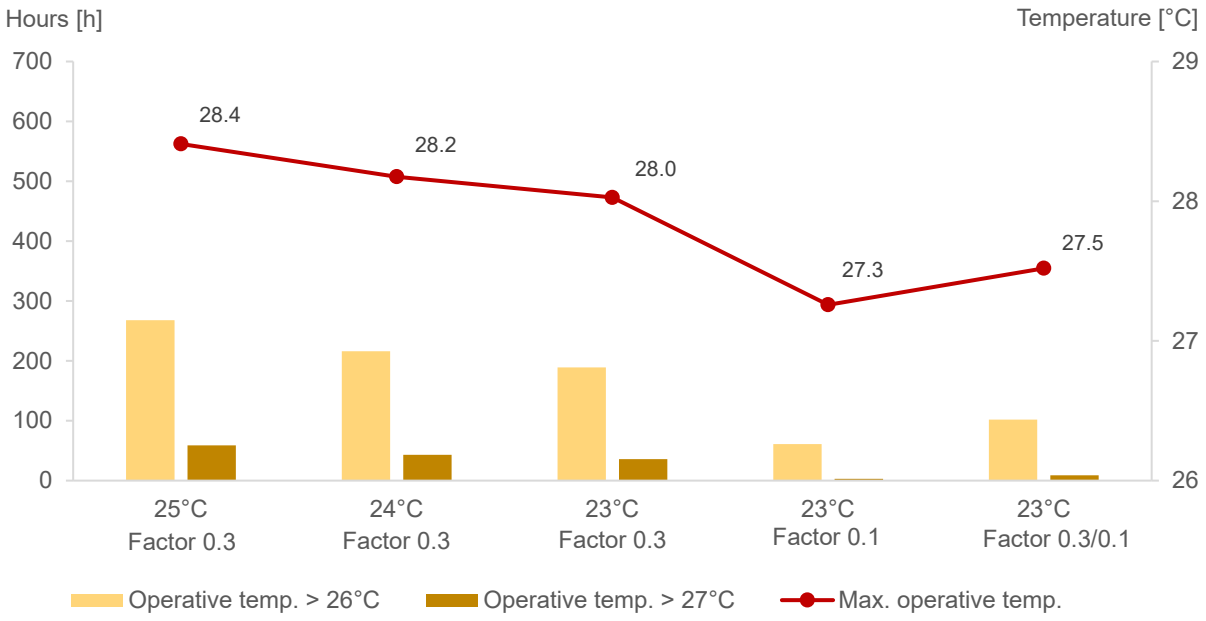

Figure 63: Overheating dependent on design temperature and reduction factor of shading devices (scenario 3)

With a design temperature of 24°C, the initial 268 hours with values greater than 26°C are reduced to 216. It is warmer than 27°C during 43 hours of the year instead of 59, and the maximum operative temperature drops by 0.2 degrees. At a threshold of 23°C, an additional improvement of about 10% is seen. The maximum temperature reached in this case is 28°C.

Thus, adjusting the activation time of the sun protection based on the interior temperature results in a moderate improvement of the indoor environment. However, greater impact is made when the western shutters are closed almost completely (reduction factor 0.1). Here, the operative temperature climbs higher than 26°C for as many as 61 hours and higher than 27°C for only 3. This indicates that the low afternoon sun reaching the west façade during July and August is the main driver for rising temperatures inside the cabin. During particularly hot days, when temperatures never sink below the 23°C threshold, this setting can lead to insufficient provision of daylight. Therefore, the last column in Figure 63 shows the results of an alternative case, in which a distinction is made between the shading parameters assigned to the ground floor glazing and the windows of the upper level. Through this setting, the number of hours with operative temperatures above 26°C rises to 102, but the limit of 27°C is surpassed for only 9.

Because of the shading cast by the courtyard walls, only some areas of the glazing are reached by solar radiation. This can be taken advantage of by designing flexible shading elements that allow occupants to adjust them in varying ways. In doing so, both the requirements of natural lighting and sun protection can be met. Moreover, based on the layout of the interior space in the final architectural design, the option of a lesser percentage of glazing towards the west should be considered. The present evaluations are intended to represent the most extreme scenario.

Figure 64 aids in understanding the cooling strategies discussed above. It shows the operative temperature inside the cabin from August 17 to August 21. The orange line represents the final building variant without night ventilation and with the initial settings for solar protection (25°C, factor 0.3). The blue line shows the effect of night cooling at an air change rate of 5 1/h. The green curve indicates the impact of adjusting the shading parameters to match the rightmost column of Figure 63.

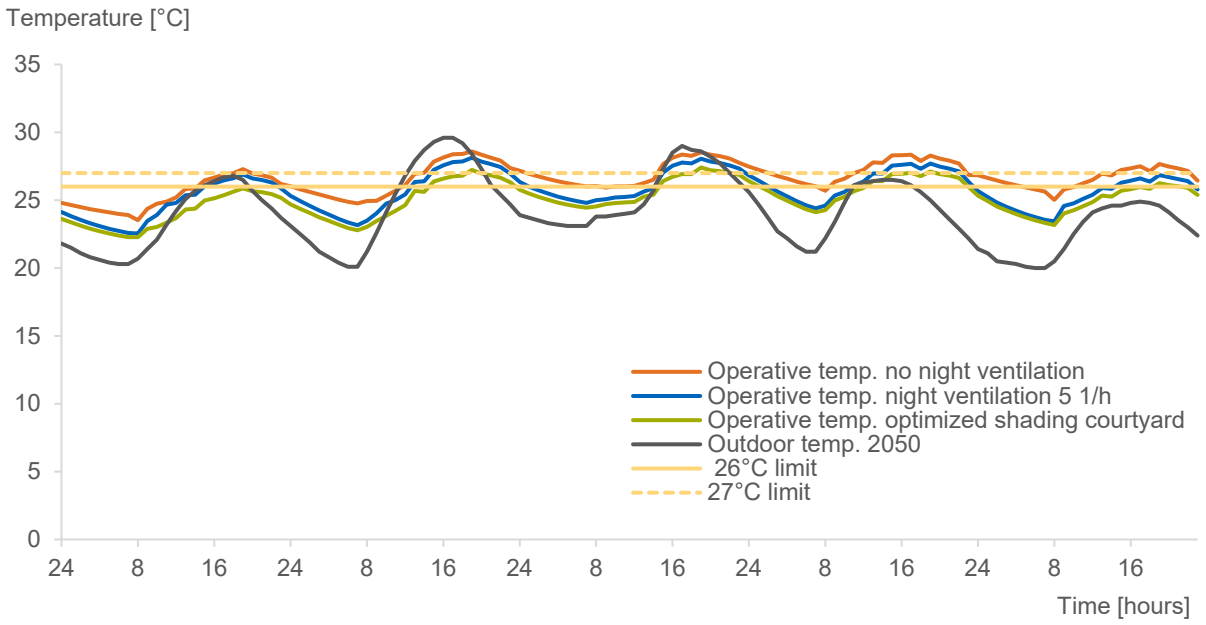

Figure 64: Operative temperature from August 17 to August 21 (scenario 3)

It can be concluded that the increased risk of overheating caused by the interior insulation and west-facing glazing can be significantly reduced through night ventilation and external shading devices. Nevertheless, a final assessment is carried out on the impact of reducing the area of the roof's glazing in scenario 3 (Figure 65). In all simulations, the design temperature at which solar protection devices are activated is set to 23°C and the reduction factor of the west shading to 0.3. The rate for night ventilation is 5 1/h.

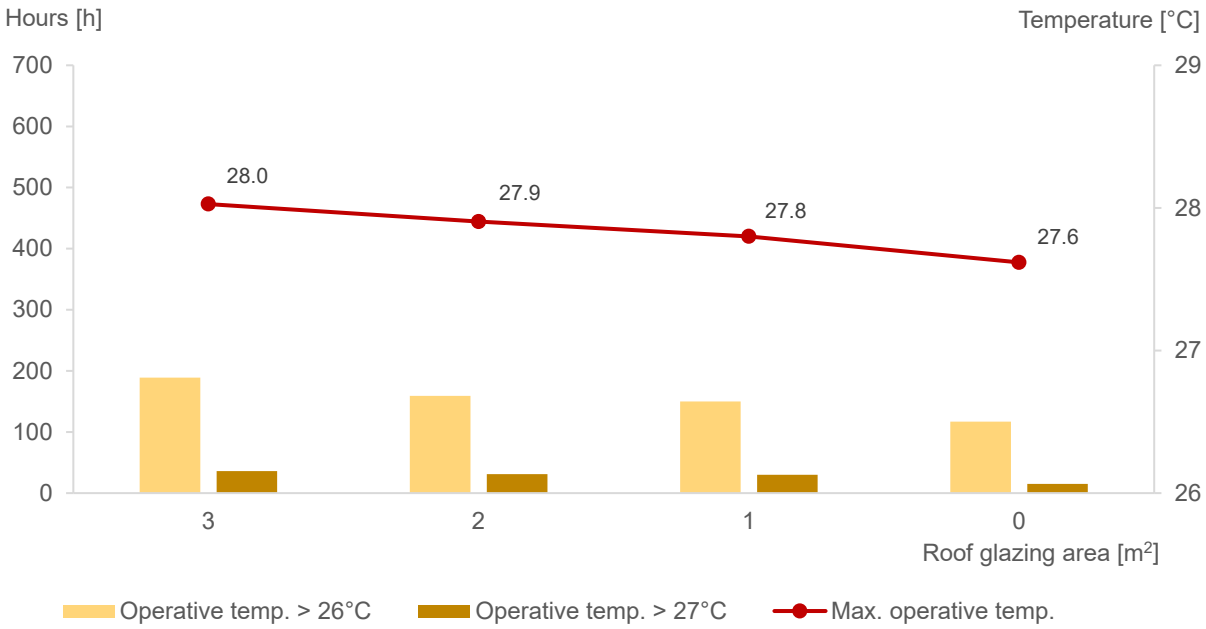

Figure 65: Overheating dependent on the roof's proportion of glazing (scenario 3)

As the glazing area decreases, so do the number of warm hours and the maximum operative temperature. At the same time, it becomes evident that even without any glazing on the roof, the reduction is not as significant as that achieved by the optimizing the western shading elements. A larger window area is favorable during the heating period (see "Optimization 4: Proportion of roof glazing," p. 65). Therefore, in the final model, the glazed area of the roof is maintained at 3 m^2.

6.4.8. Final model

The findings from the preceding parameter studies are now applied to a final building variant. Instead of creating three new openings in the south wall, the size of the westmost existing opening is enlarged to 2 by 1.5 meters. Additionally, its glazing is aligned with the exterior edge of the wall. For all windows, the overall Uw-value is changed from 1.8 to 1.4 W/m^2K. The Uf-value of the glazing is 1.1 W/m^2K. Frames are made, in accordance with the intervention guideline, of oak or chestnut wood, which corresponds to a Uf-value of 1.5 W/m^2K (Neuffer, 2024). They make up 30% of the window surface.

Compared to the initial model, a larger glazing area of 3 m^2 is assigned to the southern plane of the roof. A further optimization encompasses the sun protection of the large glazing area with views to the courtyard. The shading parameters used in the final model are the same as under "Optimization 1: Shading courtyard" (p. 62). Lastly, a 5 cm thick loam infill is added to the assembly of the intermediate floor.

Figures 66 and 67 compare the final model to the initial variant, i.e., reference case A (see Figure 52, "Optimization strategy," p. 62), in terms of thermal comfort and heating energy. The first graph shows the result without heating. In the second, an ideal heating system is set to maintain the interior temperature at 21°C from November 1 to April 30.

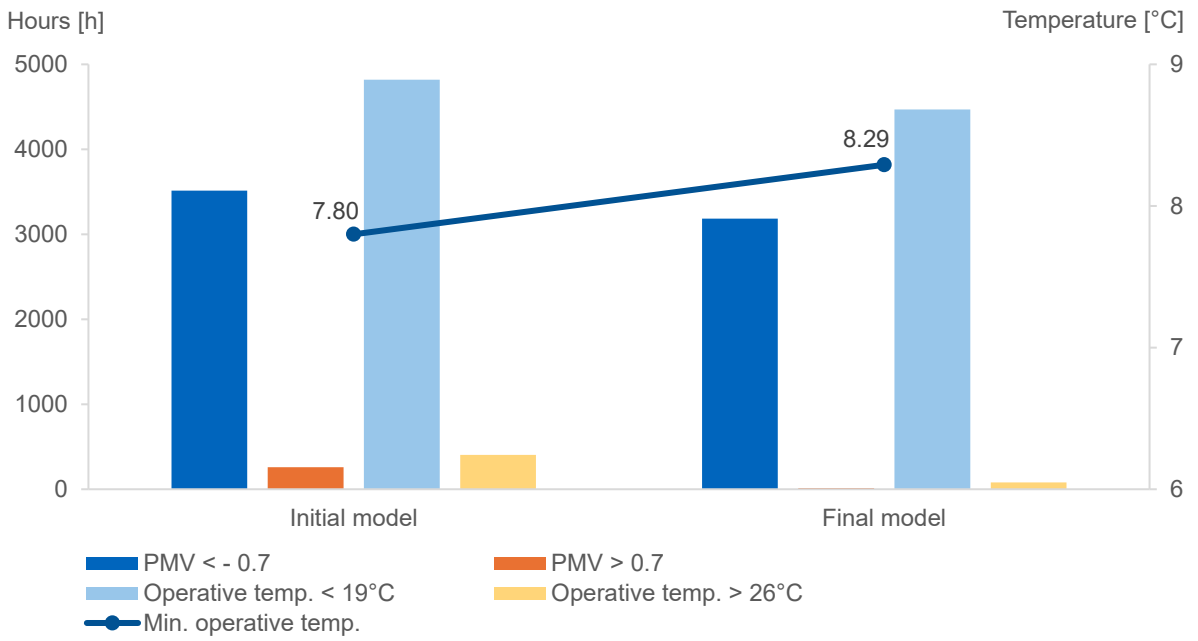

Figure 66: Thermal comfort, final model (single, 2005, unheated)

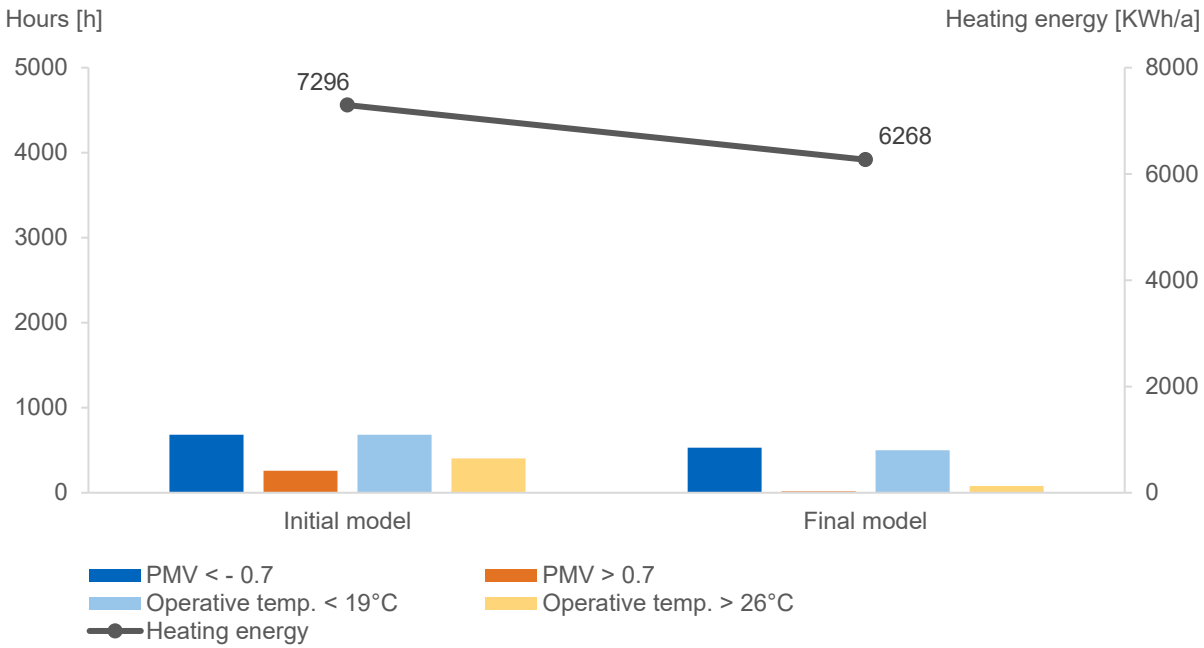

Figure 67: Thermal comfort, final model (single, 2005, heated)

Through the optimizations, improvements are achieved across all considered criteria. Compared to the reference model, the number of hours perceived as too cold by occupants is reduced from 3,514 to 3,165. Hours with operative temperatures below 19°C decrease from 4,820 to 4,469 and the minimum operative temperature rises from 7.8°C to 8.3°C. In other words, a 10% increase in thermal comfort is attained during the colder period of the year.

When examining the simulated heating energy required (Figure 67), savings amount to 14%. Operative temperatures beneath 19°C decrease by 27% compared to the reference building but still occur during 499 hours of the year. Hours with a PMV < -0.7 decrease from 682 to 529 and are spread throughout all months outside the heating period. In most cases, users can adapt to temperature fluctuations by adjusting their clothing. However, the months with the highest number of uncomfortably cold hours are May (170 hours) and October (136 hours), indicating that active heating might be required. According to DIN EN 16798-1, the limit for heating in category III buildings is 18°C. In the first two weeks of May, temperatures inside the cabin sink below this threshold for 150 hours. The same is true for 115 hours from October 24 to October 31. Therefore, a simulation with an extended heating period (from October 24 to May 15) is run to estimate the increase in energy demand. Calculation results reveal an annual increment of roughly 500 KWh (6766 KWh/a).

In addition to improving the interior climate during winter and enhancing the energy efficiency of the building, the final model is also more resilient against overheating. The number of hours with operative temperatures above 26°C decrease from 404 to 80. The maximum temperature reached is lowered from 30°C (see “Assessment of preliminary revitalization concept,” p. 59f.) to 27.0°C, occurring on August 20 at 6:00 pm. Users feel uncomfortably warm for only 14 hours. These results are calculated without using the passive cooling strategies discussed under “Influence of thermal mass and night ventilation” (p. 69ff.), ensuring the building’s adaptability to changing conditions in the future.

6.4.9. Discussion

One of the main findings of the simulation is the confirmation that installing internal insulation significantly influences the energy performance of the construction during the heating period. Further passive design strategies aimed at improving the interior climate of the cabin are strongly limited due to conservation constraints and thus yield a smaller effect. For instance, with regard to thermal comfort, larger glazing areas would be better oriented towards the south rather than the west. Despite optimizations, the building still requires active heating.

However, internal insulation also increases the risk of overheating. Therefore, identifying suitable and long-term solutions to this issue is crucial. According to the evaluation, the glazing facing the courtyard is the primary cause of uncomfortably elevated temperatures inside the building. Although the final simulation model considers this façade to be mostly transparent, a lower proportion of glazing is preferable in terms of thermal comfort, energy efficiency, and the higher carbon footprint associated with glass manufacturing. The optimum proportion should be determined using calculations of visual comfort and interior layout design. The former is beyond the scope of this thesis, whereas the latter will be addressed in the following chapter.

There are limitations associated with the simulation model used. While the thermal simulation aims to predict the indoor environment, it won’t perfectly match reality. Some degree of inaccuracy results from the climate file used, which contains interpolated data from nearby weather stations. This information is based on measurements taken in 2005 and thus cannot reflect the future climatic conditions at the site. Further imprecisions arise from the standardized profiles used to describe user behavior and occupancy numbers. As demonstrated by the evaluation of different scenarios, changes in occupancy directly affect the internal heat loads and can therefore substantially impact the interior climate.

Simplified assumptions must also be made for the material parameters, the rates of natural ventilation and infiltration, and shading provided by the tree. The values set in the model do not necessarily mirror actual circumstances. Due to the lack of more detailed information, input uncertainties are unavoidable at this early stage in the design process. The evaluation is therefore primarily intended to gain insights into the building's overall thermal performance and to inform design decisions. Given the available options and constraints, the thermal simulation enables adjustments to the preliminary design, optimizing both the living conditions and the energy efficiency of the cabin.

7. Architectural design proposal

Building on previous iterative investigations and a creative design process, an architectural proposal is developed to repurpose the case study building for residential use. The design explores how the interior space of the forsaken structure can be reimagined and transformed by interweaving the threads of the past and present. It aims to highlight the richness of its history and its modest, functional character, while simultaneously integrating modern features.

In the following pages, two site location plans identify the property's position within a broader geographical context, followed by a more detailed site plan that showcases the cabin and its immediate surroundings. Floor plans for both the ground and first floors, along with sections and elevations, illustrate the proposed interventions. Subsequently, alternative options for increasing the building's occupancy, such as flexible partitions and the potential expansion discussed under "Volume" (p. 47), are explored.

The proposal encompasses minimal alterations to the building's exterior appearance. These are: the creation of three small new openings, the enlargement of one existing window, and the removal of approximately 15% of the roof cladding. The latter, while nearly imperceptible from the outside, revitalizes the cabin by introducing a light-filled void, or courtyard.

Internally, open spaces span between the courtyard and an enclosed core placed near the short access façade. The simple rhythm of the roof structure, characteristic of this building type, informs the transversal division of interior space. On the ground floor, corridors along the southern and northern walls create axes connecting the building's front and rear, leading from the entrance into the living, dining, and kitchen area. This space, featuring expansive views through a large south-facing window, is intended to be the heart of the cabin. Full-height bi-fold doors open onto the courtyard, allowing a seamless transition between both environments and enhancing the sense of space.

In addition to maximizing natural light, the courtyard is conceived to channel breezes into the interior. Cross-ventilation can be achieved by opening both doors on the opposite side of the cabin. A double-height space around three sides of the central core improves air circulation, while the core itself directs airflow to the building's periphery, aiding in moisture removal from the internal insulation surfaces. Sliding doors enable separation of the main living area from the rest of the cabin as needed.

The central core extends upwards through both levels of the building and contains sanitary and storage functions, as well as a flight of stairs. On the first floor, a hardwood plank floor spans between the core and the courtyard, and horizontal ribbon windows distribute light evenly throughout the space. The bathroom, fully enclosed within the vertical nucleus, features a roof window for the use of daylight and moisture removal.

As was originally the case, the first floor can additionally be accessed externally via the massive staircase on the eastern façade. A catwalk made of grating panels bridges the double-height space, connecting the external entrance to the upper level. Grating provides a good flow of air and lighting, while lending the interior an abstract, contemporary feel. The choice of materials for it, such as steel or fiberglass, should be carefully considered for both

environmental impact and aesthetic appeal. In the entrance area of the cabin, the visual connections between both levels, along with the dynamic interplay of natural light filtering through the various openings, create an inviting and dynamic environment.

Overall, the design balances the preservation of the *cabaña pasiega*'s original character, a comfortable indoor environment, and the incorporation of contemporary design elements. It transforms the cabin into a secluded home that retains its compact constitution, with thick sandstone walls and small, irregular openings, while allowing contemporary open-plan living.

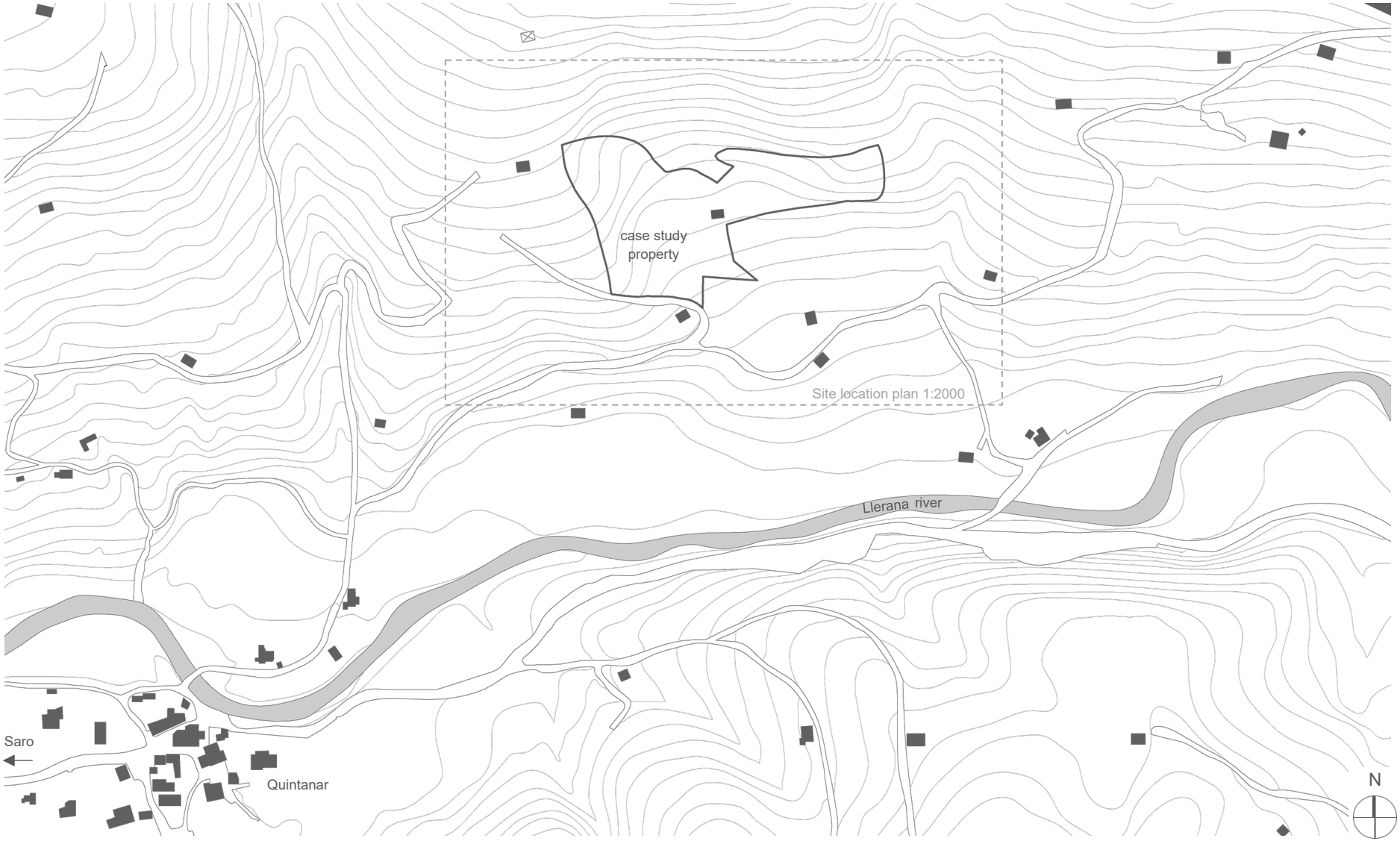

Figure 68: Site location plan, 1:5000

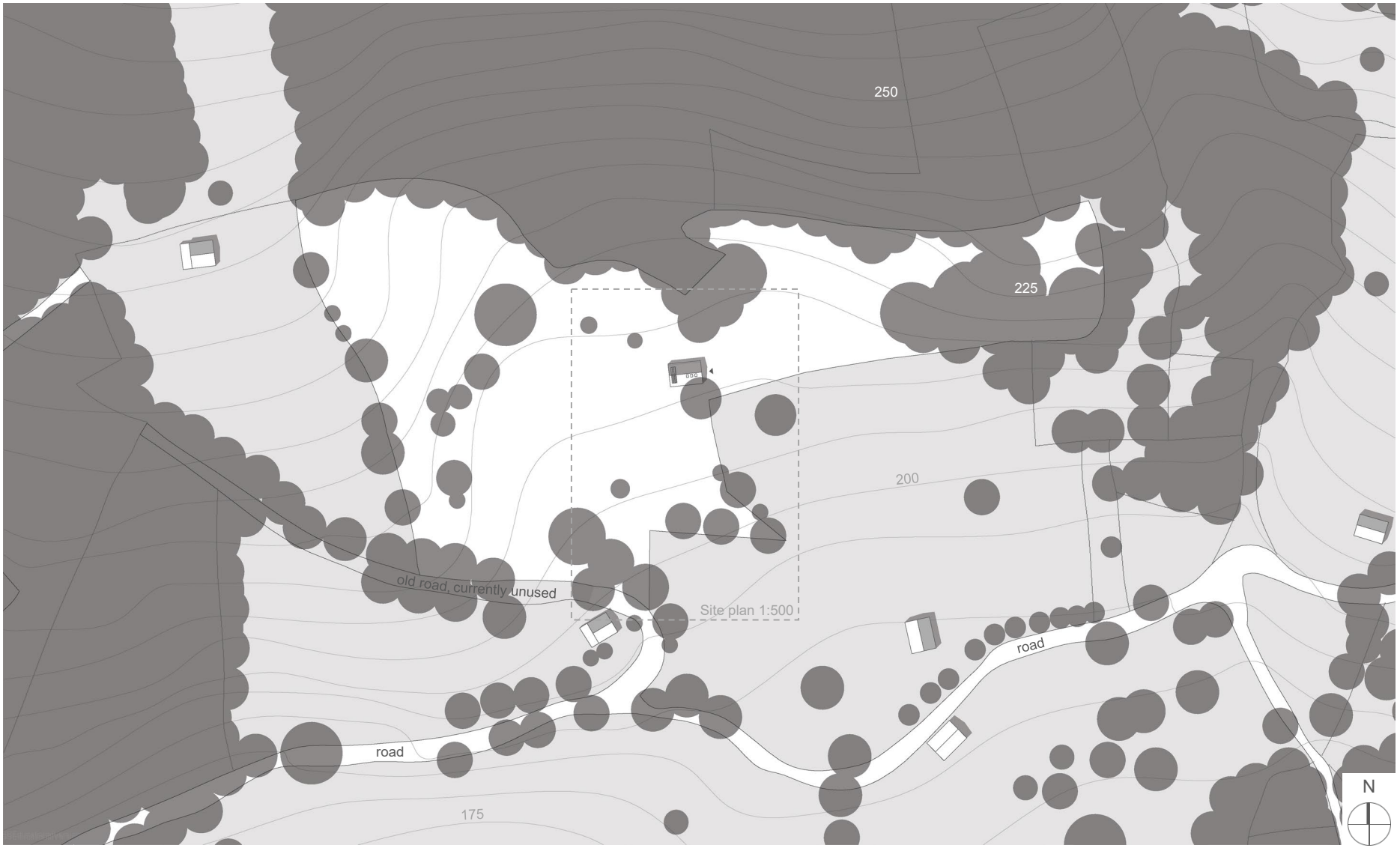

Figure 69: Site location plan, 1:2000

Figure 70: Site plan, 1:500

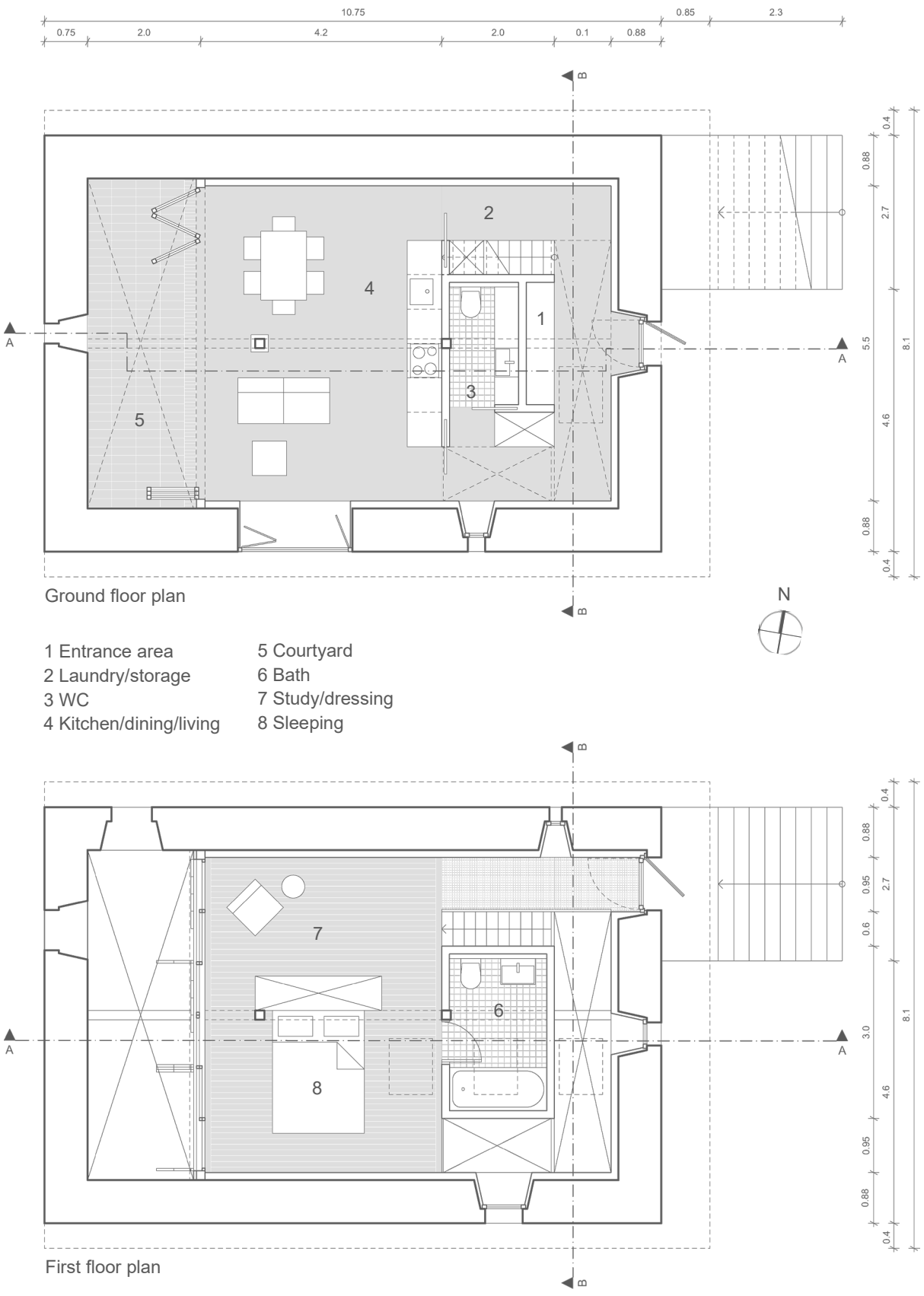

Figure 71: Floor plans, 1:100

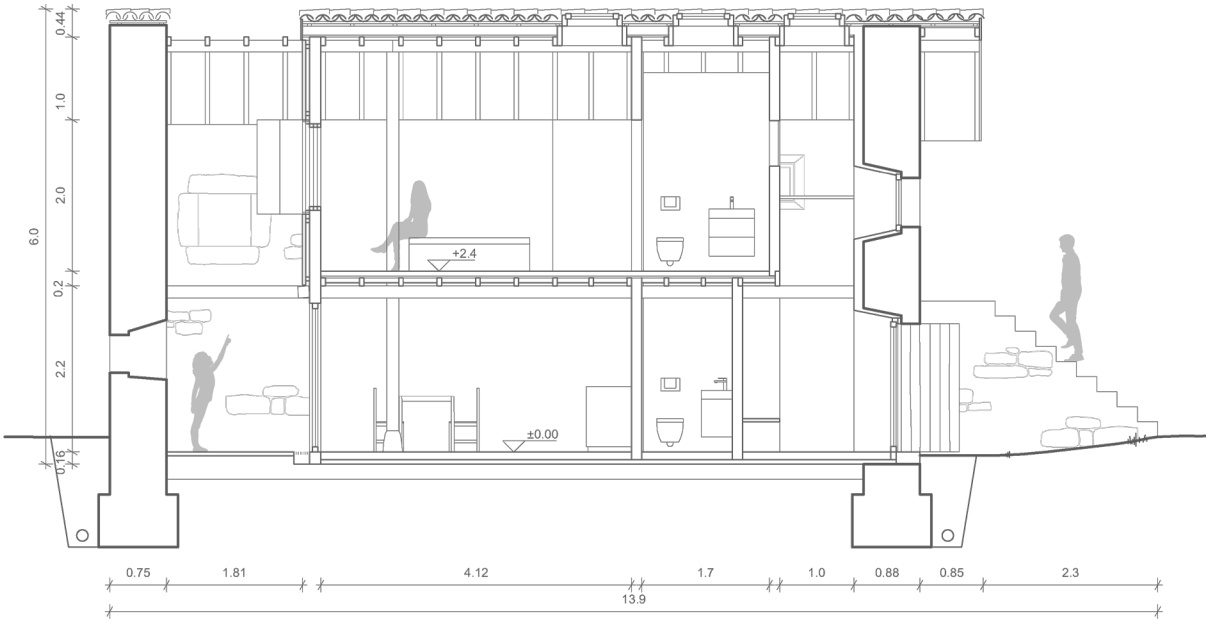

Figure 72: Section A-A, 1:100

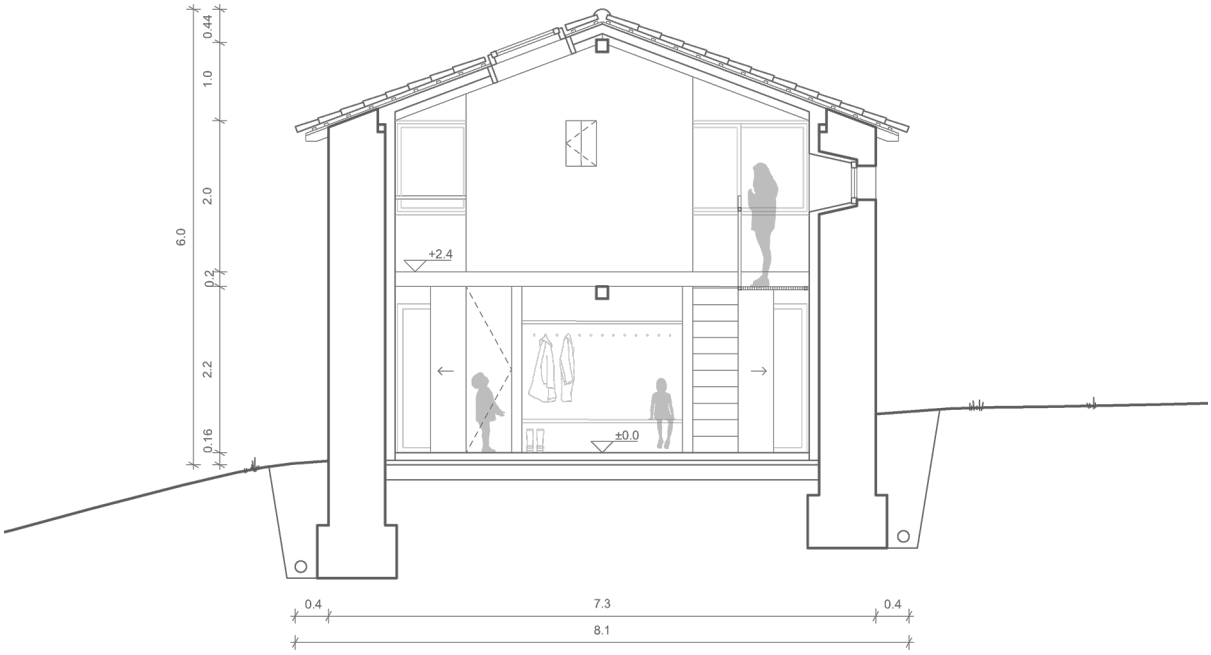

Figure 73: Section B-B, 1:100

Figure 74: East elevation, 1:200

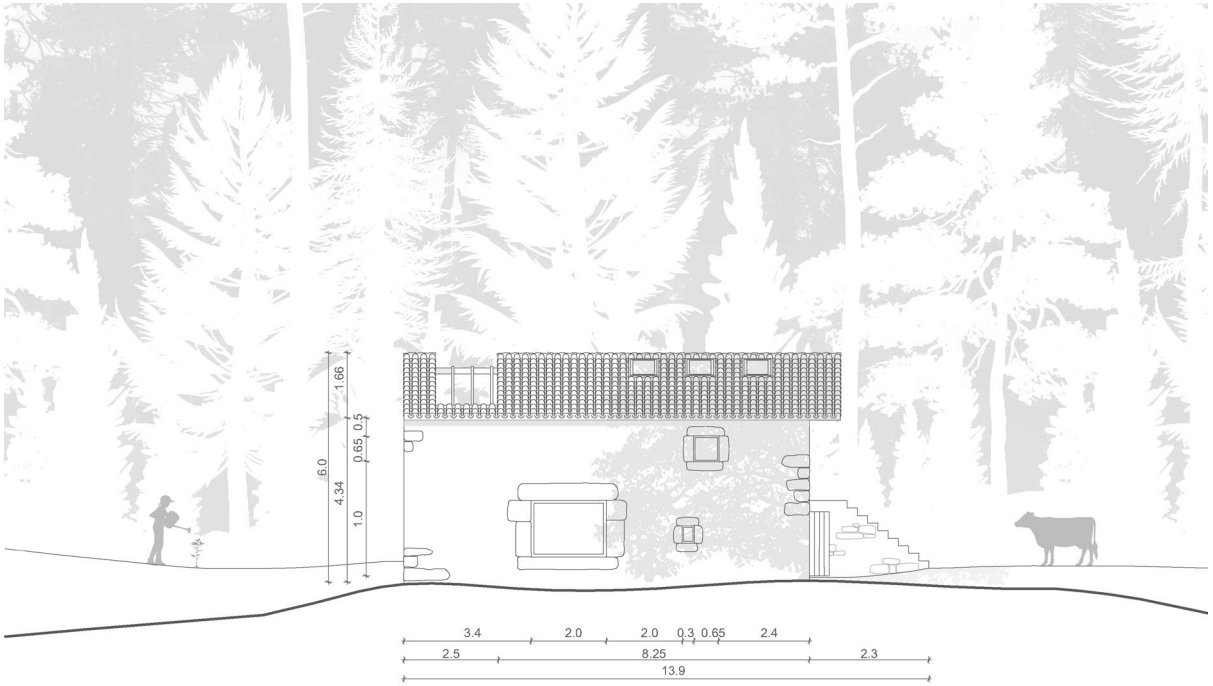

Figure 75: South elevation, 1:200

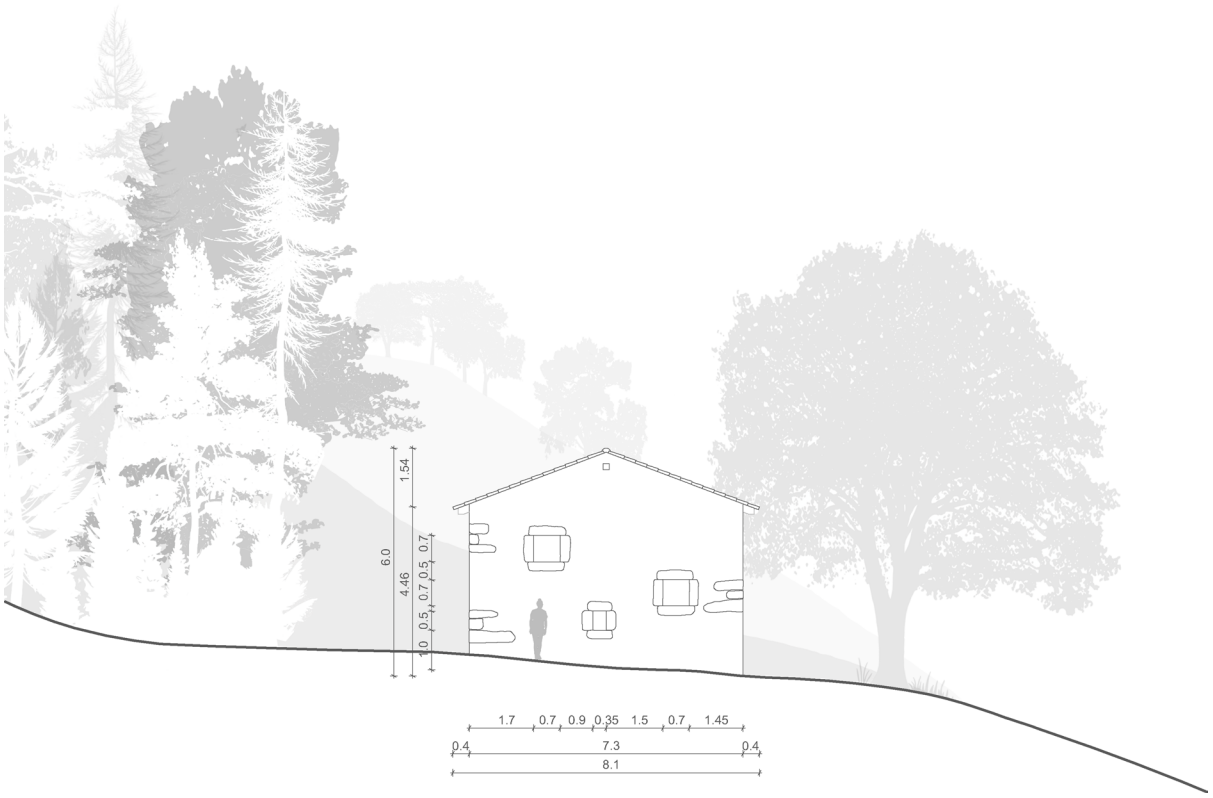

Figure 76: West elevation, 1:200

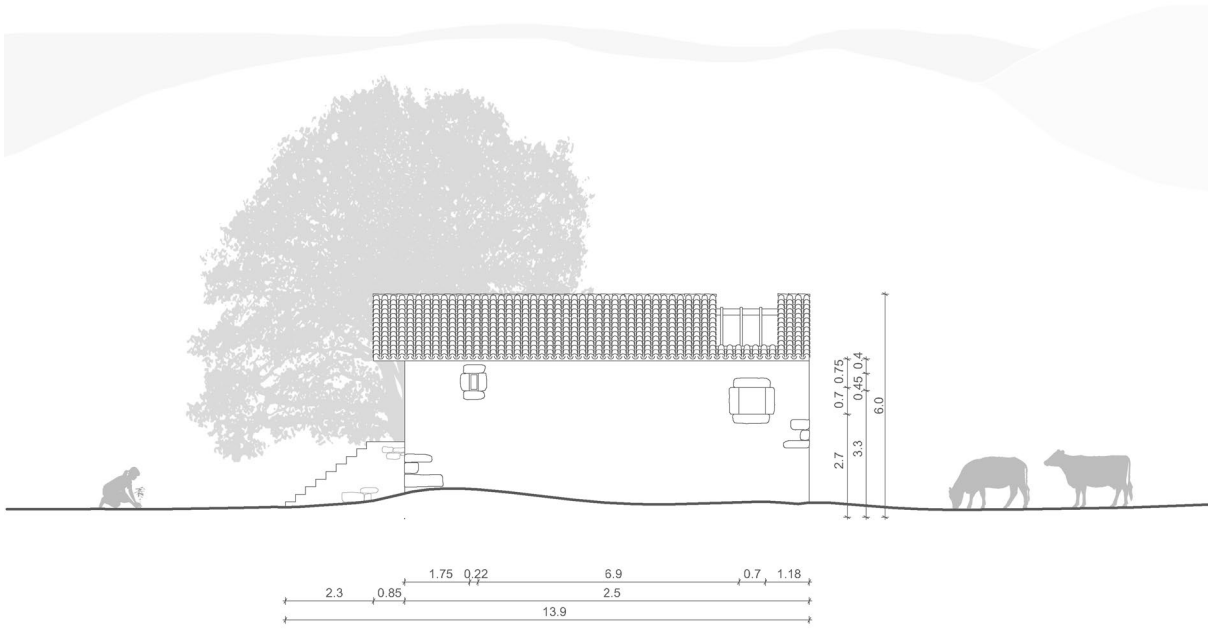

Figure 77: North elevation, 1:200

The cross-section below illustrates the courtyard and an adjacent volumetric addition, formed by extending a portion of the roof northward. The original building footprint flows into the new extension through an opening on the ground floor (Ground floor plan in Figure 79). Although conservation regulations limit the floor area of the expansion, it remains large enough to accommodate a separate bedroom. Given the generous height of the space, two single high-beds can be positioned on either side of the room, with storage space such as a closet and a large desk beneath them.

The upper level of the cabin can be divided into two individual bedrooms, with the option to optimize space by stacking the beds on top of storage units (First floor plan in Figure 80). As the number of residents grows, privacy becomes increasingly relevant. To address this, a partition with two additional sliding doors is proposed for the first floor, creating a corridor illuminated by one of the roof windows. This arrangement ensures that the bathroom can be accessed and used independently by all residents.

Figure 78 also presents the proposed design for the new façade facing the courtyard. Compared to the simulation model, the proportion of glazing is reduced. This modification results from the layout of interior spaces and the design of shading elements, which includes sliding bi-fold timber shutters manually operable from the inside. When closed, the shutters blend in perfectly with the exterior vertical paneling and are hardly perceptible. When open, they remain perpendicular to the façade, allowing natural light to enter while maintaining shade. The shutters can also be manually slid to the margins of the window ribbon to provide unobstructed views and increased lighting. On the gound level, two awnings positioned above the bi-folding doors provide additional shade while enabling unrestricted access to the courtyard.

.

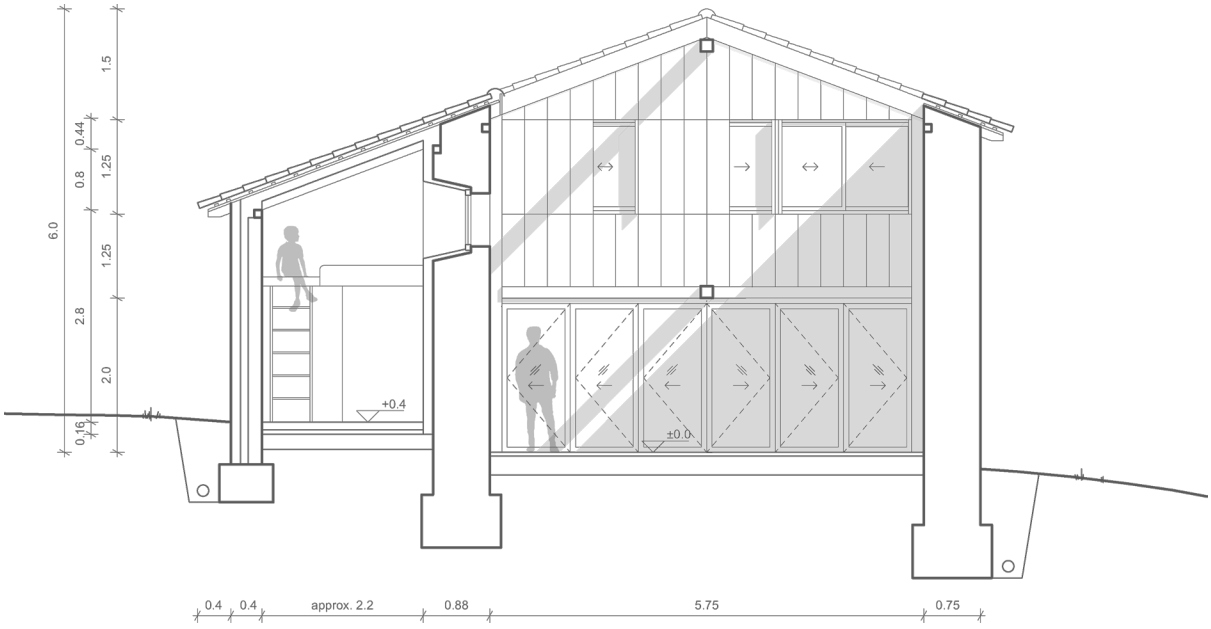

Figure 78: Section C-C, 1:100

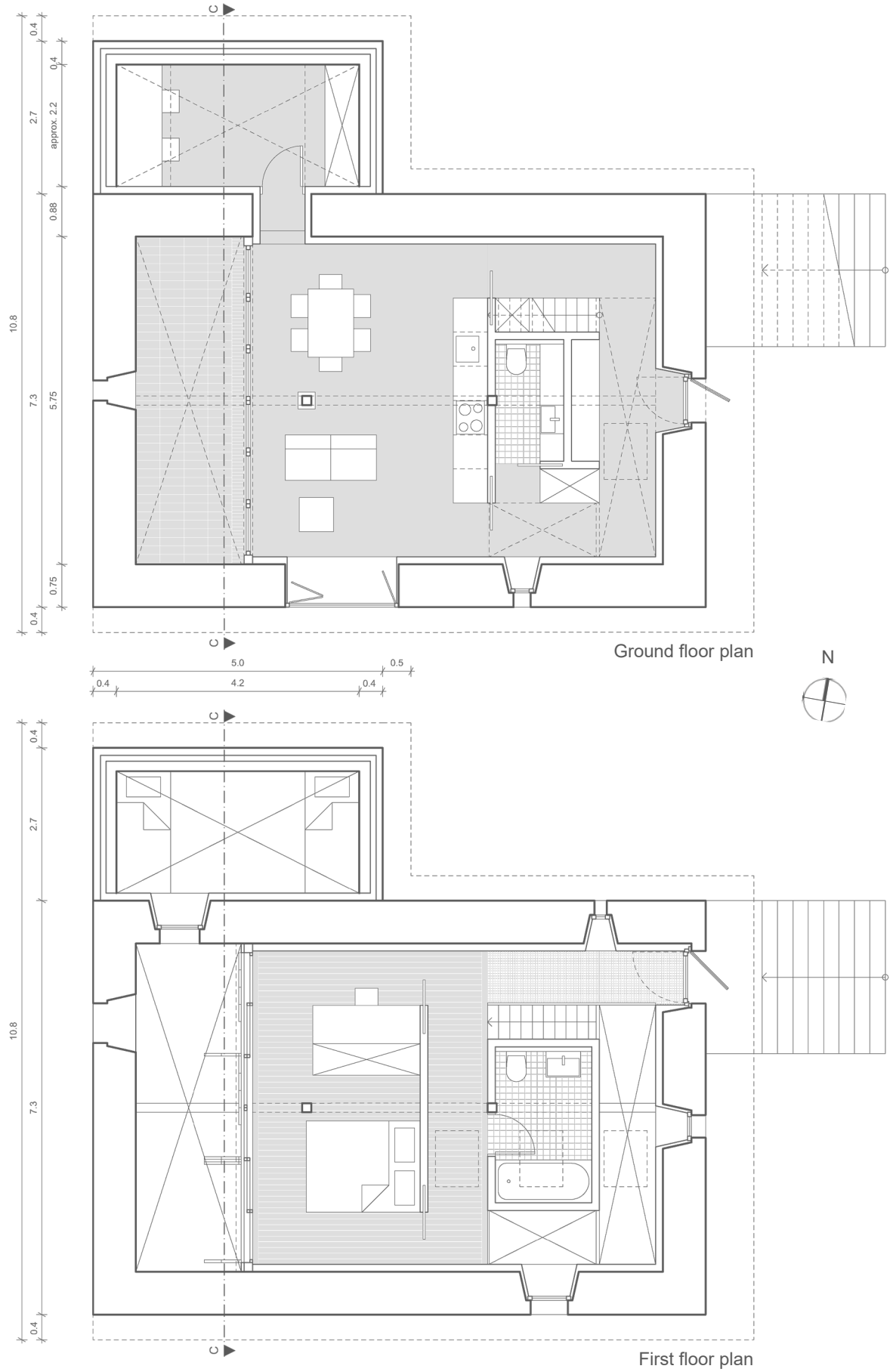

Figure 79: Floor plans future expansion (variant 1), 1:100

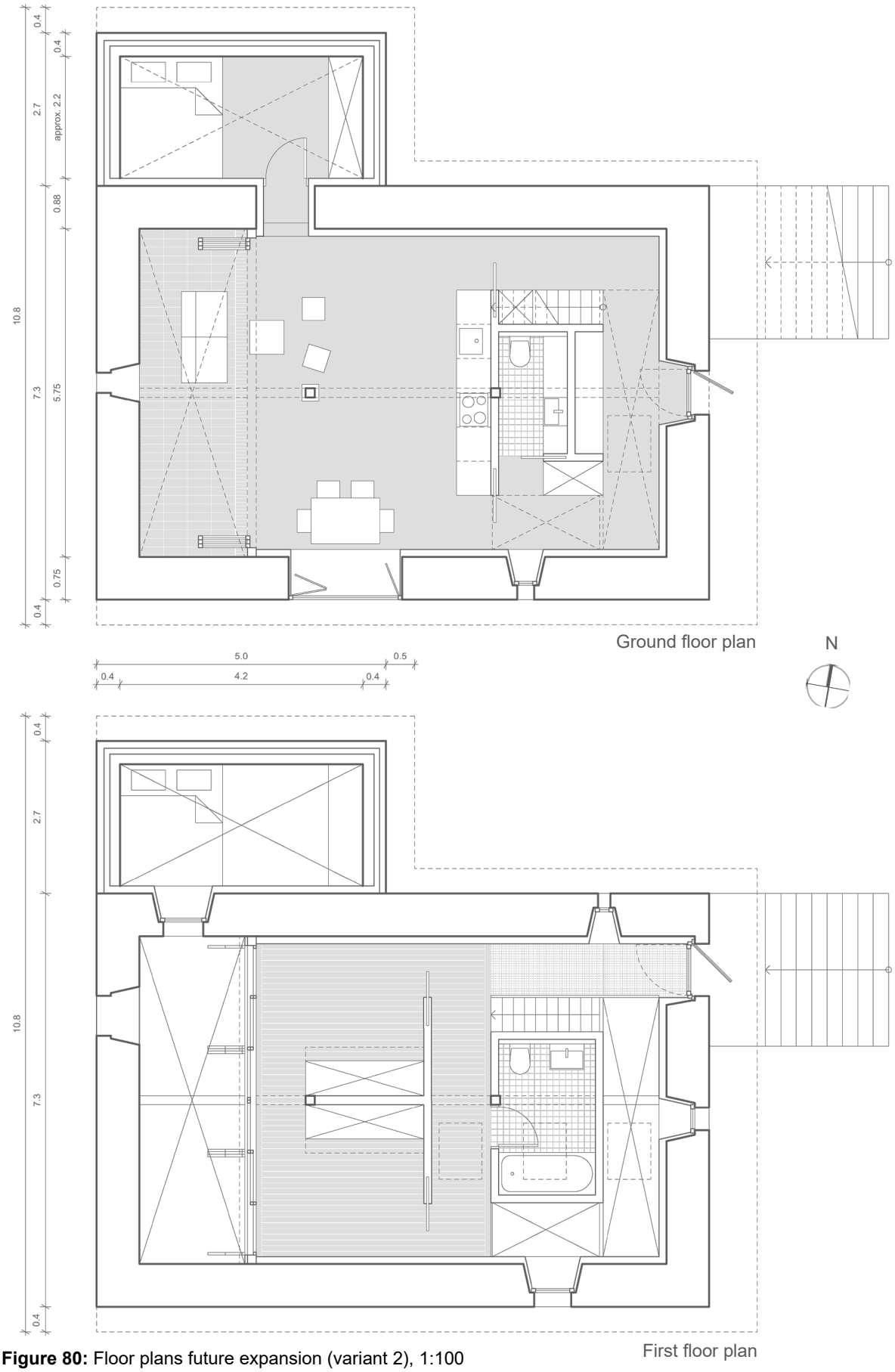

Figure 80: Floor plans future expansion (variant 2), 1:100

Conclusion

The revitalization of the *cabaña pasiega*, as explored in this thesis, underscores the delicate balance between preserving architectural heritage and adapting to modern comfort and sustainability standards. At the outset, a thorough investigation on the historical and cultural background of the *cabaña pasiega* highlighted its significance as a testament to the region's vernacular heritage, and intervention criteria established by local authorities offered a framework for design decision-making. Following, a detailed climate analysis provided valuable insights into the specific meteorological challenges of the Pasiego valleys. These investigations were critical in guiding the selection of appropriate retrofitting measures, which were tailored and applied to a case study building.

Thermal insulation showed to be pivotal to ensure both thermal comfort and energy efficiency. However, the use of internal insulation presented challenges related to moisture management. Therefore, the selected insulation system was evaluated using the dynamic simulation software WUFI Pro. The results revealed water uptake from outside and the reduced internal drying potential to be the biggest source of concern, prompting the decision to create a courtyard protecting the façade most exposed to driving rain. In addition, the analysis identified the need for adequate ventilation and an airtight construction.

Subsequently, the study shifted focus to the evaluation and optimization of the interior climate using the tool WUFI Plus. Initial simulations assessed the impact of interior insulation on thermal comfort and heating energy demand. While internal insulation effectively reduced heating energy consumption by over 50%, it also increased the risk of temperatures exceeding comfort thresholds during warm summer days. Hence, further simulations were conducted to explore strategies for mitigating this risk.

The study found a high proportion of glazing towards the courtyard to be the main driver for overheating. As options to create new openings and thus meet daylight requirements are constricted by preservation, this issue poses a point of conflict. The layout of the façade proposed in the final chapter consideres the interior arrangement of spaces as well as the operability of the shading system. However, further evaluations are needed to determine if daylight-needs can be met by this design. If this should not be the case, simulations demonstrated that the strategic use of external shading devices in combination with night ventilation can be an effective passive cooling strategy, even in scenarios of higher outdoor temperatures and increased internal heat gains.

During the colder months, it was possible to optimize the indoor environment by adjusting variables such as window quality and maximizing south-facing glazing. Nevertheless, active heating of the cabin remains necessary to achieve thermal comfort.

This thesis presents a comprehensive framework for the revitalization of the *cabaña pasiega*, though further research is required to refine and expand the proposed strategies. For instance, future studies could examine the long-term performance of retrofitted buildings and explore the integration of renewable energy systems.

Overall, the study emphasizes the need for policies and resources dedicated to preserving vernacular heritage, as undervaluation poses a serious threat to its existence. By demonstrating the feasibility and benefits of sustainable rehabilitation, it advocates for greater recognition and protection of vernacular architecture, and it underscores the importance of adopting a holistic approach that integrates both ecological and cultural considerations.

While applied to an individual case study building, the relevance of this work lies in that it aims to serve as a replicable model, thereby representing a significant step towards preserving cultural heritage in rural Cantabria while addressing contemporary environmental challenges.

References

Agencia Estatal de Meteorología & Ministerio para la Transición Ecológica (Eds.). (2018). *Mapas climáticos de España (1981-2010) y ETo (1996-2016).* https://doi.org/10.31978/014-18-004-2

Agencia Estatal de Meteorología, Ministerio de Medio Ambiente y Medio Rural y Marino & Instituto de Meteorología de Portugal (Eds.). (2011). *Iberian Climate Atlas.* https://www.aemet.es/documentos/es/conocermas/recursos_en_linea/publicaciones_y_estudios/publicaciones/Atlas-climatologico/Atlas.pdf

Alatalo, E. (2019, July 28). *Defensive and spiritual tata sombas of the Batammariba.* Field Study of the World. https://www.fieldstudyoftheworld.com/defensive-and-spiritual-tata-sombas-of-the-batammariba/

Arneill, P. (2023, October 19). *Yurt.* National Geographic Education. https://education.nationalgeographic.org/resource/yurt

Balak, M., & Pech, A. (2008). *Mauerwerkstrockenlegung: Von den Grundlagen zur praktischen Anwendung* (2. Aufl). SpringerWienNewYork.

Bc Maps. (n.d.). *Mapas vectoriales de Cantabria.* Retrieved September 18, 2024, from http://www.bc-maps.com/mapa-vectorial-eps/provincia-cantabria-illustrator/

Claytec. (2023). *Trockenbauleitfaden* [Brochure]. https://claytec.de/wp-content/uploads/2022/11/Claytec-Trockenbauleitfaden-Online_05-2023_RZ_EN_web.pdf

Claytec. (2024). *Arbeitsblatt Innendämmung* [Brochure]. https://claytec.de/wp-content/uploads/2022/11/Arbeitsblatt_Innendaemmung.pdf

Comisión Regional de Ordenación del Territorio y Urbanismo (Ed.). (n.d.). *Guía de Buenas Prácticas para la Intervención en el Patrimonio Arquitectónico Pasiego.* https://www.territoriodecantabria.es/documents/4279954/7432395/Gu%C3%ADa+de+Buenas+Pr%C3%A1cticas+para+la+Intervenci%C3%B3n+en+el+Patrimonio+Arquitect%C3%B3nico+Pasiego.pdf/2eeaa515-8791-f8d1-28be-ddd993243c15?t=1667562392750

Council of Europe. (Ed.). (2008). *The rural vernacular habitat, a heritage in our landscape.* Futuropa: For a new vision of territory and landscape (1). A Council of Europe Magazine. https://rm.coe.int/090000168093e668

Deutsches Institut für Normung. (2010, May). DIN EN ISO 10456: *Building materials and products – Hygrothermal properties – Tabulated design values and procedures for determining declared and design thermal values* (ISO 10456:2007 + Cor.

1:2009); German version EN ISO 10456:2007 + AC:2009.

Deutsches Institut für Normung. (2013, February). DIN 4108-2:2013-02: *Thermal protection and energy economy in buildings – Part 2: Minimum requirements to thermal insulation.*

Deutsches Institut für Normung. (2017, September). DIN EN 12831-1: *Energy performance of buildings – Method for calculation of the design heat load – Part 1: Space heating load*, Module M3-3; German version EN 12831-1:2017.

Deutsches Institut für Normung. (2018, April). DIN EN ISO 13789: *Thermal performance of buildings – Transmission and ventilation heat transfer coefficients – Calculation method* (ISO 13789:2017); German version EN ISO 13789:2017.

Deutsches Institut für Normung. (2018, September). DIN V 18599-2:2018-09: *Energy efficiency of buildings – Calculation of the net, final and primary energy demand for heating, cooling, ventilation, domestic hot water and lighting – Part 2: Net energy demand for heating and cooling of building zones.*

Deutsches Institut für Normung. (2020, November). DIN 4108-4:2020-11: *Thermal insulation and energy economy in buildings – Part 4: Hygrothermal design values.*

Deutsches Institut für Normung. (2022, February). DIN 68800-2:2022-02: *Wood preservation – Part 2: Preventive constructional measures in buildings.*

Deutsches Institut für Normung. (2022, March). DIN EN 16798-1: *Energy performance of buildings – Ventilation for buildings – Part 1: Indoor environmental input parameters for design and assessment of energy performance of buildings addressing indoor air quality, thermal environment, lighting and acoustics* – Module M1-6; German version EN 16798-1:2019.

Deutsches Institut für Normung. (2023, April). DIN EN ISO 7730: *Ergonomics of the thermal environment – Analytical determination and interpretation of thermal comfort using calculation of the PMV and PPD indices and local thermal comfort criteria* (ISO/DIS 7730:2023); German and English version prEN ISO 7730:2023.

Deutsches Institut für Normung. (2024, March). DIN 4108-3:2024-03: *Thermal protection and energy economy in buildings – Part 3: Protection against moisture subject to climate conditions – Requirements, calculation methods and directions for planning and construction.*

Dipasquale, L., Mecca, S., & Correia, M. (Eds.). (2020). *From vernacular to world heritage.* Firenze University Press. https://media.fupress.com/files/pdf/24/4872/16898

European Commission. (n.d.). *Renovation Wave: doubling the renovation rate to cut emissions, boost recovery and reduce energy poverty.* Retrieved March 2, 2024, from https://ec.europa.eu/commission/presscorner/detail/en/IP_20_1835

Fachverband Innendämmung (Ed.). (2016). *Praxis-Handbuch Innendämmung: Planung - Konstruktion - Details - Beispiele.* Rudolf Müller.

Fraunhofer IBP (Ed.). (2017). *WUFI Plus 3.1 Manual. https://wufi.de/de/wp-content/uploads/sites/9/2017.07_WUFI-Plus-Manual_en.pdf*

Fraunhofer IBP (Ed.). (2017, July). *WUFI How to: Guideline for assessing condensation problems in hydrophobic mineral fiber [PowerPoint slides]. https://wufi.de/de/wp-content/uploads/sites/9/2017.07_2_How_To_Condensation_Risk.pdf*

Fraunhofer IBP (Ed.). (2024, January). *WUFI: Guideline for assessing the risk of mould growth with WUFI [PowerPoint slides]. https://wufi.de/de/wp-content/uploads/sites/9/Guideline_MouldGrowthRisk_20240122.pdf*

Gamazo, J. V. (2020). *Rehabilitación de cabañas pasiegas, cabañas con Encanto* [Final degree project]. Universidad de Valladolid. http://uvadoc.uva.es/handle/10324/44646

García Alonso, M. (2004). *La cabaña pasiega origen y evolución arquitectónica* (2da Edición). Gobierno de Cantabria – Consejería de Cultura, Turismo y Deporte.

García-Lomas, A. G. (1960). *Los Pasiegos: Estudio crítico, etnográfico y pintoresco (años 1011 a 1960).* Editorial Cantabria S.A.

Giménez, N. D., & Álvarez, D. F. R. (2016). *Los temporales costeros en Cantabria: Caracterización e impactos sobre el territorio.* http://hdl.handle.net/10902/8519

Gobierno de Cantabria. (n.d.). *Catálogo de cabañales, cabañas y elementos singulars del patrimonio Pasiego.* Territorio de Cantabria. Retrieved September 12, 2024, from https://www.territoriodecantabria.es/cabanas-y-cabanales

Haupt, A. (2017). *Entwicklung eines passiven Energiekonzeptes am Beispiel eines Tiny House mit Stampflehmwänden* [Unpublished master's thesis]. Technical University Munich.

Hausladen, G., de Saldanha, M., & Liedl, P. (2012). *Building to Suit the Climate: A handbook.* Birkhäuser.

Hegger, M., Fuchs, M., Stark, T., & Zeumer, M. (2008). *Energy Manual: Sustainable architecture.* Birkhäuser; Edition Detail.

Hoffmann T. (2015 - 2024). *SunCalc sun position- und sun phases calculator.* Retrieved Mai 3, 2024, from https://www.suncalc.org

Intergovernmental Panel on Climate Change (Ed.). (2000). *IPCC Special Report: Emissions scenarios; Summary for policymakers. https://archive.ipcc.ch/pdf/special-reports/spm/sres-en.pdf*

International Council on Monuments and Sites (Ed.). (1999). *Charter on the built vernacular heritage.* https://www.icomos.org/images/DOCUMENTS/Charters/vernacular_e.pdf

Kölsch, P. (2015). *Hygrothermal Simulation of ventilated pitched roofs with effective transfer parameters. https://publica-rest.fraunhofer.de/server/api/core/bitstreams/bb218b68-ff54-4ea6-a518-19fae49cb75a/content*

Künzel, H. (2015). *Bauphysik und Denkmalpflege* (2. erw. Aufl). Fraunhofer IRB Verlag.

Lautensach, H. (1969). *Die Iberische Halbinsel* (2nd edition.). Keysersche Verlagsbuchhandlung GmbH.

Lin, Z., & Deng, S. (2008). *A study on the thermal comfort in sleeping environments in the subtropics - Developing a thermal comfort model for sleeping environments.* Building and Environment, 43(1), 70–81. https://doi.org/10.1016/j.buildenv.2006.11.026

Loidi, J. (2017). *Introduction to the Iberian Peninsula, General Features: Geography, Geology, Name, Brief History, Land Use and Conservation* (pp. 3–27). https://doi.org/10.1007/978-3-319-54784-8_1

Marsh, A. J. (2018). *Psychometric chart.* Retrieved September 16, 2024, from https://drajmarsh.bitbucket.io/psychro-chart2d.html

MASEA deprüfte Datenbank (n.d.). *Blähton 1.* Materialdatensammlung für die energetische Altbausanierung. Retrieved June 20, 2024, from https://www.masea-ensan.de/

Meteotest (Ed.). (2017). *Meteonorm Handbook part II: Theory.* https://meteonorm.com/assets/downloads/mn72_theory.pdf

Ministerio de Transportes, Movilidad y Agenda Urbana (2022, June 14). *Documento Básico HE Ahorro de energía.* Códico Técnico de la Edificación (CTE). https://www.codigotecnico.org/pdf/Documentos/HE/DcmHE.pdf

Minke, G. (2009). *Building with earth: Design and technology of a sustainable architecture* (2nd and revised edition.). Birkhäuser.

Murioz, M. V. (2005). *El régimen de vientos en la Cornisa Cantábrica.* Nimbus, 15–16, 203–222. https://www.divulgameteo.es/uploads/Vientos-Cornisa-Cant%C3%A1brica.pdf

Musso, F. (2012). *Hülle: Sonnenschutz.* In Skript EBB. Lehrstuhl für Baukonstruktion und Baustoffkunde, TUM.

Neuffer Fenster + Türen GmbH. (2024). *Gute U-Werte für Fenster, Informationen zu Energieeinsparverordnung (EnEV) und KfW-Förderung für effiziente Fenster.* Retrieved July 17, 2024, from https://www.neuffer.de/u-werte-fenster.php

Oswald, R. (Ed.). (2011). *Baupraktische Detaillösungen für Innendämmungen (nach EnEV 2009).* Fraunhofer IRB Verlag.

Pazold, M. (2015, December 17). *Natural Ventilation – Infiltration* [Online forum post]. https://www.wufi-forum.com/viewtopic.php?p=3432&hilit=infiltration&sid=9c60f01b4f378e8b6c383955cd057f09#p3432

Pilz, A. (Ed.). (2012). *Lehm im Innenraum: Eigenschaften, Systeme, Gestaltung* (2., erw. Aufl). Fraunhofer IRB Verlag.

Rudofsky, B. (1964). *Architecture without architects, an introduction to nonpedigreed architecture.* The Museum of Modern Art: Distributed by Doubleday, Garden City, N.Y. https://www.moma.org/documents/moma_catalogue_3459_300062280.pdf

Scheffler, G. A. (2016). *Bauphysik der Innendämmung.* Fraunhofer IRB Verlag.

Schmidt, Th. (2002). *Online-Hilfe für WUFI-pro 3.3 (d), 71 help topics.* Fraunhofer IBP. https://wufi.de/download/wufi_pro33_d_help.pdf

Schneider, R. (n.d.). *Holzbalkendecke mit Holzfaserdämmung.* Retrieved September 18, 2024, from https://holzlehm.de/2015-holzfaserdaemmung/balkendecke.htm

Schröder, H., & Schroeder, H. (2010). *Lehmbau: Mit Lehm ökologisch planen und bauen: mit 55 Tabellen* (1. Aufl). Vieweg + Teubner.

Schulstelle-traunstein. (2005). *Fensterlüftung.* Retrieved July 16, 2024, from http://www.schulungsstelle-traunstein.de/Energieberatung/background/printable/53040296650896a21/530402966a05262f6/530402966a0715b5f/index.html

Sobaos y Quesadas Joselín S.L. (2019). *Heritage built around the Pasiego valleys.* Retrieved September 18, 2024, from https://www.sobaosjoselin.com/en/Pasiegos-valleys/

Solargis. (2024). *Global Solar Atlas.* Retrieved September 18, 2024, from https://globalsolaratlas.info/map

Soprema GmbH (Ed.). (2024). Pavatex: *Holzfaser-Dämmsysteme, Dach-Technik Systemlösungen, Planung und Verarbeitung für den Profi* [Brochure]. https://www.pavatex.de/fileadmin/user_upload/40_Broschueren/Broschuere_PAVATEX_Dach-Technik.pdf

UNESCO World Heritage Centre. (2024). *World Heritage List.* Retrieved September 11, 2024, from https://whc.unesco.org/en/list/

Upton, D. (2006). *Residence.* JSTOR. Retrieved September 18, 2024, from https://jstor.org/stable/community.8758482

Valles Pasiegos - El secreto de Cantabria. (n.d.). *The Pasiegas Cabins: An Immense Heritage Legacy of the Region.* Retrieved September 18, 2024, from https://www.vallesPasiegos.eu/en/the-pasiegas-cabins/

Vickery, R. L. (n.d.). *Stone farmhouse, Portugal.* JSTOR. Retrieved September 17, 2024, from https://jstor.org/stable/community.22119538

Volhard, F. (2021). *Bauen mit Leichtlehm: Handbuch für das Bauen mit Holz und Lehm* (9., aktualisierte Auflage). Birkhäuser.

Volhard, F., Röhlen, U., & Breidenbach, P. (with Dachverband Lehm). (1999). *Lehmbau-Regeln: Begriffe, Baustoffe, Bauteile.* Vieweg.

Wissenschaftlich-Technische Arbeitsgemeinschaft für Bauwerkserhaltung und Denkmalpflege e.V. (2016, October). WTA Guideline 6-4*: Internal thermal insulation according to WTA I: planning guide*, edition 10.2016/E, Fraunhofer IRB Verlag.

Wissenschaftlich-Technische Arbeitsgemeinschaft für Bauwerkserhaltung und Denkmalpflege e.V. (2014, April). WTA Guideline 6-5: *Interior insulation according to WTA II: Evaluation of internal insulation systems with numerical design methods*, edition 04.2014/D, Fraunhofer IRB Verlag.

Wissenschaftlich-Technische Arbeitsgemeinschaft für Bauwerkserhaltung und Denkmalpflege e.V. (2016, August). WTA Guideline 6-8: *Assessment of humidity in timber constructions – simplified verifications and simulation*, edition 08.2016/D, Fraunhofer IRB Verlag.

List of figures

List of tables

Annex

A1: Map global horizontal radiation

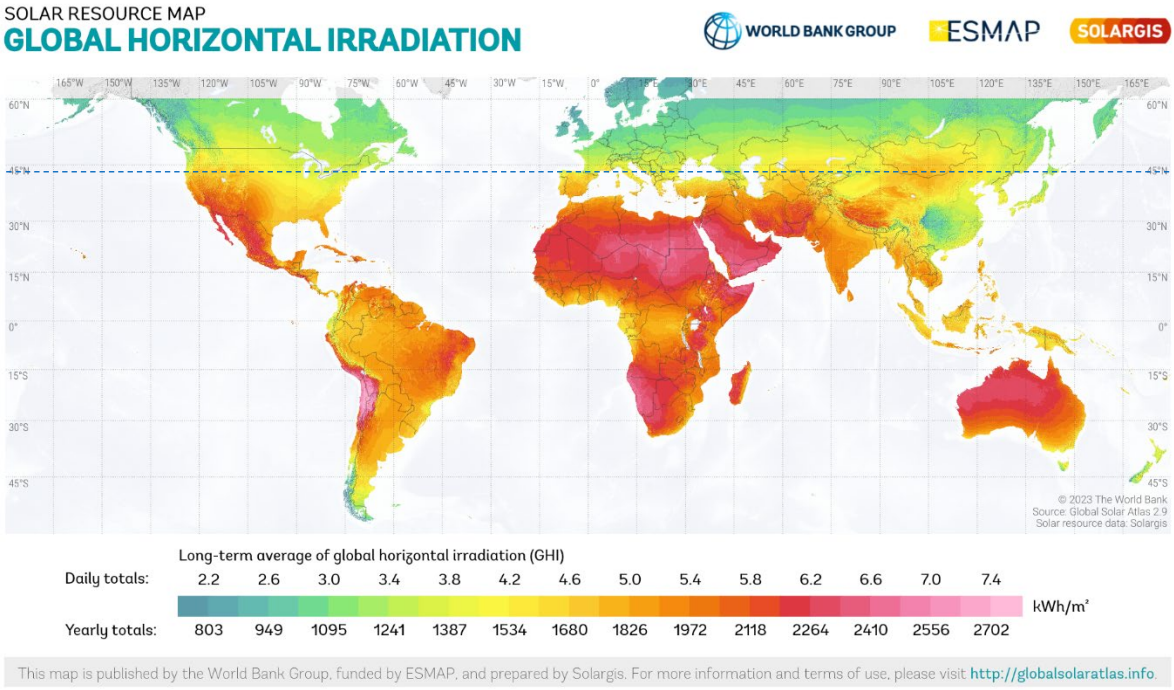

(Solargis, 2024)

A2: Psychometric chart (monthly averages)

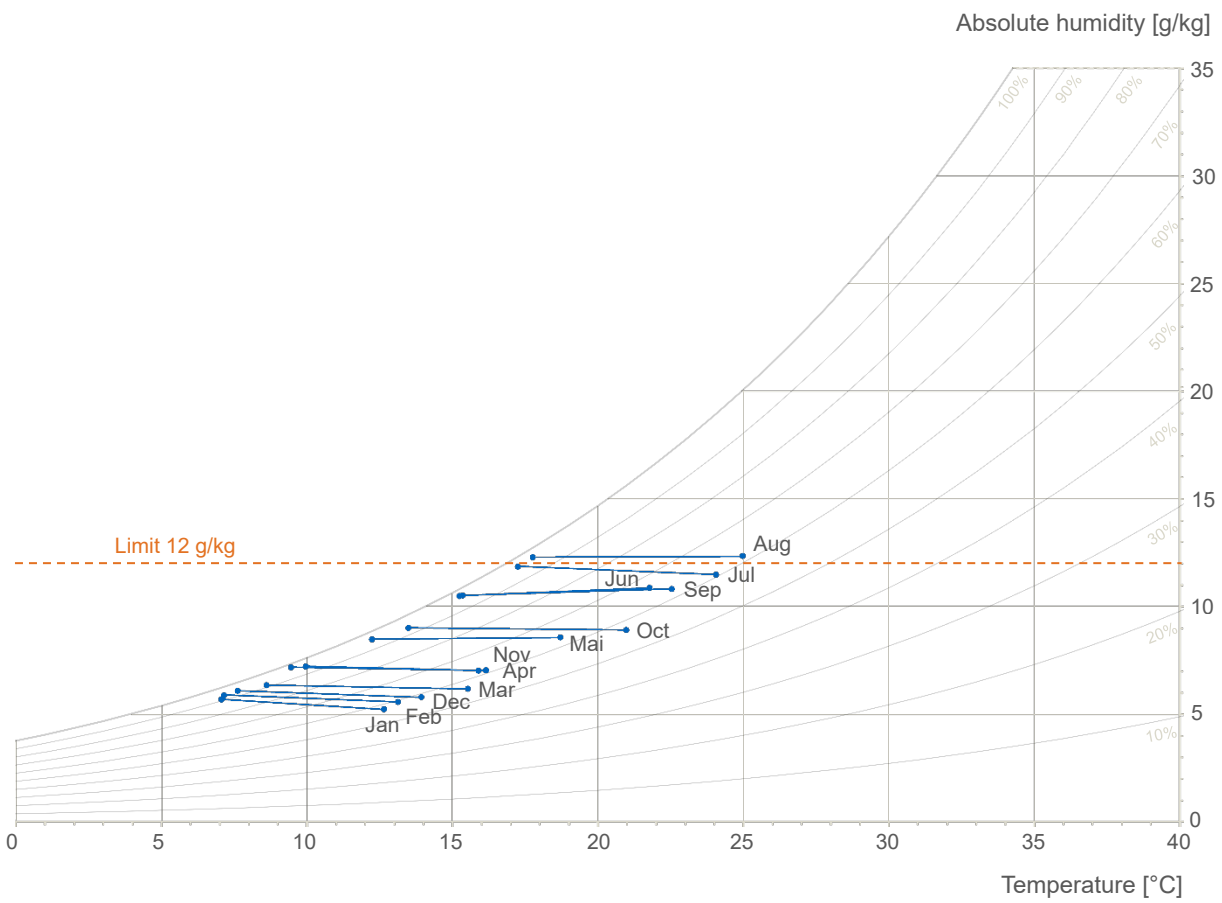

(own creation after Meteonorm and Marsh 2018)

A3: Parameters used in WUFI Pro simulation

Parameter	**Setting**
Orientation	North
Building height	Short building, height up to 10 m
Driving rain coefficients	R1 [-]: o; R2 [s/m]: 0.07
Heat transfer coefficient	Exterior surface: 17 W/m²K Interior surface: 8 W/m²K
Sd-value	Exterior and interior surface: no coating
Short-wave radiation absorptivity	0.9 (sandstone with patina)
Ground short-wave reflectivity	0.2 (standard value)
Adhering fraction of rain	0.7 is defined as the standard, depending on the inclination of the component. Comparison with 0.5, 0.3 and 0.1 in simulations using the Bad Bentheim sandstone (see Figure 40, p. 44).
Initial moisture in component	The existing wall is simulated for a 15-year period. The resulting average water content is then set as the initial moisture content for the three sandstone variants as follows: Bad Bentheim: 12.5 kg/m³ Baumberger: 43 kg/m³ Zeitzer: 7.8 kg/m³ The initial moisture content of the materials conforming the insulation system is assumed to be constant across all layers at 80% relative humidity.
Initial temperature in component	20°C constant across component

A4: Material properties sandstone Bad Bentheim

Property	Unit	Value
Bulk density	[kg/m³]	1933
Porosity	[m³/m³]	0.27
Specific Heat Capacity, Dry	[J/(kg K)]	910
Thermal Conductivity, Dry, 10°C	[W/(m K)]	2.584
Water Vapour Diffusion Resistance Factor	[-]	10
Reference Water Content	[kg/m³]	1.5
Free Water Saturation	[kg/m³]	147
Water Absorption Coefficient	[kg/(m² s^0.5)]	0.666
Moisture-dep. Thermal Cond. Supplement	[%/M.-%]	8
Temp-dep. Thermal Cond. Supplement	[W/(m K²)]	2.00000E-4

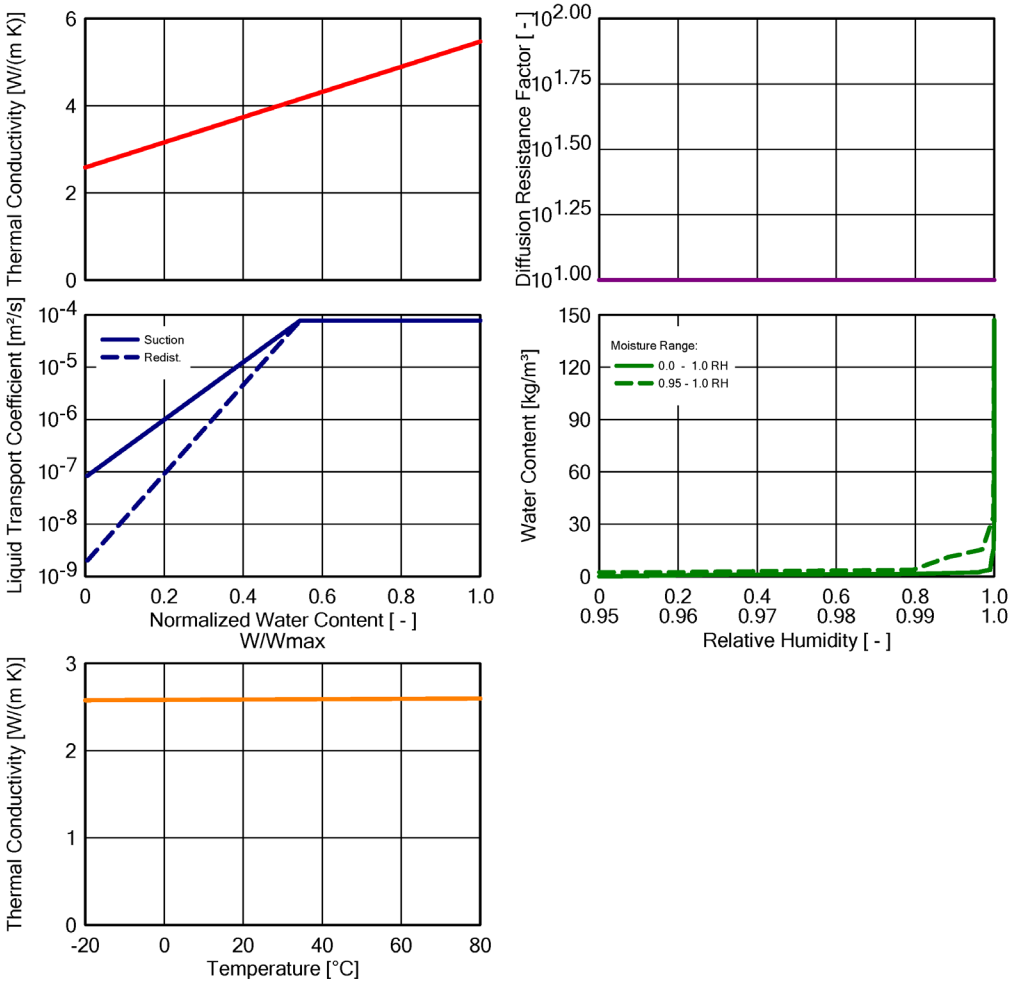

(WUFI Pro report)

A5: Material properties sandstone Baumberger

Property	Unit	Value
Bulk density	[kg/m³]	1980
Porosity	[m³/m³]	0.23
Specific Heat Capacity, Dry	[J/(kg K)]	850
Thermal Conductivity, Dry, 10°C	[W/(m K)]	1.7
Water Vapour Diffusion Resistance Factor	[-]	20
Moisture-dep. Thermal Cond. Supplement	[%/M.-%]	8
Temp-dep. Thermal Cond. Supplement	[W/(m K²)]	2.00000E-4

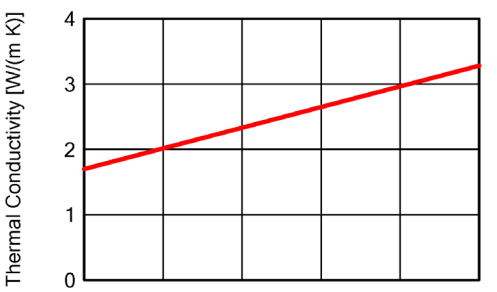

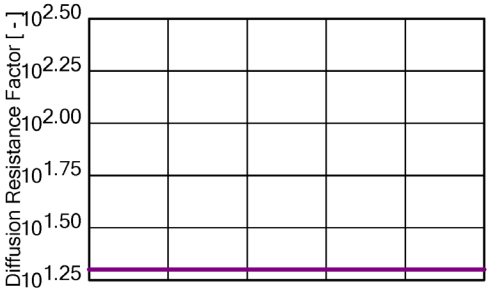

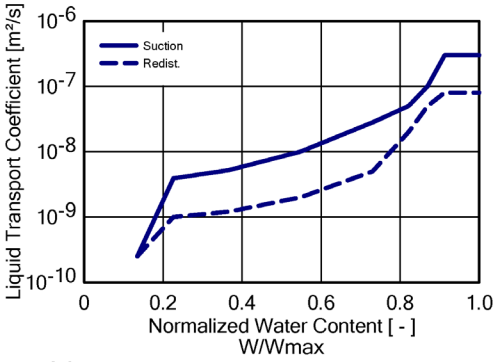

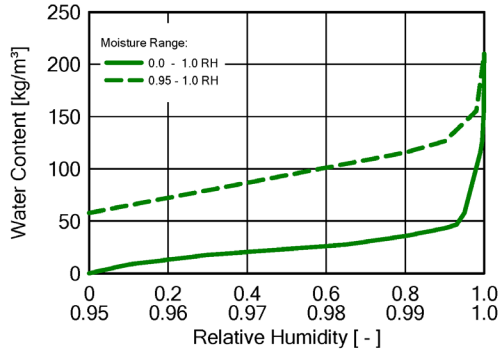

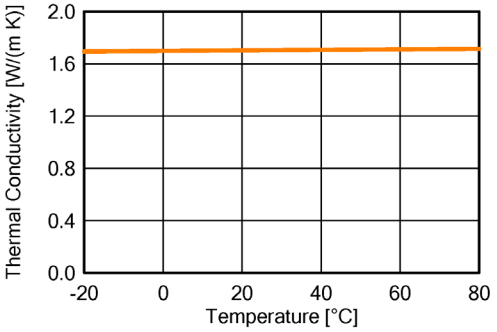

(WUFI Pro report)

A6: Material properties sandstone Zeitzer

Property	Unit	Value
Bulk density	[kg/m³]	2300
Porosity	[m³/m³]	0.05
Specific Heat Capacity, Dry	[J/(kg K)]	850
Thermal Conductivity, Dry, 10°C	[W/(m K)]	2.3
Water Vapour Diffusion Resistance Factor	[-]	70
Moisture-dep. Thermal Cond. Supplement	[%/M.-%]	8
Temp-dep. Thermal Cond. Supplement	[W/(m K²)]	2.00000E-4

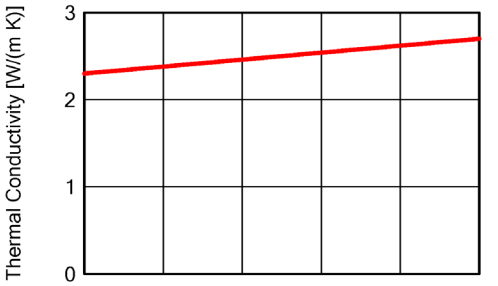

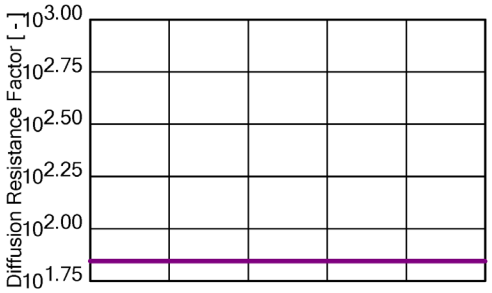

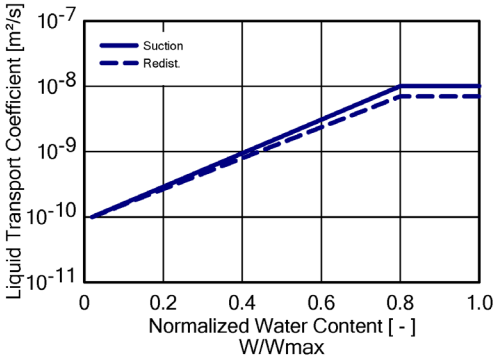

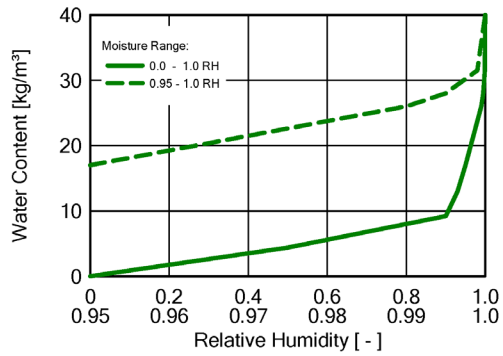

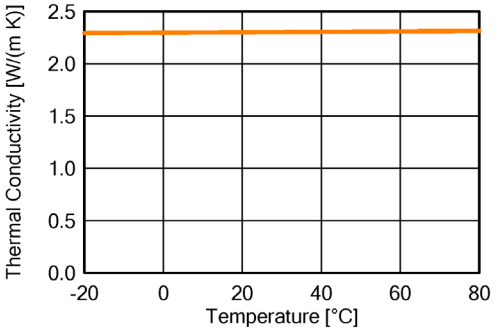

(WUFI Pro report)

A7: Material properties AiF Wood-Fiber Insulation Board WF low density

Property	Unit	Value
Bulk density	[kg/m³]	140
Porosity	[m³/m³]	0.91
Specific Heat Capacity, Dry	[J/(kg K)]	1400
Thermal Conductivity, Dry, 10°C	[W/(m K)]	0.039
Water Vapour Diffusion Resistance Factor	[-]	3
Reference Water Content	[kg/m³]	21
Free Water Saturation	[kg/m³]	350
Water Absorption Coefficient	[kg/(m² s^0.5)]	0.0075
Moisture-dep. Thermal Cond. Supplement	[%/M.-%]	0.5

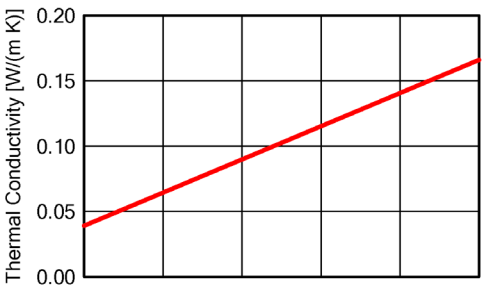

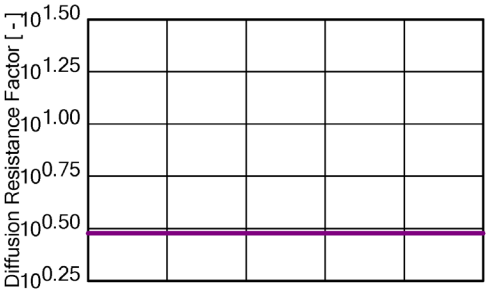

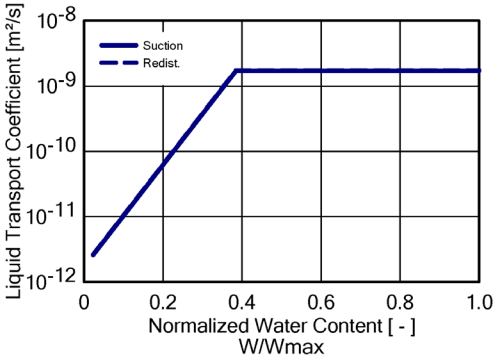

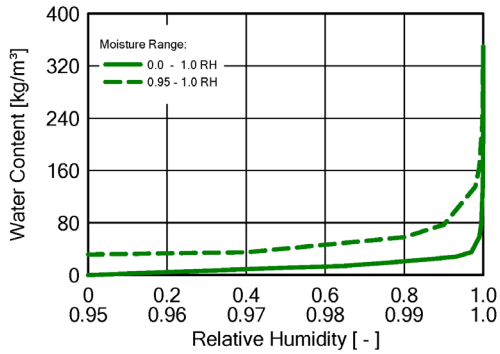

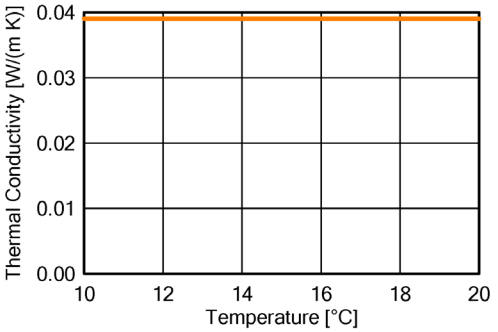

(WUFI Pro report)

A8: Material properties Expanded Clay

Property	Unit	Value
Bulk density	[kg/m³]	719
Porosity	[m³/m³]	0.67
Specific Heat Capacity, Dry	[J/(kg K)]	850
Thermal Conductivity, Dry, 10°C	[W/(m K)]	0.119
Water Vapour Diffusion Resistance Factor	[-]	7
Reference Water Content	[kg/m³]	17
Free Water Saturation	[kg/m³]	97
Water Absorption Coefficient	[kg/(m² s^0.5)]	0.02
Moisture-dep. Thermal Cond. Supplement	[%/M.-%]	4
Temp-dep. Thermal Cond. Supplement	[W/(m K²)]	2.00000E-4

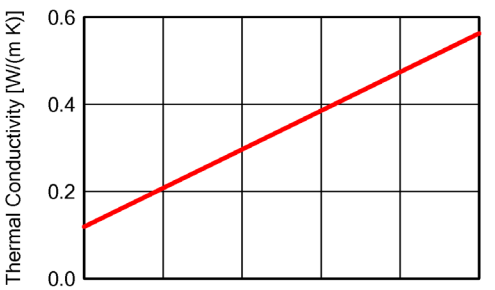

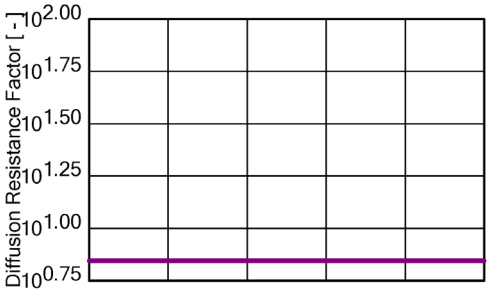

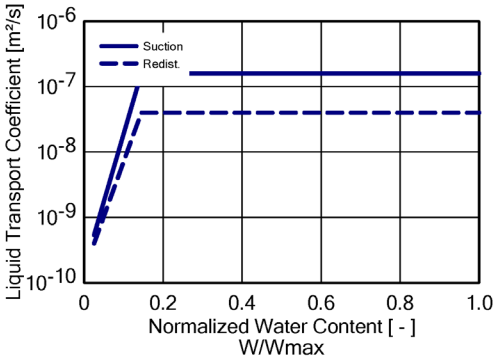

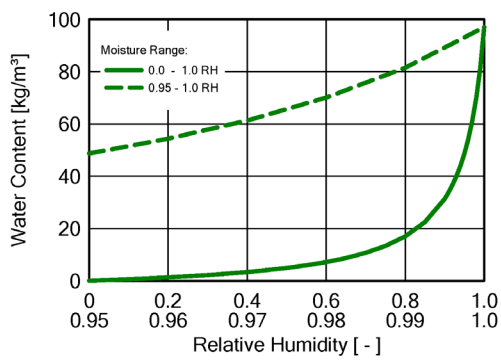

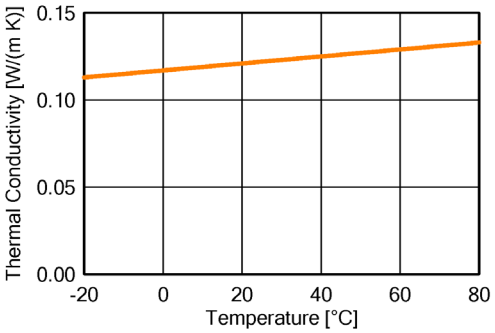

(WUFI Pro report)

A9: Material properties clay rendering

Property	Unit	Value
Bulk density	[kg/m³]	1514
Porosity	[m³/m³]	0.42
Specific Heat Capacity, Dry	[J/(kg K)]	850
Thermal Conductivity, Dry, 10°C	[W/(m K)]	0.65
Water Vapour Diffusion Resistance Factor	[-]	11.3
Moisture-dep. Thermal Cond. Supplement	[%/M.-%]	8

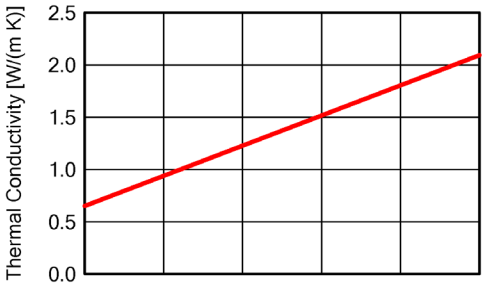

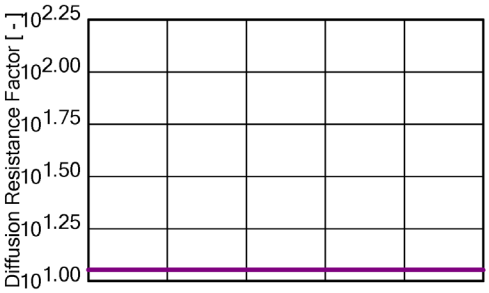

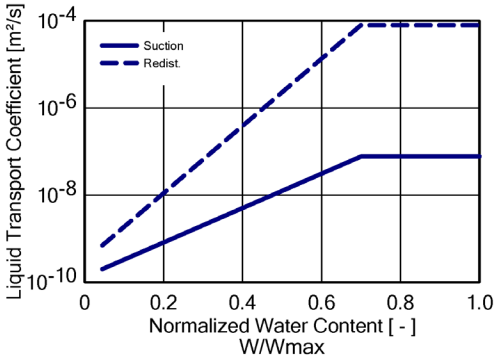

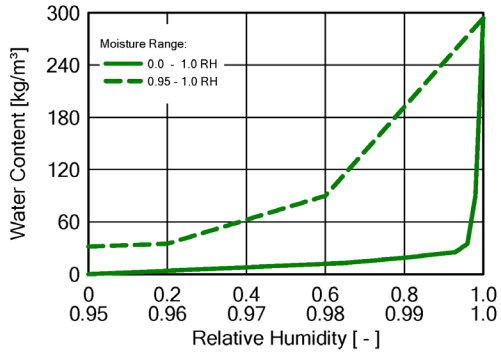

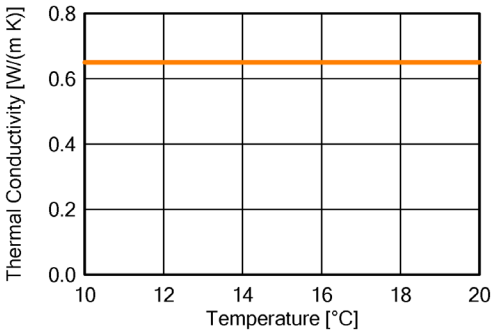

(WUFI Pro report)

A10: Isopleths interior surface

Bad Bentheim

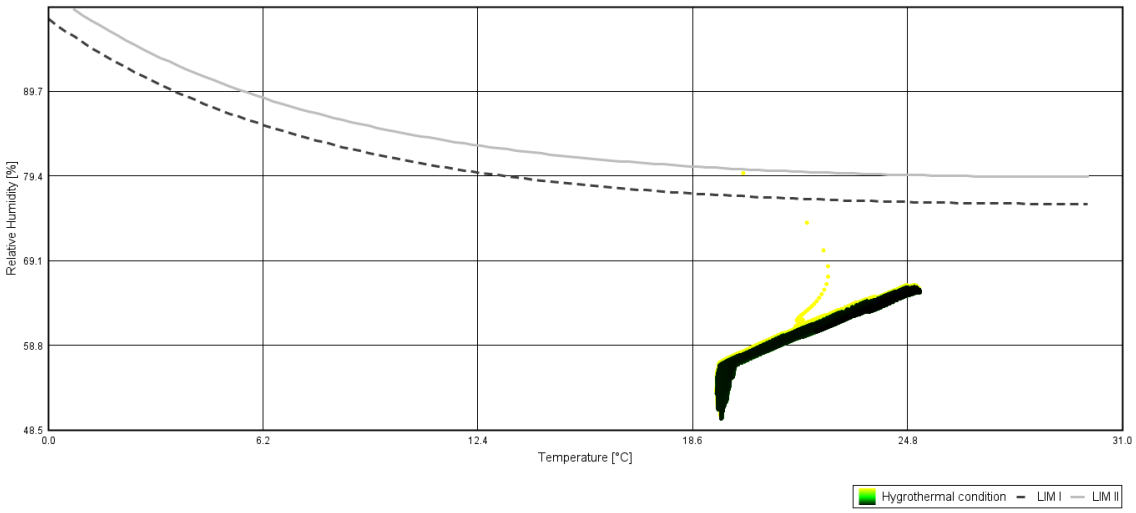

Baumberger

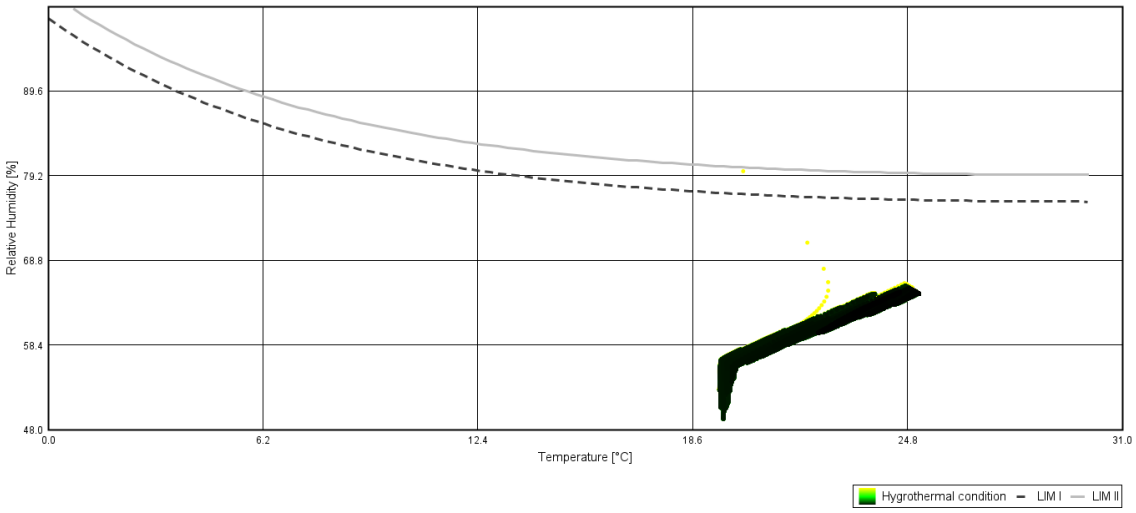

Zeitzer

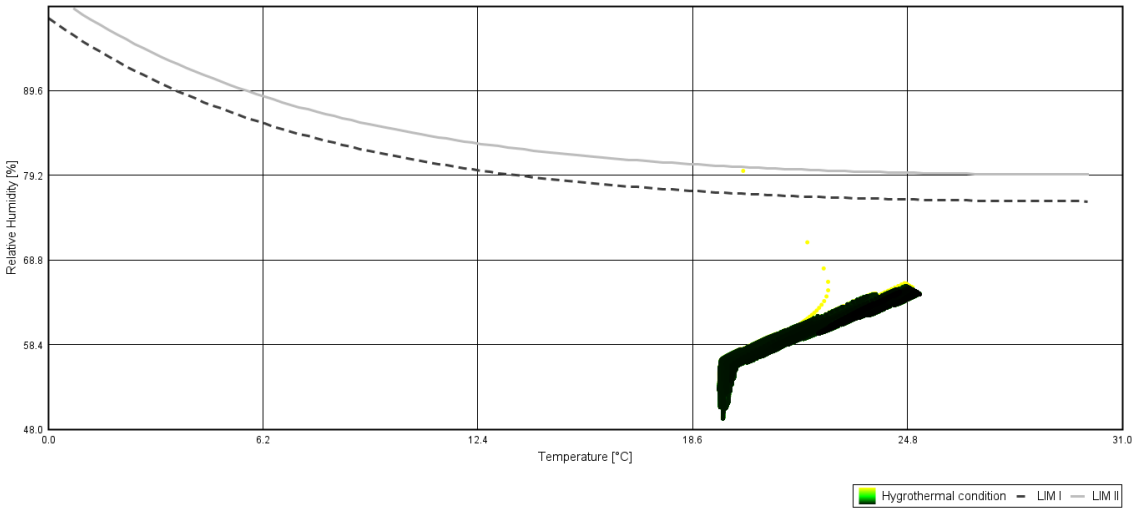

(WUFIGraph)

A11: Assemblies

Exterior wall – U-value: 0.415 W/m²K

Assembly	Material	**λ** [W/mK]	**cp** [J/kgK]	**ρ** [kg/m³]	**d** [m]
Outside					
Top coat render	Clay finishing plaster	0.45	850	1514	0.005
Reinforcement	Embedded glass fabric	-	-	-	-
Basecoat render	Clay plaster	0.45	850	1514	0.005
Insulation	Wood fiber board	0.039	1400	140	0.06
Adhesive	Clay adhesive	0.45	850	1514	0.01
Leveling layer	Lightweight mineral loam	0.17	850	719	0.06
Existent wall	Sandstone	2.3	850	2300	0.7
Inside					

Roof – U-value: 0.298 W/m²K

Assembly	Material	**λ** [W/mK]	**cp** [J/kgK]	**ρ** [kg/m³]	**d** [m]
Outside					
Roof covering	Arabic clay tiles	-	-	-	-
Counter battens	Timber 30/50	-	-	-	-
Battens	Timber 30/50	-	-	-	-
Sub-roof	Underlayment	-	-	-	-
Insulation	Wood fiber softboard	0.04	1400	165	0.12
Vapor barrier	Membrane	-	-	-	-
Tongue and groove cladding	Timber boards (oak/chestnut)	0.13	1400	650	0.024
Rafters	Timber (oak/chestnut)	-	-	-	-
Inside					

Floor – U-value: 0.633 W/m²K

Assembly	Material	**λ** [W/mK]	**cp** [J/kgK]	**ρ** [kg/m³]	**d** [m]
Inside					
Coating	Natural sealant	-	-	-	-
Flooring	Tamped earth	1.28	1000	2000	0.1
Moisture barrier	PE film	-	-	-	-
Insulation	Foamglas	0.045	1000	125	0.06
Separation layer	Geotextile fabric	-	-	-	-
Capillary break layer	Gravel with drainage	-	-	-	-
Outside					

Intermediate floor

Assembly	Material	λ [W/mK]	cp [J/kgK]	ρ [kg/m³]	d [m]
Flooring	Floorboards oak	0.13	1400	650	0.024
Sound insulation	Wood fiber softboard	0.04	1400	165	0.04
Tongue and groove cladding	Timber boards (oak/chestnut)	0.13	1400	650	0.024
Infill between beams	Loam	1.28	1000	2000	0.05
Protective layer	Oilpaper	-	-	-	-
Tongue and groove cladding	Timber boards (oak/chestnut)	0.13	1400	650	0.024
Beams	Timber oak/chestnut	-	-	-	-

Single stud wall (non-load bearing)

Assembly	**Material**	**λ** [W/mK]	**cp** [J/kgK]	**ρ** [kg/m³]	**d** [m]
Top coat render	Clay finishing plaster	0.45	850	1514	0.003
Reinforcement	Embedded glass fabric	-	-	-	-
Basecoat render	Clay plaster	0.45	850	1514	0.003
Planking	Clay building board	0.3	1100	900	0.022
Studs	Softwood 60/80	-	-	-	-
Insulation	Wood fiber softboard	0.06	1400	165	0.06
Planking	Clay building board	0.3	1100	900	0.022
Basecoat render	Clay plaster	0.45	850	1514	0.003
Reinforcement	Embedded glass fabric	-	-	-	-
Top coat render	Clay finishing plaster	0.45	850	1514	0.003

Material parameters after Wufi Pro database; Wufi Plus database; DIN 4108-4; DIN EN ISO 10456; Volhard et al., 1999, p. 85

Assemblies are own creation after Claytec, 2024; Soprema GmbH, 2024, p. 42ff.; Minke, 2009, p. 111; Haupt, 2017, p. 44; Volhard, 2021, pp. 108, 155, 230, 238; Claytec, 2023; Schneider, n.d.

A12: Simulated heating energy requirement

Simulation	Parameter	Heating energy [KWh/a]
110_h	Uninsulated	15184
210_h	Insulated (REF. CASE A)	7296
OPTIMIZATION REF. CASE A		
Optimization1: Shading courtyard		
211_W_Shading	Red. factor 0.3, > 25°C, **Optimization 1**	7296
Optimization 2: Quality of glass		
212_Uw_2.0	Uw=2.0	7683
212_Uw_1.6	Uw=1.6	6908
212_Uw_1.4	Uw=1.4, **Optimization 2**	6520
Optimization 3: Proportion and position of glazing facing south		
213_small_windows	All windows facing south: reveal 0 cm	6436
213_big_window_tree	Reveal 0 cm, red. factor 0.5 (tree)	6340
213_big_window	Reveal 0 cm, red. factor 0.7, > 25°C, **Optimization 3**	6340
Optimization 4: Proportion of roof glazing		
214_roof_0	No glazing	6490
214_roof_1	1m2, shade from tree (red. factor 0.5 Apr-Oct)	6414
214_roof_3	3m2, (Id.), **Optimization 4,** (REF. CASE B)	6272
EVALUATION REF. CASE B		
B_2050	Scenario 1	5491
B_family	Scenario 2	5054
B_family_2050	Scenario 3 (REF. CASE C)	4303
OPTIMIZATION REF. CASE C		
Thermal mass ground floor (F) and intermediate floor (C)		
TM_F_5	Rammed earth (floor) 5 cm	4328
TM_F_15	Rammed earth (floor) 15 cm	4304
TM_F_20	Rammed earth (floor) 20 cm	4312
TM_F_25	Rammed earth (floor) 25 cm	4320
TM_F_30	Rammed earth (floor) 30 cm	4322
TM_C_2.5	Loam infill 2.5 cm	4284
TM_C_5.0	Loam infill 5.0 cm, **Optimization 5,** Final 2050	4282
TM_C_7.5	Loam infill 7.5 cm	4283
TM_C_10	Loam infill 10 cm	4287
FINAL MODEL		
Final_2005_21	Heated to 21°C, Nov 1st – April 30th	6268
Final_2005_21_longer	Heated to 21°C, Oct 24th – Mai 15th	6766
Final_2005_19_longer	Heated to 19°C, Oct 24th – Mai 15th	6019
Final_2005_uninsu	Heated to 21°C, Nov 1st – April 30th, Uninsulated	11192

(WUFI Plus)

A13: Periodic day-profiles for human activity level (family household)

(own creation after WUFI Plus)

Declaration of authorship

I confirm that this master's thesis is my own work and I have documented all sources and material used. This thesis was not previously presented to another examination board and has not been published.

Munich, October 28, 2024

_____

Ayelén Arceo